THE ABUNDANCE OF LITHIUM IN THE ATMOSPHERES OF COOL STARS

Thesis by
Walter Karl Bonsack

In Partial Fulfillment of the Requirements
For the Degree of
Doctor of Philosophy

California Institute of Technology
Pasadena, California
1959

ACKNOWLEDGMENTS

The active interest of many persons has made possible the prosecution of this research. I am happy to gratefully acknowledge the contributions of

Dr. Jesse L. Greenstein, who suggested the problem and as research advisor freely gave valuable suggestions and criticism throughout the investigation;

the Council of the Mount Wilson and Palomar Observatories, who made available the necessary instruments;

Dr. Olin C. Wilson, who at the cost of much labor provided absolute magnitude estimates for many of the stars studied here; and

Drs. W. A. Fowler, H. L. Helfer, and G. Wallerstein, who enlightened me in conversation upon many important points in both the analysis and the interpretation of the results.

It is also my privilege to acknowledge the financial support of the California Institute of Technology through the van Maanen Fellowship, which I held for part of the time during which this research was carried out.

ABSTRACT

The abundance of lithium relative to vanadium, or its upper limit, has been determined for forty-six normal stars of spectral types from G8 to M0, inclusive. These results are based upon high-dispersion spectrograms obtained with the coudé spectrograph of the Hooker telescope. The abundance ratio for the sun has also been determined, using the equivalent width for lithium measured by Greenstein and Richardson and measurements of vanadium lines in the Utrecht Atlas.

Values have also been obtained of quantities related to the physical conditions in the stellar atmoshperes.

A range of up to a factor of one hundred in the abundance ratio is found among stars of similar surface characteristics. However, the maximum abundance ratio observed among similar stars declines with surface temperature.

It is not likely that a significant part of the variation is due to changes in the vanadium abundance.

Greenstein and Richardson have proposed that the lithium in the solar surface has been depleted by convective mixing to hotter regions. It is suggested that this hypothesis may explain both the trend and the variations observed in the cooler stars.

TABLE OF CONTENTS

I. INTRODUCTION

a) The Significance of Lithium

A basic requirement for any successful theory of the origin of the chemical elements is that it must account quantitatively for all elements found in nature. A theory which is currently under intensive study proposes that all the elements are formed in the stars, with hydrogen as the primordial material. A detailed review of the present state of this theory has been given by Burbidge, Burbidge, Fowler, and Hoyle (1957), who also give an extensive bibliography.

The light elements deuterium, lithium, beryllium, and boron present a considerable problem to any such theory of stellar synthesis, since they are easily destroyed by proton bombardment at the temperatures at which most stellar matter exists. Therefore they cannot remain in significant abundance in stars except in the surface layers, and there only if the matter is not rapidly mixed to the higher temperatures of the interior. Any process which might form these elements in the interior must be coupled with a mechanism to transport them quickly to the surface, and any method for producing them at the surface must involve non-equilibrium processes.

Thus the question of the abundances of these elements in stellar atmospheres assumes a double significance. Not only is quantitative information necessary in order to permit understanding of the elements' history from a nuclear-physics standpoint, but such data will also bear upon the astrophysical problems of mixing and atmospheric disturbances.

These elements are fairly common at the surface of the earth. The atomic abundance curve given by Burbidge, Burbidge, Fowler, and Hoyle, which is based upon the data of Suess and Urey (1956), shows that lithium, beryllium, and boron are slightly more abundant than the heavy, neutron-rich elements, and several orders of magnitude less abundant than the "iron group" and the other elements lighter than iron. Deuterium is more abundant than the iron group, but about 10^4 times less than hydrogen. These low abundances, which are based primarily on terrestrial and meteoritic measurements, are in qualitative agreement with the instability of these elements in stellar interiors.

However, the surface of the earth cannot be regarded as a fair sample of cosmic matter. It is essential to know how the abundances of these elements at the surfaces of stars compare with each other and with the

terrestrial values. Very few data have been made available on this problem. Boron is not observable in stars. The wave lengths of the deuterium lines are so close to the extremely strong hydrogen lines that there is little hope of seeing them if they exist. Lithium and beryllium have been observed but few quantitative results have been forthcoming. Clearly there is a need for more information on the abundances of the light elements in stars, and at least in the case of lithium and beryllium there is considerable hope that the information can be provided by astrophysical observations.

It is the purpose of this study to add to the available information on the abundance of lithium in stellar atmospheres. Lithium is somewhat less difficult to observe than beryllium, since its strongest lines are in the red region of the spectrum which can be recorded spectroscopically at high dispersion with modern equipment and materials, and in which the problems of the blending of crowded lines are not severe. The strongest lines of beryllium, on the other hand, are the doublet of Be II at λ3130, where the observational problems are considerable. Only the brightest and hottest stars provide sufficient energy at that wave length to permit the making of spectrograms of sufficient dispersion to resolve the frequent blends. More useful information can be provided by reasonable expenditure of time in observation and analysis by concentrating at first on lithium.

b) Previous Observations

Observations of lithium depend upon the resonance doublet of Li I at λ6707.74 and λ6707.89. Since very high resolution is required to separate these lines, the doublet is usually seen as a single blended feature. It arises from a transition analogous to the "D" lines of Na I and the "H" and "K" lines of Ca II. Other lines of Li I are much weaker and would not be detected unless the resonance doublet were very strong. Li II is not detectible because the first excited state has an excitation potential of almost 60 ev, and would not be significantly populated in any stellar atmosphere. Since only this one feature in the lithium spectrum can be expected to be visible, identification must depend primarily on wave length co-incidence, and also upon the appearance of the feature if the spectrographic dispersion is sufficient to partially resolve the blend.

The ionization potential of Li I is only 5.37 ev; therefore it should be observable only in cool stars. In these, the identification is streng-

thened by the fact that no observable atomic lines are listed in the Revised Multiplet Table (Moore 1945) within 2 A of the wave length of the Li I doublet.

The only previous quantitative result on the abundance of lithium in stars is the determination for the sun by Greenstein and Richardson (1951). Their study was based upon spectrograms taken at 0.7 A/mm with the 150-foot solar tower on Mount Wilson. Plates of both the solar disc and sunspot penumbra were used. On the solar disc the lines were extremely weak, having a total equivalent width of only 3.7 mA. This equivalent width was compared with that of a line of Ca I at λ6573 in order to obtain a relative abundance. The analysis was carried out using a model atmosphere of Stromgren and the Milne-Eddington approximation, and yielded an abundance ratio of lithium to calcium of about 100 times less than the terrestrial value. Unsöld (1955) has criticized this analysis on the grounds that the Li I doublet but not the Ca I line is on the linear part of the curve of growth, and that the chemical dissimilarity of lithium and calcium reduces the significance of the comparison with terrestrial abundances. To overcome these objections, he has compared the Li I equivalent width of Greenstein and Richardson with that of a line of K I at λ4044 and obtained the abundance ratio of lithium to potassium. His result is the same as that of the other authors: the abundance of lithium is lower in the sun than in the earth by a factor of about 100.

The Li I doublet has been observed in many other stars, but no quantitative analyses have been made. Much interest in lithium was aroused by McKellar's (1941) discovery of an extremely strong feature in the cool carbon star WZ Cassiopeiae. Lines of various strengths were subsequently found in other carbon stars. McKellar and Stilwell (1944) discuss the spectra of thirty such stars and find that the strengths of the doublets of Li I and Na I are not correlated. These authors give the equivalent width of the lithium doublet in WZ Cas as 8.4 A, about 2×10^3 that in the sun. They conclude that there is not sufficient evidence to assert that the great strength of the Li I line is due to a high abundance, since it may be caused by low excitation. However, other of their stars which have similar Na I doublet strengths do not show as much Li I. Keenan and Morgan (1944) classify WZ Cas as a very cool carbon star, and suggest that the low temperature may account for the lithium strength.

A lithium feature slightly stronger than in WZ Cas is present in another carbon star, WX Cygni, where Sanford (1950) reports an equivalent width of 10 A. Feast (1953) found a lithium line strong enough to be seen at 230 A/mm in the southern carbon star T Arae. Relatively weak Li I features have been seen in S stars (Keenan and Teske 1956, Merrill and Greenstein 1956, and Teske 1956). Hunger (Burbidge, et. al. 1957) has observed a strong feature in a T Tauri star. In addition, the writer has inspected a number of spectrograms obtained by J. L. Greenstein, and has found the element in normal K stars of several luminosity classes, M0 stars (but not M1 stars), and several carbon stars. It would appear that lithium is observable in fairly normal stars in which the temperature is high enough to avoid blending by molecular lines.

Spitzer (1949) looked for interstellar lithium and beryllium, but failed to detect any. He obtained upper limits of the lithium and beryllium abundances as respectively 1/10 and 5×10^{-4} that of sodium. In addition, lithium, beryllium, and boron nuclei have been found in cosmic rays in abundances comparable to carbon, nitrogen, and oxygen (Burbidge, et. al. 1957).

c) The Present Study

In view of the appearance of the lithium doublet in stars of various sorts--both normal stars and spectroscopically peculiar ones--and the apparent failure of the line strength to be correlated with other obvious features, it seemed worthwhile to attempt a quantitative survey at sufficient dispersion to detect and measure weak lines. Since it would not be practical to cover all stars in which this element might be detectible, it was thought best to confine the survey at first to the bright, normal stars about which the most information was available from other sources. For such stars there would be a maximum possibility of correlating variations in the lithium abundance with other characteristics of the stars, and a minimum probability of unusual surface or mixing phenomena. If it were to prove possible to correlate the lithium abundance with certain regular properties of the normal stars, a valuable basis would be provided for the study of the peculiar stars.

The considerations of ionization and blending by molecular lines which were mentioned above suggested that the K stars constituted the most promising field to search for this element.

The use of the yellow-red region of the spectra of K stars, which can be photographed together with the Li I doublet, offers other attractions. Lines of the elements of the iron group and the lighter metals abound, but are not present in such numbers as to obscure the continuum. Molecular features are practically absent. Furthermore, the continuous opacity, due to the H^- ion, has a particularly simple analytical form which greatly speeds the quantitative analysis. Using the coudé spectrograph of the Hooker telescope, spectrograms of a sixth magnitude star at 7 A/mm dispersion in this region can be obtained in about four hours. This dispersion is adequate for the measurement of line intensities in this spectral region, and there are enough stars of type K brighter than the sixth magnitude to provide material for such a survey. It was therefore decided to obtain such spectrograms of as many K stars as possible in a reasonable time, restricting the observations to stars having reliable spectral classifications on the MK system, and including as many luminosity classes as possible in each spectral class.

Obtaining the absolute abundance of lithium in a number of K stars would not only be difficult and necessarily inaccurate, but not particularly meaningful. It seems better to follow the example of Greenstein and Richardson, and obtain the abundance relative to another element which is not likely to suffer capricious variations from star to star. Such a relative determination minimizes the number of physical properties of the stellar atmosphere that need to be determined, since presumably both elements would be affected similarly. This procedure permits a maximum accuracy from a minimum amount of work, and in attempting a survey it is important to minimize the labor expended on each star.

It is interesting to list the criteria for a comparison line which Unsöld gives in discussing the paper of Greenstein and Richardson. He states that the line to which the Li I strength is compared should be

(1) similar to the Li I lines in excitation and ionization state,

(2) on the linear part of the curve of growth,

(3) near λ6708 in wave length, and

(4) due to an element chemically similar to lithium.

In the context of the present survey, several other general conditions should be noted:

(5) for maximum efficiency, only one high-quality plate should be obtained of each star,

(6) no model atmospheres are available, and

(7) comparison between stars is more important than comparison with the earth.

For this program, Unsöld's criteria (1) and (3) seem most weighty. Since the atmospheres of the cool giants are undoubtedly distended and complex, it is likely that one sees into regions of different temperatures and turbulent velocities. If one were to compare the Li I lines arising from the ground state with lines from a highly excited state of another atom--perhaps in order to fulfill condition (2)--it is likely that considerable error would arise because the lines were formed under different physical circumstances. Violation of Unsöld's condition (3) might entail also violation of condition (5). However, if the wave length difference were not sufficient to require violating (5), condition (3) is not so important because the wave length variation of the continuous opacity is known. Condition (4) is most weighty with respect to comparison with the earth. If it proves convenient or better in a nuclear-physics sense to compare lithium with a chemically dissimilar element in surveying stars, it is still possible to compare with the earth by placing the sun on the same system as the stars studied. Finally, it would seem that rigid adherence to condition (2) would cost as much accuracy as it would add. Certainly if the line is weak enough to be on the linear part of the curve of growth, the result will be minimally affected by the conditions of the stellar atmosphere. However, a line on the linear part of the curve of growth in a K5 giant would be invisible in a K0 giant. Thus it would be necessary to choose different lines, possibly not of the same element, for the cooler stars as compared with the hotter ones. Furthermore, lines weak enough to be on the linear part of the curve are often too weak to be measured accurately in stellar spectra. Although the lithium line is generally in this class, it seems better for minimum errors and in order to maintain condition (5) to use a number of lines of a suitable element for comparison, and instead of insisting on condition (2), use the comparison lines to determine a curve of growth appropriate to lines obeying condition (1), with reference to a specific set of theoretical curves of growth.

In view of the many lines of the elements of the iron group which exist in the yellow-red region, and since the abundances of these elements are not likely to change significantly during the stable lifetime of a star, or vary greatly relative to each other in different stars (see

Burbidge, et. al. 1957), it was decided to compare the lithium line to a number of weak, low-excitation lines of an iron-group element. The same lines and a standardized reduction procedure were maintained throughout the program.

II. OBSERVATIONS AND MEASUREMENTS

a) The Observations

The observational material upon which this study is based is a series of spectrograms obtained by the writer with the coudé spectrograph of the 100-inch Hooker telescope on Mount Wilson. Use of the 73-inch camera of the spectrograph and the second order of a 10,000 lines/inch grating produced spectrograms at 6.8 A/mm dispersion; the grating's blaze at λ6000 permitted exposures of useful density over the wave length range λλ5300-6800. A Kodak "K2" filter was placed in the stellar beam ahead of the spectrograph to remove the interfering third order spectrum.

The plateholder of the 73-inch camera accepts two standard 2x10-inch plates. Each spectrogram for this study was made with two plates of different sensitizations--a Kodak type "D" plate for the wave lengths shortward of λ6000, and a type "F" plate longward of λ6000. Many of the brighter stars observed were recorded on IIa-D and IIa-F plates. These have very fine grain and give excellent contrast. For the fainter stars, and for all stars when the limited supply of IIa-F plates was exhausted, 103a-D and 103a-F(3) plates were used. The 103a-F(3) plates were approximately three times faster than the IIa-F, but much more grainy. The difference in speed between the two sensitizations on each emulsion was not great. For all spectrograms, the projected width of the slit was 19 μ, near the limit of resolution of the plates. The projected slit length was 0.5 mm for most of the spectra taken on the IIa emulsion, and ranged from 0.5 mm to 1.5 mm for the spectra recorded on the 103a emulsion. In general if the star was sufficiently bright to be recorded in two hours or less on the IIa plates, these were used, until the supply was exhausted. After this, such stars were recorded on 103a plates using a projected slit 1.5 mm long. Fainter stars were recorded on 103a plates using shorter slits; in no case was the slit image shorter than 0.5 mm. It was found that the 1.5 mm-wide spectrograms made on the 103a emulsion yielded microphotometer tracings quite comparable in noise level to those made on the IIa emulsion with a width of 0.5 mm. A few very bright stars were recorded on the IIa emulsion with slit images longer than 0.5 mm.

All plates were developed in a mechanically-rocked tank for four minutes, using "D-19" developer.

In accord with the purpose of the investigation set forth in the

Introduction, the list of stars for observation was selected from lists of stars classified on the MK system by Johnson and Morgan (1953), Keenan and Morgan (1951), and Roman (1952). The stars selected were brighter than the sixth visual magnitude, and were of spectral types from G8 to M0, inclusive. All luminosity classes were included. As many stars meeting these criteria were observed as time permitted, but only one spectrogram was taken of each star. Table 1 lists the forty-six stars for which spectrograms of good photometric quality were obtained, giving the number in the Henry Draper catalogue, the name, the spectral class, the apparent visual magnitude, the co-ordinates for the epoch 1950, the plate number, the emulsion type, and the spectrum width in mm.

b) Wave Length Calibration

In order to calibrate the wave length scale on each plate, the spectrum of an iron arc and of a neon discharge tube were impressed on each side of the stellar spectrum. Since the iron spectrum has relatively few lines in the wave length region of interest, no filter was placed in the beam of the arc lamp and both the second and the third order spectra were recorded. The third order spectrum ($\lambda\lambda$3500-4500) is rich in lines. The iron spectrum was impressed both at the beginning and at the end of the stellar exposure, so that small changes in the plate's position would not affect the deduced wave lengths, and so that any large movement could be detected at once. No such large movements were found. The neon spectrum has very few lines, all of them in the yellow-red region. They are, however, useful for quick visual identification of wave length regions. The neon spectrum was impressed only after the end of the stellar exposure, and after increasing the separation of the prisms which deflect the light from the comparison source into the slit. This step made the neon lines easily identifiable on the plate. This spectrum was not used for wave length measurements.

c) Intensity Calibration

Two methods are available at the 100-inch telescope for the photometric calibration of spectrograms. The first is part of the coude spectrograph itself. A movable lamp housing mounted on rails atop the spectrograph room illuminates a set of slits of different widths on the spectrograph head. The light from the slits is reflected by a pair of plane mirrors

Table 1

Stars Observed

HD	Name	Type	m_v	α (1950) h	m	δ °	'	Plate no. Ce	Emul.	width mm.
3627	δ And	K3III	3.5	0	36.6	+30	35	11416	IIa	1.0
4128	β Cet	K0III	2.2	0	41.1	-18	16	11633	103a	1.5
6805	η Cet	K2III	3.6	1	06.1	-19	27	11671	103a	1.5
6860	β And	M0III	2.4	1	06.9	+35	21	11425	IIa	0.5
8512	e Cet	K0III	3.8	1	21.5	-08	26	11420	103a	1.1
9270	η Psc	G8III	3.7	1	28.8	+15	05	11573	IIa	0.5
								11681*	103a	0.5
10476	107 Psc	K1V	5.2	1	39.8	+20	02	11415	103a	0.5
11909	i Ari	K1p	5.2	1	54.6	+17	34	11580	103a	0.5
12533	γ AndA	K2III	2.3	2	00.8	+42	05	11426	IIa	0.5
12929	α Ari	K2III	2.2	2	04.3	+23	14	11427	IIa	0.5
20468	HR 991	K2II	4.9	3	15.6	+34	02	11629	103a	0.5
20644	HR 999	K3II-III	4.7	3	17.3	+28	52	11574	103a	0.8
22049	ε Eri	K2V	3.8	3	30.6	-09	38	11755	103a	1.5
27371	γ Tau	K0III	3.7	4	16.9	+15	31	11630	103a	0.8
27697	δ Tau	K0III	3.9	4	22.6	+17	49	11655	IIa	0.5
28305	ε Tau	K0III	3.6	4	25.7	+19	04	11673	103a	1.5
29139	α Tau	K5III	2.2	4	33.0	+16	25	11653	IIa	1.2
30504	HR 1533	K4II	5.1	4	46.5	+37	24	11672	103a	0.6
35620	ø Aur	K3p	5.3	5	24.3	+34	26	11668	103a	0.5
50778	e CMa	K4III	4.2	6	51.9	-11	58	11663	103a	1.5
62345	κ Gem	G8III	3.7	7	41.4	+24	31	11664	IIa	0.5
69267	β Cnc	K4III	3.8	8	13.8	+09	20	11657	103a	1.2
76294	ξ Hya	K0III	3.3	8	52.5	+06	08	11658	103a	1.5
81797	α Hya	K3III	2.2	9	25.1	-08	26	11666	103a	1.5
90432	μ Hya	K4III	4.1	10	23.7	-16	35	11676	103a	1.5
90537	β LMi	G8III-IV	4.5	10	25.0	+36	58	11632	103a	0.6
96833	ψ UMa	K1III	3.2	11	06.9	+44	46	11665	103a	1.5
98262	ν UMa	K3III	3.7	11	15.8	+33	22	11659	103a	1.0
98430	δ Crt	G8III-IV	3.8	11	16.8	-14	30	11757	103a	1.5
104979	o Vir	G8III	4.2	12	02.7	+09	01	11677	103a	0.5
108381	γ Com	K1III-IV	4.6	12	24.4	+28	33	11670	103a	0.8
124897	α Boo	K2IIIp	-0.1	14	13.4	+19	27	11237	IIa	1.5
165341	70 OphA	K0V	4.3	18	02.9	+02	31	11422	IIa	0.5
168723	η Ser	G8IV	3.3	18	18.7	-02	55	11412	IIa	0.5
176670	λ Lyr	K3II	5.1	18	58.1	+32	04	11417	103a	0.5
186791	γ Aql	K3II	2.8	19	43.9	+10	29	11248	IIa	0.5
189319	γ Sge	K5III	3.7	19	56.5	+19	21	11577	IIa	0.5
196321	70 Aql	K5II	5.2	20	34.1	-02	43	11578	103a	0.5
197989	ε Cyg	K0III	2.4	20	44.2	+33	47	11255	IIa	0.5
200905	ξ Cyg	K5Ib	4.1	21	03.1	+43	44	11413	IIa	0.5
201091	61 CygA	K5V	5.2	21	04.7	+38	30	11418	103a	0.6
201092	61 CygB	K7V	6.0	21	04.7	+38	30	11571	103a	0.5
201251	63 Cyg	K4II	4.9	21	04.9	+47	27	11419	103a	0.6
206778	ε Peg	K2Ib	2.4	21	41.7	+09	39	11257	IIa	0.5
219615	γ Psc	G8III	3.8	23	14.6	+03	01	11579	IIa	0.5
225212	3 Cet	K3Ib	5.2	0	01.9	-10	47	11424	103a	1.2

*obtained by W. G. Melbourne

toward the collimating mirror. The result on the plate is a set of twelve continuous spectra of known relative intensity, placed six on each side of the stellar spectrum. The intensity of illumination of the slits can be changed by moving the lamp housing and by changing the size of the lamp. Normally the light passes throug a diffusing glass and a "bull's-eye" filter--blue with a clear center--in the lamp housing, and another diffuser and a diaphragm near the slits. For the present exposures, a Kodak "K2" filter was also placed in the beam to suppress the third order spectrum.

The second calibration system, which was not installed until after approximately one-third of the observations for this program had been completed, is a separate grating spectrograph. This instrument is equipped with a wedge-shaped slit, so that the intensity incident upon the plate varies in proportion to the distance perpendicular to the dispersion. The light incident upon the slit comes from a diffusing screen, which is illuminated by a lamp mounted some distance away. The illumination of the screen can be changed by changing the size of the lamp or by changing a diaphragm placed in front of it. The dispersion at the plate is approximately 50 A/mm, so that the entire spectrum from the ultraviolet to the infrared can be impressed upon a single 2 x 5-inch plate. There were no significant overlapping orders in the spectral regions of interest in this study. The zero-intensity point on the spectrogram is located from the image of a rectangular slit which is cut in the slit-plate a known distance below the point of the wedge. Plates used in this instrument are taken from the same box as the stellar plate being calibrated, and are developed together with it.

Exposures with the first system, hereafter referred to as the "step" calibration, were made on all plates. Calibration spectrograms were made with the second, or "wedge," system for the "F" plate of all stellar exposures subsequent to plate Ce 11570. The dispersion of the wedge spectrograph is too small to make it practical to expose two plates of different sensitizations in their proper spectral regions simultaneously. In a few cases, a separate exposure for the "D" sensitization was made. Calibration exposure times were approximately equal to the total time that a given point on the stellar spectrogram was illuminated.

In both calibration systems, it is necessary that the slits be uniformly illuminated, and both systems provide methods for testing this.

In the step system, two apertures of uniform width may be slid into the place of the set of slits. Unfortunately moving the test apertures into place also moves the field lens, somewhat reducing the value of the test. An exposure through the uniform apertures should leave on the plate two spectra of uniform density perpendicular to the dispersion, if the apertures are uniformly illuminated and the optics are properly aligned. Such tests were made, and it was found that the apertures were not in general uniformly illuminated, and that the intensity gradient varied in an irregular manner with the position of the lamp. Thus it did not seem practical to take into account the non-uniformity in the photometric reductions--each exposure would require a separate illumination gradient determination. However, since the calibration slits are arranged so that slits of consecutively increasing width are on alternate sides of the stellar beam, the main effect is the introduction of scatter in the calibration curve. The difference in intensity of illumination between the strongest and weakest calibration spectrum on one side of the plate is small compared to the difference between two spectra of consecutive strength, which are on opposite sides of the plate.

In the wedge spectrograph, the slit can be removed and replaced with another one of uniform width. When uniformly illuminated, this will give a spectrogram with uniform density perpendicular to the dispersion. A test indicated that this condition was fulfilled.

The advantage of the step system is that the emulsion and development given the calibration spectrograms are as nearly as possible identical to those of the stellar spectrogram. However, with the non-uniform illumination introducing scatter, and with only twelve points to define a calibration curve, the accuracy of the result suffers considerably. The wedge spectrograph calibration may be subject to some systematic errors, but has very little scatter, and an infinity of points is available to define the curve.

Since the wedge spectrogram can produce a well-defined calibration curve, it is of interest to investigate the differences between wedge and step calibration curves made for the same plate. This was done in several cases, and the results for a typical one (plate Ce 11659, HD 98262) are shown in Figure 1. The abscissa is the logarithm of the intensity, in arbitrary units, and the ordinate, ρ, is defined as the ratio of the microphotometer deflection below the clear plate level caused by the blackened plate to that caused by the dark current. Thus it is a measure of the blackening in terms of the maximum possible blackness. This quantity was used as a measure

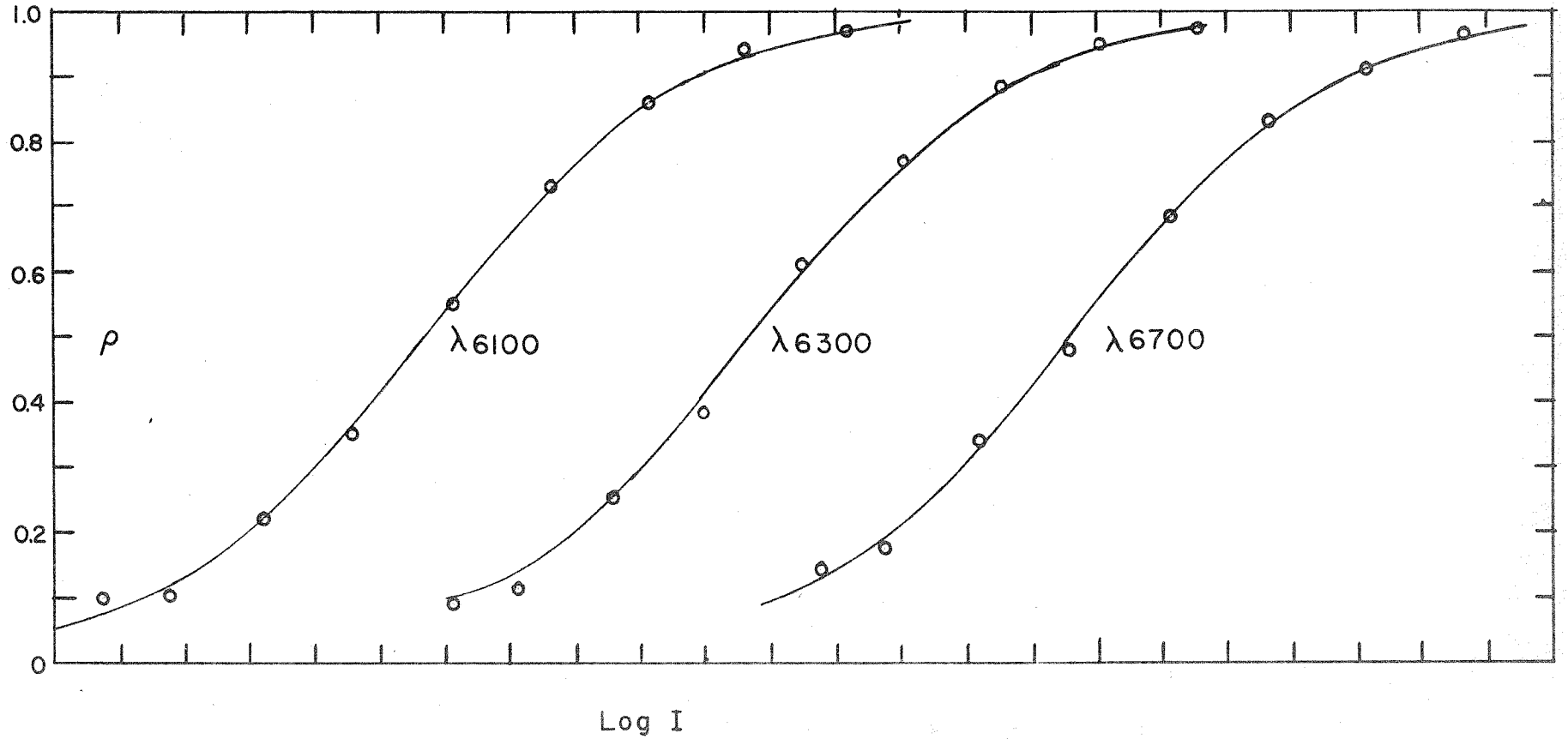

Figure 1. Comparison of calibration methods for plate Ce 11659 (HD 98262). The ordinate is a measure of plate blackening, and the abscissa the logarithm of the intensity (arbitrary units). The curves are from the wedge calibration, the circles from the step calibration. Fit is forced at $\rho = 0.5$.

of the exposure density throughout the reductions to remove the effects of variable plate background and varying microphotometer sensitivity. The curves in the figure are the results of reducing the wedge spectrograms at the wave lengths indicated. The points are from the step calibration at the same wave lengths. Agreement between the wedge curve and a curve through the step points was forced at $\rho = 0.50$. There is no indication of a significant systematic difference between the two methods. Thus there seems to be no reason to prefer the step calibration to the wedge method, and since the latter gives a better-defined curve, it was used whenever a wedge spectrogram was available.

In a few cases, the calibration spectrograms were either overexposed or underexposed compared to the stellar spectrogram, and extrapolation was necessary. It was found that two calibration spectrograms exposed for about the same length of time on plates with the same emulsion number gave essentially identical calibration curves, even if not developed together. Since the conditions of development were kept fairly constant throughout the whole program, serious differences are not to be expected. Thus when extrapolation was necessary, a calibration curve was selected from a spectrogram made under as nearly identical conditions as possible and used to extend the inadequate curve.

d) Identification and Selection of Lines

Complete wave length measurements and line identifications were carried out for one star only. This star was HD 206778 (ε Peg), spectral type K2Ib. The plate of this star was one of the best ones taken early in the observing program, and the star itself has about an average surface temperature for the stars in this study. Micrometer measurements were made of all spectral features in the wave length region from λ5300 to the beginning of the "B" band of atmospheric O_2 at λ6867. The measurements were reduced to apparent wave lengths by reference to the iron comparison spectrum, and corrected for radial velocity after identifying some of the stronger features.

The primary reference for identifications of the spectral lines was the Revised Multiplet Table. The Revision of Rowland's Preliminary Table of Solar Wave Lengths (St. John, et. al. 1928) provided identifications of terrestrial atmospheric lines. Davis' (1947) list of identifications in the M giant β Pegasi was most helpful in confirming certain identifications and in provi-

ding wave lengths of molecular lines. The list given by Burbidge and Burbidge (1957) for K Geminorum was also consulted, as was Hacker's (1935) for α Boötis. Satisfactory identifications were obtained for most lines strong enough to be certainly real, considering that only a single spectrogram was measured. The complete list of the measured lines will not be given here, since it is not relevant to the present study. Table 2 gives the lines selected for photometry.

The wave lengths of all the measured lines were marked on the microphotometer tracings of the spectrogram of HD 206778. Since all tracings used were made at the same scale, comparison with the marked tracing provided rapid identifications of the lines in the other stars. The considerable differences in atmospheric conditions encountered in the stars studied were not sufficient to make identifications by this method difficult.

The resonance doublet of Li I at λ6707.74 and λ6707.89 was not found in the spectrum of HD 206778. However, the identification of five fairly strong lines in the region λλ6700-6720 permitted the construction of a paper scale by which the wave lengths of the Li I lines could be located to within a few hundredths of an Angstrom on any of the tracings. It should be repeated that no other lines of this ion are sufficiently strong to be seen in the spectrum. Identification depends on wave length coincidence, and upon the fact that the blended doublet must appear broader than any unblended atomic lines of comparable strength.

It was pointed out in the introduction that considerable simplification is provided if the abundance of lithium is measured relative to an element of the "iron group." The lines used for comparison should preferably be as weak as possible (and still be measurable in all the stars studied) and of low excitation, so that no systematic errors are introduced by comparing lines formed at different levels in the extended atmospheres of the cool giants and supergiants. A group of lines was found that conforms rather well to these criteria, and in addition has transition probabilities determined in the laboratory. The lines selected are in the spectrum of neutral vanadium, and arise from levels of approximately 0.3 and 1.1 ev excitation. Thirty-four lines were chosen in the wave length region λλ5600-6300. These lines are all sufficiently free from blends so that fairly accurate equivalent widths could be obtained; furthermore most of the lines are in parts of the spectrum where the continuum is clearly defined. Table 2 lists the

lines used by multiplets, giving the multiplet number and transition, wave length, change in total angular momentum quantum number, excitation potential, and gf-value. The data in the first five columns are from the RMT, while those in the sixth are from the laboratory measurements of King (1947) for V I (relative values), and from Allen (1955) for Li I (absolute values).

In order to determine the state of ionization in the atmosphere of each star, lines of neutral and ionized scandium were measured. Unfortunately no lines of ionized vanadium are available in the wave length region covered by the spectrograms, making it necessary to substitute lines of another element of similar ionization properties. Four lines of Sc I and three of Sc II were used in the ionization determination. Spectroscopic data for these lines are also given in Table 2. No measurements of transition probabilities are available for scandium.

e) Photometry

The wave length regions λλ5600-5780, λλ6020-6320, and λλ6700-6720 of each spectrogram used in this study were registered on the Sinclair Smith recording microphotometer of the California Institute of Technology. An overall magnification of approximately 220 was used. The intensity calibration spectrograms were also registered (at a lower magnification) at the wave lengths λ5700, λ6100, λ6300, and λ6700 for most of the stars. In some of the stellar spectrograms an appreciable part of the wave length region λλ6020-6320 fell on the "D" plate; in this case an additional calibration of this plate was made at λ6000, and the "F"-plate calibrations were made at λ6200 and λ6700. The tracings of the calibration spectrograms were reduced to curves similar to Figure 1. As mentioned previously, wedge calibrations were used in preference to step calibrations when available.

Generally, the level of the continuum at a line to be measured could be accurately interpolated from nearby regions of uninterrupted continuum. In a few stars with broad lines, this could not be done for perhaps five of the lines measured. Even here, a reasonable estimate of the continuum could be made by inspection of the spectrum tracing for a distance of 25 Å or so on each side of the line. Further, on some underexposed regions on grainy plates the continuum could not be seen with certainty. The latter effect tends to produce random errors which cancel on the average, and the former affects relatively few lines; consequently the location of the continuum cannot

Table 2

Lines Measured

Multiplet		λ	J	E.P.	gf
		Li I			
1	$2^2S-2^2P^\circ$	6707.74	0.5-1.5	0.00	1.0)*
		6707.89	0.5-0.5	0.00	0.5)
		V I			
1	$a^4F-z^6D^\circ$	5632.469	4.5-3.5	0.07	2.4 †
19	$a^6D-z^6D^\circ$	6251.83	3.5-3.5	0.29	173
		6256.906	2.5-2.5	0.27	32
		6292.858	3.5-2.5	0.29	109
		6285.185	2.5-1.5	0.27	102
		6274.670	1.5-0.5	0.27	72
		6199.202	3.5-4.5	0.29	102
		6216.368	2.5-3.5	0.27	156
20	$a^6D-z^6F^\circ$	6150.132	4.5-5.5	0.30	83
		6189.350	2.5-3.5	0.27	5.4
		6213.874	4.5-4.5	0.30	45
		6224.507	3.5-3.5	0.29	49
		6233.187	2.5-2.5	0.27	43
		6245.214	0.5-0.5	0.26	3.5
		6266.32	2.5-1.5	0.27	26
34	$a^4D-z^4P^\circ$	6090.184	3.5-2.5	1.08	2500
		6119.505	2.5-1.5	1.06	1370
		6135.36	1.5-0.5	1.05	510
		6039.690	2.5-2.5	1.06	640
		6081.421	1.5-1.5	1.05	720
		6111.622	0.5-0.5	1.04	570
		6058.113	0.5-1.5	1.04	121
35	$a^4D-y^4F^\circ$	5727.024	3.5-4.5	1.08	5000
		5703.562	1.5-2.5	1.05	3200
		5706.973	0.5-1.5	1.04	2200
		5737.040	2.5-2.5	1.08	920
		5727.662	1.5-1.5	1.05	700
36	$a^4D-z^2G^\circ$	5670.827	3.5-4.5	1.08	1900
		5776.670	3.5-3.5	1.08	145
37	$a^4D-y^4D^\circ$	5627.628	3.5-3.5	1.08	2400
		5626.014	0.5-0.5	1.04	260
		5668.369	3.5-2.5	1.08	390
		5657.449	2.5-1.5	1.06	510
		5646.112	1.5-0.5	1.05	320
		5604.943	0.5-1.5	1.04	270

Table 2 cont'd.

Multiplet		λ	J	E.P.	gf
		Sc I			
2	$a^2D-z^2D^o$	6305.671	2.5-2.5	0.02	--- ≠
		6210.676	1.5-1.5	0.00	
12	$a^4F-z^4G^o$	5671.805	4.5-5.5	1.44	
		5717.30	3.5-3.5	1.43	
		Sc II			
28	$a^3P-z^3D^o$	6245.629	2-3	1.50	--- ≠
29	$a^3P-z^3P^o$	5657.870	2-2	1.50	
		5640.971	1-2	1.49	

* Lines blended. Absolute gf.
† Relative gf(King, 1947).
≠ No gf available.

be considered a significant source of photometric error.

The equivalent width, W, of an absorption line is defined by the relation

$$(1) \qquad W = \int \frac{F_o - F_\lambda}{F_o} \, d\lambda \quad ,$$

where F_o is the interpolated flux in the continuum, and F_λ is the flux in the line. The integral is taken over the range in λ in which the integrand is greater than zero. The direct way to obtain W is to derive values of F_o and F_λ at a sufficient number of points on the observed profile, and proceed by numerical or graphical integration. A numerical integration method was used on the first two tracings reduced, those of HD 206778 (ε Peg) and HD 28305 (ε Tau). It was apparent from these that the method was too slow in view of the volume of work to be done--a more rapid approximate method was needed. It was further seen that this method is quite sensitive to errors from blending in the wings of the line.

A plot of the integrand of equation 1 as a function of λ for a typical line indicated that the profile could be fairly well approximated by a triangle, and the equivalent width computed by the ordinary relation for the area of a triangle. Indeed, this method is often used. The equivalent width is determined by measurements of the line depth and the line width at the continuum. Unfortunately the latter quantity is subject to much uncertainty. Even weak lines have some wings, and it is difficult to decide where the line profile "ends." Further, the importance of blending lines increases with distance from the center of the line being measured. Thus, in an uncrowded region, the triangle method, which neglects the rounded bottom of the line and the wings, may underestimate the true equivalent width, and in a crowded region the influence of blends may cause it to overestimate this value.

An improved estimate of the equivalent width could be obtained by measuring the total width of the line at the half-depth point (the "half-width"). This would not only reduce the effect of blending, but since the product of the depth and the half-width gives in general the area of a trapezoid, the value would be correct if the line had a flat bottom of arbitrary width. This would partially compensate for the true rounded profile. However, having performed the added labor of measuring the half-width (involving an additional intensity determination), no further work is re-

quired to compute the equivalent width on the assumption that the profile is Gaussian. For a line whose central flux is $\underline{F_c}$ and whose half-width is $\underline{\Delta\lambda}$, the equivalent width on the assumption of a Gaussian profile is

$$(2) \qquad W = \Delta\lambda \left(\frac{F_o - F_c}{F_o}\right) \sqrt{\pi} \,/ 2\sqrt{\ln 2} = 1.064 \Delta\lambda \left(\frac{F_o - F_c}{F_o}\right) .$$

Equivalent widths in HD 206778 and HD 28305 have also been computed in the Gaussian approximation. In addition, certain lines in HD 81797 (α Hya) were selected for freedom from blending and were measured by both methods. Analysis of the measurements of half-widths in this star indicated considerable broadening by damping, which would tend to produce line wings stronger than the Gaussian approximation predicts. Thus the values for HD 81797 should be given high weight in testing the approximation. Figure 2 shows the results. The ordinate is the equivalent width calculated by a numerical integration of the apparent profile, and the abscissa is the equivalent width calculated on the Gaussian approximation. Values from different stars have different symbols. The full line is drawn through the origin with a slope of 45°, and the dashed line represents the expected slope of the relation if the trapezoidal profile were a better approximation. The difference between the two lines (6.4 per cent, according to equation 2) is negligible in terms of the main results of this study; nevertheless the points lie very close to the 45° line and systematically above the dashed line. There is no indication of error due to neglected damping wings. In view of these results, the Gaussian approximation was applied to all the lines measured in this investigation. The intention was to resort to numerical integration for any line which showed noticeable wings, but none was found. It was noted in the case of HD 28305 that a curve of growth constructed from the results of integrated profiles showed much more scatter than one constructed from equivalent widths computed on the Gaussian approximation, indicating the value of the approximation in suppressing blends.

Since the Li I feature is a blended doublet, the profile is not symmetrical. Nevertheless, the Gaussian approximation is still valid, since it may be thought of as nothing more than the trapezoid formula--which does apply in the absence of symmetry--with a correction factor for rounding at the bottom and edges.

Some of the lines measured were partially blended so that the half-width could not be determined. In these cases, a mean half-width was

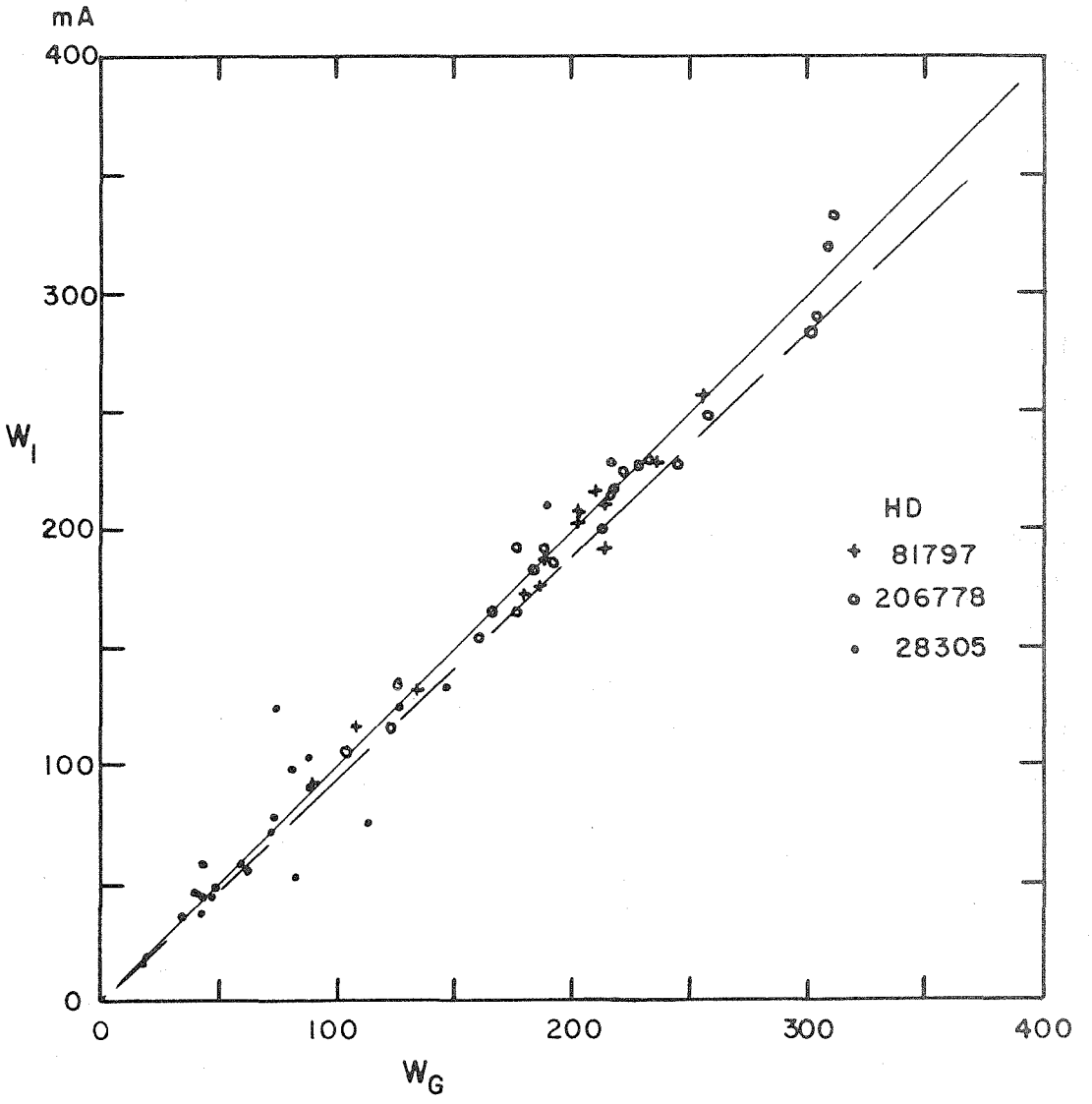

Figure 2. Comparison of equivalent widths derived by numerical integration of the apparent profiles (ordinate) and by the Gaussian approximation (abscissa). The solid line is at 45°; the dashed line shows the relation expected if the trapezoid approximation were correct.

used, which was calculated from all of the measured half-widths for each star. For lines sufficiently weak that the half-width is determined by the instrumental profile or by motions in the atmosphere, it is independent of central depth. All of the lines used were of this class in stars of spectral types earlier than K3. In later types, a dependence upon depth was found for the stronger lines, and the relation between depth and width was determined and used. In the coolest stars, the half-widths of a few weak lines not in Table 2 were measured in order to fix the weak-line end of the relation.

It is to be expected that equivalent widths derived from mean half-widths are less accurate than those from measured half-widths. In the latter case, errors in measuring the central depths will be partially cancelled by consequent errors in the half-widths. It is easily shown that if the line profile is exactly triangular and the central depth is inaccurately estimated, the resultant shift in the estimated position of half-depth will cause an error in the width measurement which will cancel the error in the depth measurement to the first order. If a mean half-width is used, no such cancellation results. If the error in the central depth is due to erroneous placement of the continuum, the effect of the shift in the half-depth position is to square the error. However, as mentioned above, the position of the continuum is usually well determined.

Tracings were made of a number of weak comparison lines to estimate the width of the instrumental profile. These gave instrumental half-widths of about 0.20 A. The half-widths for weak lines observed in the stellar tracings ranged from 0.23 A to 0.42 A.

It is of value to compare the results by this method with those obtained by other investigators for common stars. K. O. Wright (1951b) has measured many of the lines listed in Table 2 in HD 124897 (α Boo). Comparison of Wright's values with those of this study is made in Figure 3. Wright used approximately the same dispersion as was used here, and measured equivalent widths by fitting empirically determined standard profiles to the lines. Figure 3 indicates that Wright's values agree fairly well with those derived here, but are systematically slightly higher. The standard profiles used by Wright, which are plotted in his paper, show considerable wings, even for weak lines. There is no evidence for the existence of such

wings in the tracings made for this study. It should be pointed out that such discrepancies between equivalent widths measured by Mount Wilson and Victoria observers have been noted before.

E. M. and G. R. Burbidge (1957) have measured equivalent widths in HD 62345 (K Gem), using plates from the 100-inch telescope coudé spectrograph, but at a lower dispersion than used here. They used the triangle approximation. As a consequence of increased blending and decreased central depth at the lower dispersion, these authors did not measure most of the lines of Table 2. A comparison diagram similar to Figure 3 for the lines in common indicated a systematic difference, with the lines from this study weaker. This is to be expected from the increased effect of blends upon the lower dispersion measurements.

In spite of the above discrepancies, it would seem that the Gaussian approximation is an efficient method for obtaining an accurate estimate of the equivalent width of an absorption line showing no obvious wings. It certainly surpasses in accuracy the often-used triangle approximation. Perhaps the fitting of Voigt functions (van de Hulst and Reesinck 1947), which is again more difficult, would improve the accuracy, but it is difficult to see how the agreement in Figure 2 could be improved. No approximation is better (in the absence of blends) than the numerical integration of the observed profile; thus the agreement shown in Figure 2 is sufficient justification for the use of the Gaussian approximation.

Since only one plate of each star was used in this study, there remains the possibility of systematic photometric errors not connected with the assumed line profile. To test this, two plates of the same star are needed, both reduced by the same method. W. G. Melbourne obtained a spectrogram of HD 9270 (η Psc) in approximately the same spectral range used here. He had kindly permitted the writer to use it in this program. Mr. Melbourne's spectrogram (Oe 11681) was made on 103 a emulsion, while that obtained by the writer is on IIa emulsion. Since the division between the two plates in the different spectrograms occurred at different wave lengths, the calibration curves were constructed for different wave lengths. Hence ample opportunity for systematic differences is provided. Yet as the comparison of equivalent widths given in Figure 4 shows, no systematic effects are apparent. Completely separate analyses were made of these two spectrograms, but the equivalent widths for the star given in Table 4 are means

from the two plates, weighted 2:1 in favor of the plate made on the IIa emulsion.

f) The Li I Doublet

For those spectra in which the blended doublet of Li I is either absent or too weak to permit half-width measurements, it is necessary to devise a method to obtain the equivalent width (or its upper limit) taking into account the doublet nature. Since even at its strongest the Li I feature showed a roughly triangular profile, it seems sufficient to represent it in the case of very weak lines as the sum of two triangular profiles. Since the atomic weight of lithium is only about 1/7 that of vanadium, the broadening of the Li I profile due to thermal motion is greater than that for V I. However, the broadening effects of turbulence and the instrumental profile, which are the same for all atoms, are much greater than the effect of thermal motion; therefore the difference in width between single Li I and V I lines can be neglected, and the entire excess width of the Li feature can be ascribed to its doublet nature.

Figure 5 shows the assumed situation. The dashed line gives the undisturbed profile of the stronger member of the doublet, the dotted line represents the weaker member, and the solid line their linear sum. If the central depth of the strong line is $\underline{d}$, that of the weaker line is $\underline{d}/2$, and that of the sum is $\underline{d_t}$. This latter quantity is the only observable one. The line centers are separated by $\underline{\delta}$, and the half-width (equal also to half the width of the line at the continuum) is $\underline{\Delta\lambda}$. It follows from the figure that

$$(3) \qquad d_t = d + \frac{d/2}{\Delta\lambda}(\Delta\lambda - \delta) \quad ;$$

therefore

$$(4) \qquad d = d_t \,/\left(\frac{3}{2} - \frac{\delta}{2\Delta\lambda}\right) \quad .$$

The equivalent width of the strong line is $W = 1.064 d\Delta\lambda$ (inserting now the factor for the Gaussian approximation), and that of the weak line is half this value; therefore the total equivalent width is given by

$$W = \left(\frac{3}{2}\right)(1.064) d\Delta\lambda \quad ,$$

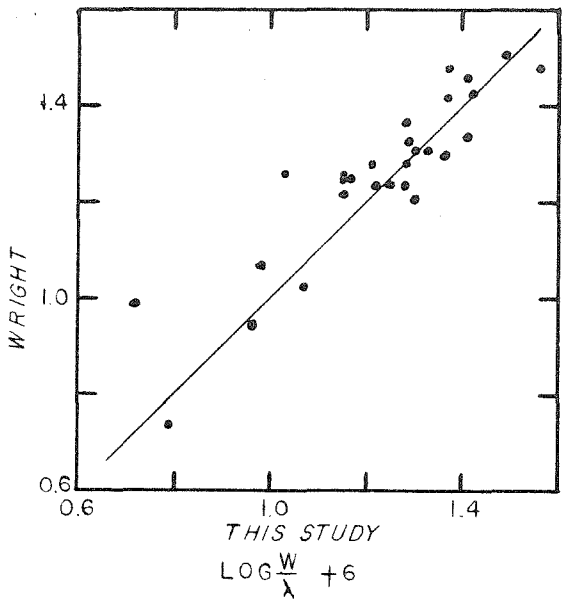

Figure 3. Equivalent widths for α Boo by Wright compared with those from this study.

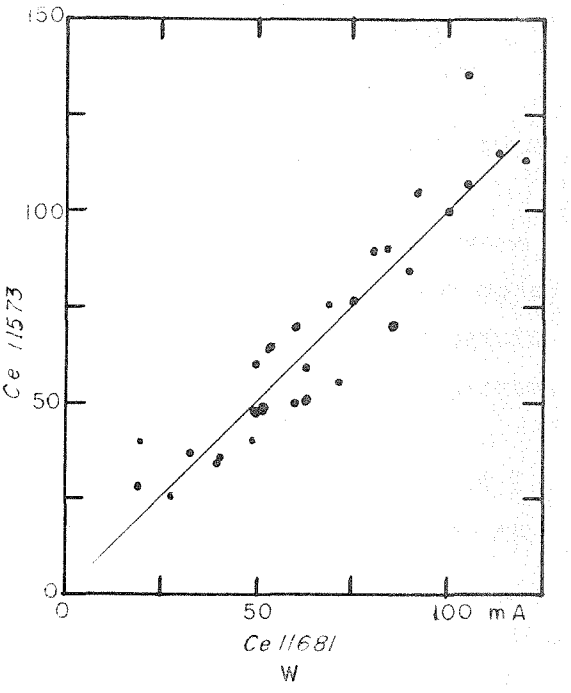

Figure 4. Comparison of equivalent widths derived from two plates of HD 9270.

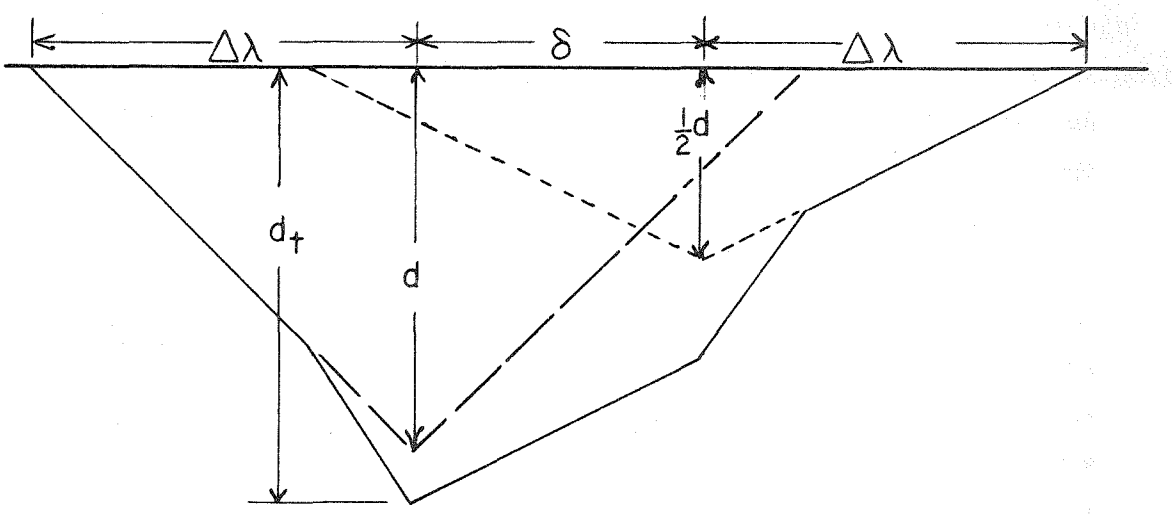

Figure 5. Synthetic profile for weak Li I doublet. Dashed lines indicate stronger component; dotted lines, weaker component; solid lines, total profile.

$$(5) \qquad W = (\tfrac{3}{2})(1.064) d_t \Delta\lambda (\tfrac{3}{2} - \frac{\delta}{2\Delta\lambda}) \quad .$$

Substituting $\delta = 0.15$ A,

$$(6) \qquad W = 1.064\ d_t \Delta\lambda / (1 - \frac{0.050}{\Delta\lambda}) \quad .$$

Thus the equivalent width of the whole feature is determined using equation 6, obtaining $\Delta\lambda$ from the weak lines of vanadium.

Equation 6 was used only when no trace of the feature was seen--in which case d_t was estimated from the noise pattern as the largest possible undetectible depth--and when the line was seen but was too weak to permit measurement of the half-width. For stronger lines, the Gaussian approximation was applied to the feature as a whole.

As a test, equation 6 was applied to two stars in which the Li I doublet was strong enough to measure directly. The results are given in Table 3 below.

Table 3

Test of Weak Doublet Formula

HD	W(A) (Gaus.)	W(A) (eq.6)
200905	0.200	0.161
11909	0.049	0.046

Since as the line becomes saturated the flux at the center falls more slowly than that in the wings, the result of equation 6 would tend to underestimate the true equivalent width by a greater amount as the total strength increased. This expectation is confirmed by the results of Table 3. The agreement for the weaker line is good, but the method underestimates the strong line equivalent width by 20 per cent.

Greenstein and Richardson (1951) take note of the considerable isotope shift in the lithium spectrum. The strong line of the less abundant isotope, Li^6, is approximately co-incident with the weak line of the strong isotope, Li^7. The wave lengths given in this study refer to Li^7. These authors found no evidence in the sun for an isotope ratio, Li^6/Li^7, in excess of the terrestrial value, 0.08. In this study, no particular allowance has been made for Li^6. In the strong features which were measured directly, any absorption due to Li^6 would have been automatically included. In the weak

lines to which equation 6 was applied, a strong Li^6 component would increase d_t, but the formula would underestimate the total strength slightly. None of the strong lines, however, indicated any appreciable abundance of Li^6. There seems to be no evidence that the isotope shift can introduce appreciable error into the results.

The Li I doublet in most of the stars is blended with a weak feature at λ6707.52. This was noticed and allowed for by Greenstein and Richardson in the sun. Davis (1947) found it in β Pegasi and ascribed it to TiO. A line at that wavelength in the carbon stars is assigned to CN by Sanford (McKellar 1944). It was always possible to free the Li I profile from the effects of the blend by simple extrapolation, since the blending feature was weak and did not contribute significantly over most of the doublet.

In the M0III star HD 6860 (β And) a broad blending feature appeared whose shortward edge corresponded closely to the longward component of the Li I doublet. In this star the depth at the intensity maximum between this feature and the one at λ6707.52 was taken as the maximum depth of the Li I feature. The increased strength of the broad feature in a good spectrogram of the M1III star δ Ophiuchi was one of the reasons for dropping this star from the program. It was felt that no meaningful upper limit to the Li abundance could be obtained.

Since the Li abundance depends on only one spectral feature, it is particularly sensitive to errors caused by plate defects. Therefore, each plate was inspected carefully in the region of the Li I doublet both before making the tracing and while it was on the microphotometer. In those few cases in which a defect appeared, the microphotometer entrance slit was adjusted to avoid it. It is fairly safe to assert that none of the Li I equivalent widths are significantly affected by defects.

g) The Case of the Sun

Since lithium has been observed in the sun, it is of interest to include the sun in the present investigation in order to put its abundance on the same scale as in the cooler stars. Because of the relatively high temperature and opacity in the solar atmosphere, the vanadium lines of Table 2 would be very weak at 6.8 A/mm, and the weaker lithium line would be unobservable. It seemed preferable therefore to use the much higher dispersion available in the intensity-scale tracings of the Utrecht Atlas (Minnaert, Mulders, and Houtgast 1940) to determine the vanadium and scandium equivalent widths, and adopt the equivalent width of the Li I feature given by Green-

stein and Richardson. As will be shown later, no important systematic differences between the sun and other stars seem to have arisen from the different source of equivalent widths.

Equivalent widths for the vanadium and scandium lines were derived by applying the Gaussian method directly to the tracings of the Atlas. To estimate possible systematic effects, these results were compared with those of other investigators for common lines. Wright (1951a) obtained the solar spectrum at a lower dispersion than the 6.8 A/mm used for the other stars in this study by exposing on the moon and the sky. He gives equivalent widths for nine lines used here. There are no sytematic differences apparent between the two sets of results. Allen (1934) has given an extensive list of solar equivalent widths obtained at the center of the disc with a high-dispersion prismatic solar spectrograph. Eleven of the lines in Table 2 were included in his study. No systematic differences appear between Allen's values and those derived here. Bell (1951) derived equivalent widths from the Utrecht Atlas by fitting Voigt profiles. She has measured thirteen of the lines in Table 2 and lists equivalent widths greater by about 0.02 in the logarithm than those derived here. This difference is trivial. Probably for such weak lines the adopted Voigt functions are no closer to the true profiles than the Gaussian functions. In view of these various results, it was decided to use directly the equivalent widths given by the Gaussian approximation.

h) The Table of Equivalent Widths

The equivalent widths derived according to the discussions of the last several sections are given in the form log W/λ + 6 in Table 4. The spectral lines are listed in the table in order of increasing wave length. The information given is as follows:

Column 1: An ordinal number.

Column 2: The wave length, according to the RMT.

Column 3: The ion causing the line.

Column 4: The multiplet number in the RMT.

Column 5: The abscissa of the curve of growth, uncorrected for temperature (see Chapter III).

Columns 6, 7, etc.: The derived values of log W/λ + 6 for each star. The equivalent width values for a star are grouped in a single column, and

the columns are ordered according to the stars' HD numbers. In these columns a "less-than" ($<$) symbol preceding an entry indicates that no trace was found and an upper limit to the central depth was estimated from the noise pattern; a "less-than-or-equal-to" ($\leq$) symbol indicates that a trace of the line was seen but it was impossible to do more than estimate a maximum depth.

All of the results of this study are based on the values in Table 4.

Table 4

The Equivalent Widths

$\log \frac{W}{\lambda} + 6$

No.	λ	Ion	Mult.	$\log \eta_o'$	HD 3627	4128	6805	6860	8512
1	5604.943	V I	37	5.57	1.20	0.85	1.10	1.41	0.79
2	26.014	"	"	5.55	1.34	1.03	1.26	1.48	0.87
3	27.662	"	"	6.52	1.45	1.35	1.45	1.54	1.28
4	32.469	"	1	3.52	1.05	<0.08	0.77	1.37	0.38
5	40.971	Sc II	29	--	1.28	1.26	1.34	1.34	1.21
6	46.112	V I	37	5.64	1.24	0.91	1.22	1.44	0.85
7	57.449	"	"	5.84	1.26	1.10	1.21	1.43	1.03
8	57.870	Sc II	29	--	1.28	1.32	1.35	1.37	1.27
9	68.369	V I	37	5.73	1.24	1.01	1.11	1.47	0.96
10	70.827	"	36	6.42	1.43	1.20	1.36	1.58	1.24
11	71.805	Sc I	12	--	1.40	1.13	1.36	1.53	1.09
12	5703.562	V I	35	6.64	1.48	1.31	1.48	1.60	1.34
13	06.973	"	"	6.82*	1.53	1.36	1.48	1.60	1.42
14	17.30	Sc I	12	--	0.92	0.44	0.81	1.19	0.25
15	27.024	V I	35	6.85	1.55	1.37	1.52	1.64	1.38
16	27.662	"	"	5.98	1.42	1.12	1.36	1.52	1.16
17	37.040	"	"	6.10	1.38	1.22	1.24	1.54	1.20
18	76.670	"	36	5.31	1.21	0.81	1.02	1.50	0.63
19	6039.690	"	34	5.95	1.40	1.18	--	1.46	1.16
20	58.113	"	"	5.23	1.38	0.84	1.06	1.48	0.92
21	81.421	"	"	6.00	1.43	1.29	1.35	1.53	1.26
22	90.184	"	"	6.54	1.52	1.24	1.39	1.59	1.27
23	6111.622	"	"	5.90	1.51	1.19	1.38	1.54	1.26
24	19.505	"	"	6.28	1.47	1.24	1.39	1.55	1.26
25	35.36	"	"	5.85	1.39	1.16	1.30	1.48	1.12
26	50.132	"	20	5.06	1.50	1.22	1.40	1.63	1.29
27	89.350	"	"	3.88	1.28	0.50	0.97	1.38	0.64
28	99.202	"	19	5.16	1.60	1.30	1.44	1.66	1.28
29	6210.676	Sc I	2	--	1.43	1.02	1.26	1.59	1.06
30	13.874	V I	20	4.80	1.41	1.03	1.31	1.49	1.10
31	16.368	"	19	5.34	1.55	1.33	1.47	1.67	1.36
32	24.507	"	20	4.84	1.41	1.13	1.29	1.50	1.13
33	33.187	"	"	4.78	1.46	1.08	1.25	1.45	1.10
34	45.214	"	"	3.69	1.14	0.41	0.82	1.25	≤0.33
35	45.629	Sc II	28	--	1.28	1.19	1.16	1.20	1.13
36	51.83	V I	19	5.39	1.56	1.25	1.40	1.56	1.28
37	56.906	"	"	4.65	1.42	--	1.24	1.44	1.04
38	66.32	"	20	4.56	1.37	1.00	1.20	1.43	0.94
39	74.670	"	19	5.00	1.46	1.20	1.31	1.44	1.15
40	85.185	"	"	5.16	1.44	1.08	1.31	1.52	1.10
41	92.858	"	"	5.18	1.50	1.22	1.34	1.62	1.26
42	6305.671	Sc I	2	--	1.57	1.27	1.41	1.69	1.17
43	6707.82	Li I	1	--	0.51	<0.12	1.20	<0.58	<0.26

*Derived from stellar W, not laboratory gf.

Table 4 cont'd.

No.	9270	10476	11909	12533	12929	20468	20644	22049	27371
1	0.67	0.59	0.36	1.22	1.08	1.25	1.26	0.18	0.82
2	0.82	--	0.82	1.36	1.16	1.28	1.37	--	0.81
3	1.30	1.06	1.23	1.48	1.33	1.52	1.53	1.03	1.30
4	<0.07	<0.13	≤0.43	0.97	0.70	1.07	0.91	<0.25	0.58
5	1.28	0.89	1.31	1.38	1.31	1.48	1.42	0.88	1.33
6	0.80	0.63	0.53	1.31	1.11	1.29	1.32	0.60	0.90
7	0.83	0.64	0.86	1.31	1.19	1.32	1.37	0.73	1.07
8	1.34	1.04	1.33	1.40	1.34	1.45	1.47	1.05	1.37
9	0.83	0.62	0.84	1.30	1.20	1.34	1.32	0.86	1.01
10	1.16	1.04	1.09	1.48	1.38	1.45	1.51	1.17	1.28
11	0.94	0.84	0.99	1.41	1.28	1.52	1.42	1.00	1.10
12	1.21	1.10	1.23	1.56	1.42	1.56	1.53	1.09	1.24
13	1.36	1.14	1.25	1.62	1.45	1.58	1.62	1.22	1.39
14	0.51	--	--	0.92	0.38	0.86	0.93	0.15	--
15	1.33	1.19	1.32	1.59	1.52	1.65	1.59	1.18	1.38
16	0.96	0.86	0.90	1.46	1.21	1.43	1.44	0.76	1.12
17	1.04	0.75	0.93	1.40	1.34	1.36	1.41	0.99	1.17
18	--	0.49	--	1.22	0.96	1.15	1.21	0.36	0.59
19	0.99	0.84	0.94	1.43	1.16	1.47	1.43	0.86	1.07
20	0.47	0.38	0.50:	1.23	0.97	1.30	1.24	0.50	0.82
21	1.07	0.80	0.98	1.48	1.23	1.50	1.45	0.98	1.14
22	1.21	1.08	1.08	1.50	1.29	1.53	1.51	1.20	1.37
23	0.99	0.86	0.98	1.46	1.20	1.46	1.44	0.89	1.11
24	1.17	0.97	1.02	1.47	1.27	1.51	1.48	1.08	1.27
25	1.04	0.70	0.83	1.41	1.14	1.43	1.41	0.95	1.11
26	1.02	0.78	0.84	1.47	1.27	1.47	1.48	0.92	1.03
27	--	--	0.44	1.24	0.82	1.14	1.17	0.46	0.41
28	1.10	0.93	0.99	1.54	1.34	1.53	1.60	1.00	1.14
29	0.74	0.56	0.71	1.39	1.14	1.34	1.35	0.68	0.85
30	0.94	0.74	0.73	1.46	1.20	--	1.44	0.84	1.00
31	1.24	0.97	1.05	1.56	1.38	1.58	1.57	1.18	1.28
32	0.87	0.75	0.80	1.46	0.99	1.42	1.44	0.78	1.07
33	0.92	0.67	0.82	1.42	1.22	1.45	1.50	0.84	1.04
34	--	--	-0.02	1.08	0.64	--	0.94	--	0.44
35	1.18	0.72	1.08	1.36	1.16	1.41	1.39	0.63	1.11
36	1.09	0.90	0.95	1.54	1.36	1.52	1.48	1.10	1.18
37	0.85	0.30	0.52	1.44	1.20	1.43	1.37	0.56	0.89
38	0.66	0.47	0.67	1.42	1.08	1.37	1.33	0.64	0.83
39	0.96	0.75	0.81	1.44	1.15	1.43	1.39	0.87	1.02
40	0.97	0.94	0.89	1.48	1.18	1.48	1.48	0.92	1.16
41	1.05	0.77	0.94	1.48	1.27	1.51	1.53	0.92	1.12
42	0.94	0.58	0.79	1.47	1.28	1.53	1.52	1.05	1.08
43	0.76	<-0.01	0.86	0.64:	<0.25	1.27	0.90	<0.84	0.64

Table 4 cont'd.

No.	27697	28305	29139	30504	35620	50778	62345	69267	76294
1	0.69	0.88	1.41	1.34	1.39	1.33	0.55	1.37	0.77
2	0.77	0.88	1.52	1.44	1.46	1.44	0.64	1.46	0.82
3	1.36	1.36	1.52	1.52	1.50	1.49	1.29	1.53	1.33
4	0.58	<0.51	1.30	1.19	1.15	1.24	<-0.06	1.19	<0.23
5	1.26	1.35	1.36	1.30	1.39	1.31	1.25	1.34	1.25
6	0.73	0.94	1.43	1.36	1.38	1.36	--	1.38	0.78
7	0.95	0.86	1.40	1.32	1.38	1.36	0.76	1.38	0.89
8	1.26	1.40	1.35	1.35	1.39	1.36	1.33	1.38	1.35
9	0.97	1.02	1.45	1.38	1.32	1.41	0.68	1.35	0.79
10	1.21	1.31	1.54	1.49	1.51	1.57	1.11	1.57	1.18
11	1.14	1.16	1.54	1.47	1.52	1.54	1.04	1.44	1.09
12	1.21	1.33	1.56	1.53	1.54	1.57	1.28	1.56	1.30
13	1.40	1.60	1.63	1.57	1.59	1.60	1.43	1.63	1.42
14	0.35	0.23	1.21	1.07	1.02	1.16	0.31	1.11	0.32
15	1.36	1.41	1.64	1.62	1.63	1.66	1.33	1.66	1.38
16	1.09	1.15	1.48	1.48	1.47	1.49	0.89	1.48	1.04
17	1.05	1.17	1.50	1.46	1.41	1.48	0.99	1.50	1.15
18	--	0.50	1.47	1.34	1.37	1.41	0.22	1.34	0.26
19	1.06	--	1.39	--	--	--	0.91	--	0.93
20	0.85	0.75	1.38	1.29	1.34	1.37	--	1.31	--
21	1.30	1.20	1.46	1.47	1.44	1.45	1.10	1.46	1.12
22	1.34	1.31	1.50	1.50	1.54	1.49	1.18	1.53	1.22
23	1.12	1.16	1.40	1.48	1.44	1.49	1.06	1.52	0.99
24	1.21	1.27	1.49	1.48	1.54	1.42	1.13	1.46	1.19
25	1.00	0.89	1.45	1.46	1.47	1.41	0.96	1.44	1.03
26	1.07	1.13	1.56	1.48	1.56	1.53	0.97	1.56	1.11
27	≤0.68	0.46	1.37	1.31	1.29	1.30	0.51	1.28	0.51
28	1.19	1.28	1.63	1.56	1.63	1.60	1.09	1.62	1.20
29	0.88	0.87	1.52	1.49	1.47	1.50	0.80	1.50	0.83
30	1.03	1.08	1.48	1.47	1.48	1.47	0.83	1.46	1.04
31	1.30	1.26	1.62	1.53	1.57	1.61	1.19	1.62	1.31
32	1.03	1.02	1.49	1.46	1.42	1.45	0.71	1.50	0.98
33	1.02	1.07	1.45	1.40	1.40	1.39	0.77	1.47	0.97
34	--	--	1.32	1.11	1.17	1.16	--	1.18	0.17
35	1.18	1.15	1.25	1.23	1.28	1.19	1.18	1.23	1.19
36	1.19	1.28	1.52	1.51	1.54	1.53	1.13	1.54	1.18
37	0.87	0.99	1.52	1.44	1.42	1.45	0.60	1.42	0.80
38	0.90	0.83	1.43	1.38	1.42	1.35	0.60	1.37	0.82
39	1.07	1.06	1.40	1.46	1.48	1.50	0.92	1.48	1.04
40	1.14	1.10	1.48	1.48	1.47	1.48	0.96	1.44	0.94
41	1.38	1.13	--	1.51	1.49	1.54	1.18	1.57	1.21
42	1.31	1.02	1.67	1.62	1.62	1.64	0.96	1.67	1.11
43	0.29	0.19	<0.82	1.25	0.57	<0.29	0.86	<0.26	≤0.23

Table 4 cont'd.

No.	81797	90432	90537	96833	98262	98430	104979	108381	124897
1	1.29	1.34	0.76	1.15	1.29	0.82	0.53	1.18	1.06
2	1.38	1.45	0.91	1.18	1.36	0.78	0.50	1.29	1.15
3	1.50	1.55	1.24	1.39	1.52	1.24	1.10	1.45	1.37
4	1.20	1.29	<0.48	0.64	1.06	0.30	<0.15	0.46	0.69
5	1.30	1.35	1.18	1.30	1.35	1.14	1.10	1.38	1.24
6	1.29	1.39	0.89	1.10:	1.34	0.81	0.45	1.20	1.15
7	1.33	1.37	0.94	1.21	1.35	0.87	0.63	1.24	1.20
8	1.33	1.35	1.24	1.37	1.37	1.23	1.30	1.38	1.33
9	1.37	1.40	0.88	1.20	1.28	0.93	≤0.25	1.24	1.17
10	1.52	1.57	1.25	1.41	1.52	1.20	0.93	1.41	1.41
11	1.48	1.56	1.12	1.26	1.42	1.10	0.69	1.37	1.29
12	1.59	1.58	1.23	1.43	1.54	1.24	1.12	1.49	1.49
13	1.65	1.67	1.32	1.48	1.60	1.31	1.29	1.49	1.55
14	1.06	1.16	0.49	0.64	0.94	≤0.38	--	0.74	0.72
15	1.66	1.67	1.31	1.49	1.65	1.35	1.23	1.51	1.50
16	1.50	1.45	1.14	1.31	1.41	--	0.61	1.36	1.28
17	1.48	1.51	1.10	1.32	1.41	1.06	0.85	1.38	1.36
18	1.30	1.49	0.60	0.80	1.33	0.62	--	1.01	0.97
19	--	--	1.02	1.20	1.28	1.02	--	--	1.25
20	1.34	1.38	0.69	--	1.26	0.68	≤0.42	1.20	1.07
21	1.54	1.50	1.09	1.27	1.42	1.13	0.91	1.37	1.33
22	1.50	1.52	1.13	1.30	1.47	1.30	1.09	1.41	--
23	1.52	1.50	1.09	1.29	1.46	1.11	0.82	1.38	--
24	1.47	1.45	1.16	1.30	1.42	1.20	1.07	1.38	1.35
25	1.41	1.45	1.04	1.23	1.41	1.06	0.74	1.33	1.30
26	1.54	1.57	1.10	1.32	1.56	1.24	0.83	1.42	1.40:
27	1.28	1.33	≤0.35	0.82	1.06	0.59	--	1.04	0.96
28	1.56	1.54	1.20	1.39	1.60	1.24	0.87	1.43	--
29	1.48	1.50	0.95	1.16	1.42	1.02	0.61	1.27	1.22
30	1.48	1.46	1.08	1.24	1.45	1.08	0.69	1.33	1.30
31	1.61	1.62	1.28	1.44	1.57	1.31	1.09	1.47	--
32	1.48	1.45	0.97	1.27	1.44	1.08	0.50	1.32	1.28
33	1.45	1.40	1.01	1.21	1.38	1.01	--	1.20	1.22
34	1.14	1.17	--	0.62	1.09	0.22	--	0.83	0.79
35	1.26	1.20	1.04	1.21	1.25	1.10	0.99	1.27	1.18
36	1.53	1.56	1.09	1.40	1.55	1.25	0.91	1.44	1.41:
37	1.34	1.41	0.96	1.19	1.42	0.99	0.69	1.29	1.28
38	1.37	1.39	0.85	1.15	1.35	1.00	0.59	1.21	1.14
39	1.45	1.45	0.96	1.29	1.43	1.05	0.84	1.23	1.29
40	1.52	1.47	1.11	1.28	1.46	1.18	0.80	1.34	--
41	1.57	1.57	1.15	1.35	1.51	1.26	0.94	1.42	--
42	1.57	1.68	1.15	1.34	1.58	1.17	0.60:	1.39	1.38
43	1.25	<0.38	<0.29	1.32	0.69	<0.00	<0.13	0.78:	≤-0.38

Table 4 cont'd.

No.	165341	168723	176670	186791	189319	196321	197989	200905	201091
1	--	0.73	1.28	1.32	1.33	1.36	0.63	1.44	0.98
2	0.16	0.79	1.25	1.40:	1.46	1.47	≤0.83	1.60	0.88
3	0.93	1.24	1.55	1.43	1.49	1.54	1.24	1.63	1.22
4	<-0.10	≤0.33	1.20	1.07	1.26	1.24	<0.10	1.28	≤0.52
5	0.86	1.17	1.22	1.38	1.30	1.30	1.20	1.48	0.55
6	0.37	0.86	1.14	1.34	1.38	1.36	≤0.83	1.49	0.94
7	0.66	0.68	1.30	1.38	1.40	1.39	0.95	1.50	0.96
8	1.02	1.23	1.45	1.42	1.31	1.34	1.26	1.51	0.86
9	0.56	0.71	1.35	1.35	1.40	1.40	0.83	1.54	1.04
10	0.93	1.15	1.51	1.48	1.55	1.54	1.21	1.63	1.34
11	0.68:	0.97	1.52	1.42	1.52	1.49	1.04	1.56	1.28
12	1.01	1.15	1.61	1.57	1.55	1.59	1.31	1.72	1.32
13	1.10	1.26	1.54	1.61	1.57	1.58	1.42	1.76	1.45
14	0.20:	0.21	1.08	0.96	1.23	1.12	--	1.20	0.68
15	1.07	1.27	1.54	1.66	1.64	1.67	1.35	1.79	1.42
16	0.55	--	1.40	1.44	1.51	1.48	1.25	1.59	1.23
17	0.76	1.01	1.44	1.39	1.54	1.50	1.04	1.59	1.30
18	--	--	0.98	1.29	--	1.38	0.48	1.53	0.51
19	0.67	0.91	1.40	1.51	1.41	1.39	1.07	1.51	1.09
20	0.27	0.52	1.29	1.42	1.38	1.37	0.61	1.50	0.82
21	0.80	1.10	1.47	1.55	1.49	1.49	1.17	1.64	1.20
22	1.03	1.18	1.50	1.55	1.54	1.47	1.25	1.65	1.25
23	0.79	0.96	1.45	1.50	1.51	1.51	1.09	1.55	1.19
24	0.82	1.12	1.47	1.54	1.45	1.47	1.19	1.60	1.14
25	0.65	0.71	1.36	1.47	1.46	1.41	1.10	1.59	1.07
26	0.64	1.05	1.51	1.54	1.56	1.52	1.11	1.62	1.27
27	≤-0.05	0.10	≤1.25	1.30	1.32	1.32	--	1.46	0.78
28	0.81	1.19	1.52	1.58	1.52	1.60	1.23	1.62	1.30
29	0.30	0.69	1.44	1.47	1.49	1.49	0.93	1.54	1.18
30	0.54	0.87	1.49	1.53	1.48	1.48	0.98	1.56	1.10
31	1.04	1.09	1.55	1.57	1.64	1.59	1.32	1.69	1.40
32	0.48	0.81	1.47	1.51	1.48	1.48	1.03	1.56	1.14
33	0.50	0.82	1.47	1.46	1.45	1.40	1.02	1.55	1.12
34	--	--	1.21	1.19	1.24	1.22	0.28	1.36	0.53
35	0.72	0.98	1.35	1.36	1.18	1.14	1.08	1.38	0.44
36	0.89	--	1.52	1.58	1.51	1.53	1.20	1.60	1.26
37	0.44	0.72	1.46	1.48	1.44	1.37	0.99	1.54	1.00
38	0.31	0.72	1.38	1.44	1.41	1.38	1.14	1.55	1.02
39	0.60	0.93	1.49	1.49	1.45	1.44	1.13	1.55	1.19
40	0.74	1.07	1.49	1.51	1.49	1.47	1.08	1.58	1.21
41	0.72:	1.04	1.54	1.56	1.61	1.55	1.23	1.61	1.25
42	0.47:	0.88	1.51	1.56	1.68	1.63	1.14	1.62	1.48
43	<-0.25	<-0.06	1.16	1.43	1.11	<0.49	<0.03	1.47	≤0.37

Table 4 cont'd.

No.	201092	201251	206778	219615	225212	(Sun)
1	1.06	1.39	1.27	0.43	1.41	-0.27
2	1.15	1.48	1.45	0.51	1.50	--
3	1.27	1.57	1.65	1.04	1.56	+0.53
4	0.47:	1.26	0.98	<0.10	1.18	<-0.35
5	0.66	1.42	1.45	1.17	1.46	+0.80
6	0.97	1.42	--	0.60	1.46	-0.16
7	1.07	1.42	1.43	0.58	1.47	-0.09
8	0.82	1.41	--	1.24	1.50	+0.94
9	1.07	1.46	1.43	0.55	1.48	-0.09
10	1.16	1.57	1.54	1.00	1.59	+0.41
11	1.19	1.49	1.49	0.60	1.53	+0.28
12	1.21	1.59	1.64	1.09	1.66	+0.71
13	1.26	1.66	1.70	1.17	1.66	+0.78
14	0.92	1.12	0.91	--	0.95	-0.32
15	1.40	1.73	1.75	1.19	1.73	+0.79
16	1.22	1.54	1.51	0.68	1.55	+0.05
17	1.23	1.53	1.52	0.76	1.51	+0.22
18	0.86	1.43	1.30	--	1.47	--
19	1.08	1.54	1.48	0.88	1.56	+0.26
20	1.00	1.44	1.34	0.34:	1.50	-0.46
21	1.17	1.64	1.55	1.02	1.65	+0.32
22	1.30	1.60	1.64	1.11	1.68	+0.66
23	1.22	1.57	1.50	0.86	1.58	+0.25
24	--	1.56	1.57	0.99	1.63	+0.56
25	1.12	1.56	1.51	0.85:	1.58	--
26	1.30	1.60	1.57	0.80	1.61	+0.24
27	0.90	1.43	--	0.41	1.45	--
28	1.28	1.67	1.66	1.06	1.71	+0.16
29	1.36	1.53	1.47	0.47	1.57	-0.44
30	1.15	1.55	--	0.68	--	-0.38
31	1.42	1.70	1.73	1.07	1.71	+0.51
32	1.16	1.53	1.54	0.73	1.60	-0.10
33	1.12	1.52	1.53	0.69	1.57	-0.06
34	0.75	1.31	1.17	--	1.30	--
35	0.41	1.41	1.44	1.02	1.47	+0.63
36	1.33	1.59	1.56	0.97	1.69	+0.30
37	1.12	1.52	1.54	0.58	1.60	-0.42
38	1.05	1.51	1.47	0.54	1.55	-0.34
39	1.21	1.54	1.55	0.76	1.61	0.00
40	1.24	1.56	1.53	0.80	1.41	+0.04
41	1.21	1.65	1.66	1.04	1.69	+0.19
42	1.52	1.64	1.73	0.76	1.73	-0.36
43	0.74	≤0.54	≤0.35	0.44	0.48	-0.26

III. THE REDUCTIONS

a) Theory

(i) Introduction: The Curve of Growth

In order to utilize the data in Table 4, a relation between the equivalent width of an absorption line and the number of atoms involved in its formation is needed. In the absence of detailed model atmospheres, the common procedure is to make use of one of the standardized curves of growth, which give this relation in terms of the physical conditions at a representative point in the atmosphere.

In computing curves of growth, two idealizations of the conditions in the atmosphere have been used frequently. In the Schuster-Schwarzschild model the atmosphere is represented as a layer in which line absorption only takes place, superimposed over a photosphere which radiates a pure continuum. From this model one may derive the number of atoms per unit area above the photosphere active in absorbing a line. In the Milne-Eddington model, the ratio of line to continuous absorption is taken as constant with optical depth. Here one may obtain the number of active atoms per gram of stellar material if the continuous opacity is known. The lines used in this analysis arise from low-excitation states which will not increase in population rapidly enough to compensate for the strong increase inward of the opacity which is to be expected in the stars studied here, but this effect is somewhat reduced by the fact that both the abundance of neutral atoms and the opacity are proportional to the electron pressure. Probably the S-S model is most appropriate, but since sets of similar lines are being compared here, it is not likely that the choice of models will have an appreciable effect on the results. Wright (1951b) found that for α Boötis no significant differences arose in the derived parameters when the data were treated by the two different models.

A very convenient tabulation of the curves of growth in the M-E approximation is provided by Wrubel (1949). These curves were calculated from Chandrasekhar's exact solution of the radiative transfer equation for this representation of the absorption coefficients; therefore the application of these curves suffers only from the inaccuracies inherent in the M-E model itself. Since these excellent tables are available, and in view of the discussion in the preceding paragraph, it was decided to make use of the M-E model for the present study.

Wrubel's curves of growth relate the two quantities log W/b and

log η_o. Here W is the equivalent width; b is the Doppler width given by

$$b = v\lambda/c \quad , \tag{1}$$

where v is the most probable velocity of the atoms and c the velocity of light; and η_o is the ratio of the "fictitious absorption coefficient" at the line center to the continuous opacity. This quantity is given by

$$\eta_o = N_{i,j} f \frac{\lambda}{K_\lambda} \frac{\sqrt{\pi}}{m} \frac{\varepsilon^2}{c^2} \frac{c}{v} \quad , \tag{2}$$

where

$N_{i,j}$ is the number of atoms per gram of stellar material in the excitation and ionization state which gives rise to the line,
f is the atomic oscillator strength,
K_λ is the continuous opacity in cm^2/gm of stellar material,
m is the mass of the electron, and
ε is the charge of the electron.

Upon introduction of the Boltzmann equation to give the distribution of atoms in the excited states, equation 2 becomes

$$\eta_o = \frac{\sqrt{\pi}\varepsilon^2}{mc^2} \frac{N_i}{B(T)} \frac{c}{v} \frac{g_j f \lambda}{K_\lambda} e^{-X_j/kT} \quad , \tag{3}$$

where

N_i is the number of atoms in the proper ionization state,
$B(T)$ is the partition function $\Sigma_j g_j e^{-X_j/kT}$,
g_j is the statistical weight of the jth level,
X_j is the excitation potential of the jth level,
k is the Boltzmann constant, and
T is the excitation temperature.

The curves of growth depend on two parameters. There is a different curve for every value of the quantity a, which is the ratio of the damping constant to the Doppler width; and for every value of the ratio B_o/B_1, which specifies the temperature gradient according to the approximation

$$B_\lambda(T) = B_o + B_1 \tau \quad , \tag{4}$$

where $B_\lambda(T)$ is the Planck intensity, and τ is the optical depth.

(ii) The Continuous Opacity

All of the stars studied here are sufficiently cool that the continuous opacity is due entirely to the negative hydrogen ion. This circumstance greatly simplifies much of the reduction procedure, as will become clear.

The absorption coefficient for H^- has been tabulated by Chandrasekhar and Breen (1946). It may be written

$$K_\lambda = \alpha_\lambda \phi(T) P_e X/M \quad , \tag{5}$$

where

α_λ is the absorption coefficient per H^- ion,
$\phi(T)$ is the ionization function for H^-,
P_e is the electron pressure,
X is the abundance of hydrogen by mass, and
M is the mass of the hydrogen atom.

The quantity $\alpha_\lambda \phi(T)$ is tabulated by Chandrasekhar and Breen. Stimulated emission is included in the factor α_λ so that this quantity is really a function of temperature also, but in the range of temperatures considered here stimulated emission can be neglected, and α_λ depends on λ only. Hence the ratio of the absorption coefficients for the same electron pressure and different temperatures depends only on the temperatures and is independent of wave length.

(iii) The Reduction Equations

(a) The empirical curve of growth.

By substituting equation 5 into equation 3, defining first

$$\alpha = \alpha_\lambda \phi(T) \quad , \tag{6}$$

one obtains

$$\eta_o = \sqrt{\pi}\, \frac{1}{X}\left(\frac{M}{m}\right)\left(\frac{\xi}{c}\right)^2 \frac{N_i}{B(T)}\, \frac{c}{v}\, \frac{gf\lambda}{\alpha P_e}\, e^{-X_j/kT} \quad . \tag{7}$$

Here the subscript j has been dropped from the statistical weight. Taking logarithms to the base 10 yields

(ii) The Continuous Opacity

All of the stars studied here are sufficiently cool that the continuous opacity is due entirely to the negative hydrogen ion. This circumstance greatly simplifies much of the reduction procedure, as will become clear.

The absorption coefficient for H^- has been tabulated by Chandrasekhar and Breen (1946). It may be written

$$(5) \qquad K_\lambda = a_\lambda \phi(T) P_e X/M \quad ,$$

where

a_λ is the absorption coefficient per H^- ion,
$\phi(T)$ is the ionization function for H^-,
P_e is the electron pressure,
X is the abundance of hydrogen by mass, and
M is the mass of the hydrogen atom.

The quantity $a_\lambda \phi(T)$ is tabulated by Chandrasekhar and Breen. Stimulated emission is included in the factor a_λ so that this quantity is really a function of temperature also, but in the range of temperatures considered here stimulated emission can be neglected, and a_λ depends on λ only. Hence the ratio of the absorption coefficients for the same electron pressure and different temperatures depends only on the temperatures and is independent of wave length.

(iii) The Reduction Equations

(a) The empirical curve of growth.

By substituting equation 5 into equation 3, defining first

$$(6) \qquad a = a_\lambda \phi(T) \quad ,$$

one obtains

$$(7) \qquad \eta_o = \sqrt{\pi}\, \frac{1}{X}\left(\frac{M}{m}\right)\left(\frac{\varepsilon}{c}\right)^2 \frac{N_i}{B(T)}\, \frac{c}{v}\, \frac{gf\lambda}{aP_e}\, e^{-X_j/kT} \quad .$$

Here the subscript j has been dropped from the statistical weight. Taking logarithms to the base 10 yields

$$(8)\qquad \log \eta_o = \log\left[\sqrt{\pi}\,\frac{1}{X}\,\frac{M}{m}\left(\frac{\varepsilon}{c}\right)^2\right] + \log N_i - \log B(T) + \log \frac{c}{v} + \log \frac{gf\lambda}{\alpha P_e} - \frac{5040}{T}\,E \quad ,$$

where E is the excitation potential expressed in electron-volts. The first term on the right contains only constants, with the exception of X, which may vary from star to star. This variation is probably small for the stars studied here, and will be neglected in what follows. This assumption is irrelevant to the principal results. The following definitions are adopted:

$$(9)\qquad \delta \equiv \sqrt{\pi}\,\frac{1}{X}\,\frac{M}{m}\left(\frac{\varepsilon}{c}\right)^2$$

$$(10)\qquad \theta \equiv \frac{5040}{T}$$

$$(11)\qquad R(\theta) \equiv \frac{\alpha(\lambda,\theta)}{\alpha(\lambda,1.4)} = \frac{\phi(\theta)}{\phi(1.4)} \quad .$$

Then equation 8 may be written in the form

$$(12)\qquad \log \eta_o = \log \delta + \log N_i - \log B(\theta) + \log \frac{c}{v} + \log \frac{gf\lambda}{\alpha(1.4)R(\theta)P_e} - \theta E \quad .$$

Let it be hereafter understood that the symbol α refers to the case $\theta = 1.4$ and is a function only of wave length.

For the lines of V I, the relative oscillator strengths have been measured by King (1947), but no absolute values of f are available. Writing the relative values as f', the calibration constant C may be defined such that

$$(13)\qquad f = Cf' \quad .$$

Then it is convenient to make the further definition

$$(14)\qquad \log \eta_o' \equiv \log \frac{gf'\lambda(A)}{\alpha \times 10^{25}} = \log\left[\frac{gf'\lambda(cm)}{\alpha} \times \frac{10^8}{10^{25}}\right] = \log \frac{gf'\lambda}{\alpha} - 17 \quad .$$

Inserting this definition into equation 12 yields

$$(15)\qquad \log \eta_o = \log N_i - \log B(\theta) + \log \frac{c}{v} + \log \eta_o' - \theta E + \log \frac{\delta C}{RP_e} + 17 \quad .$$

Now since α is a function only of wave length, it is possible to compute the quantity $\log \eta_o'$ for each line for which King has determined an f', and this value will apply to all the stars. This has been done using the gf' values in Table 2, and $\log \eta_o'$ is given in the fifth column of Table 4.

It is useful to define further

(16) $$\log \eta_o'' \equiv \log \eta_o' - \theta E \quad ,$$

and write

(17) $$\log \eta_o = \log N_i - \log B(\theta) + \log \frac{c}{v} + \log \eta_o'' + \log \frac{\delta C}{RP_e} + 17 \quad .$$

Now since the curve of growth specifies the relation between the quantity W/b and η_o, it is clear from equations 1 and 17 that for a given ion in a star a similar relation exists between W/λ and η_o''. This latter relation will be called the "empirical curve of growth."

Since two lines of the same W/λ must have the same η_o'', then if they have different excitation potentials they must have different values of η_o'. According to equation 16 from the difference of their log η_o' values and of their excitation potentials, θ may be deduced. Using this value log η_o'' can be computed for each line, and the empirical curve of growth for the ion can be plotted.

It should be noticed that for lines originating in the ground state of an ion, log η_o'' = log η_o'. Thus the curve of growth relating log W/λ and log η_o'' may be regarded as a curve of growth for lines from the ground state. The value of θ then is merely a parameter to reduce the separate curves of growth for the various excited states to a single curve for the ground state.

(b) Relative abundances.

The curves of growth for two similar ions do not differ significantly, except possibly in the region strongly affected by the damping constant a. Thus if fairly weak lines are used, the relative abundance of two ions can be determined if an empirical curve of growth can be determined. Specifically, for this investigation the relative abundance of Li I to V I is of interest. The photometric results listed in Table 4 permit the construction of an empirical curve of growth for VI. Given the value of log W/b for a single line of Li I, the corresponding log η_o will be the same as that for a V I line of the same log W/b. Hence from equation 17 there is a definite log η_o'' on the V I curve of growth corresponding to the strength of this Li I line. Equation 12 may be used to represent the log η_o of the Li I line, and equation 17 to represent the log η_o of the V I line with the same log W/b. Equating the right sides of these expressions, and using the symbols Li^o and V^o to represent the numbers per gram of Li I and V I

($\underline{Li}^+$ and $\underline{V}^+$ would be used for the singly ionized states and $\underline{Li}$ and $\underline{V}$ for the total of all states), one obtains

$$\log Li^\circ - \log B(Li\ I) + \log \frac{c}{v} + \log \frac{gf\lambda}{\alpha} - \theta E + \log \frac{\delta}{RP_e}$$

$$= \log V^\circ - \log B(V\ I) + \log \frac{c}{v} + \log \eta_o'' + \log \frac{\delta C}{RP_e} + 17 \quad ;$$

(18)
$$\log \frac{Li^\circ}{V^\circ} = \log \eta_o'' + \log \frac{B(Li\ I)}{B(V\ I)} - \log \frac{c/v(Li)}{c/v(V)}$$

$$- \log \frac{gf\lambda}{\alpha} + \theta E + \log C + 17 \quad .$$

Here $\log \eta_o''$ may be read from the empirical curve of growth for V I using the equivalent width for Li I (corrected for the difference in thermal velocities of the two atoms); the partition functions can be calculated from a spectroscopic term table; the values of $\underline{c/v}$ can be obtained by a comparison of the empirical and theoretical curves of growth as described below; and the value of $\underline{E}$ for the Li I line is zero. The remaining terms which are constants, may be left unevaluated if only the variation of the $\underline{Li/V}$ abundance ratio from star to star is of interest, or may be determined from theory and labroatory experiment.

This last equation shows how the investigation is simplified by the use of relative abundances. The ratio of neutral atoms is seen to be independent of the electron pressure, the temperature-dependent part of the continuous opacity, and the abundance of hydrogen. To determine the variation of the ratio, neither the absolute $\underline{gf}$ value for the lithium lines nor the calibration of the vanadium $\underline{f'}$ values need be known.

(c) The relation between the empirical and theoretical curves of growth.

It is necessary to find the theoretical curve of growth which best represents the empirical curve for at least two reasons: to obtain the most probable velocity of the atoms $\underline{v}$, and to extrapolate the empirical curve when the Li I line is weaker than the weakest V I line. Other interesting information about the stellar atmosphere will also be revealed by the theoretical curve.

In order to find the proper theoretical curve, it is first necessary to consider the temperature gradient parameter $\underline{B_o/B_1}$. This ratio can be computed from the relation (Aller 1953, p. 294)

(19)
$$\frac{B_o}{B_1} = \frac{8}{3} \frac{K_\lambda}{\bar{K}} \frac{1-e^{-u}}{u} \quad ,$$

where $\bar{K}$ is the mean opacity, and $u = hc/\lambda kT$, h being Planck's constant. Thus B_o/B_1 depends both on the temperature and the wave length, and is different for every line in every star. For maximum precision, B_o/B_1 should be computed for each line and the value of log η_o'' for each line corrected by means of tables given by Wrubel, so that the final curve of growth can be represented by a single value of the parameter. To follow such a procedure would add much labor to the reductions. It was found sufficiently accurate to determine the median value of B_o/B_1 for the V I lines used, and apply the curves of growth for values of this parameter nearest the median value.

The damping constant affects both the slope of the curve of growth in the central ("transition") region and the position of the curve in the strong-line ("square-root") region. For high damping, the slope in the central region becomes large and the extent of the region in log η_o is reduced. Thus the stronger lines of the empirical curve of growth will permit an estimate of a, given theoretical curves of growth for different values of a. If the strongest V I lines are too weak to determine a, then this parameter is irrelevant to this analysis because no stronger lines than these are used. The damping constant is related to both the properties of the atomic states and the pressure in the atmosphere, but no discussion of the derived values is attempted in this study.

A convenient way of fitting the theoretical curve of growth to the empirical one is to plot the former on transparent paper and slide it vertically and horizontally over the latter until the best agreement is obtained. With a sufficient number of V I lines having a sufficient range in log η_o'', an accurate fit is possible. Then, for a line of given strength, both log W/λ and log W/b can be read from the scales. According to equation 1 the most probable velocity follows from

$$\log \frac{c}{v} = \log \frac{W}{b} - \log \frac{W}{\lambda} \quad . \tag{20}$$

The velocity v so deduced represents all motions which affect the equivalent width of a line; that is, all motions whose mean free path is of the order of the mean free path of a photon, or less. In general, then v arises from both thermal motion and microturbulence, so that

$$v^2 = v_e^2 + v_t^2 \quad , \tag{21}$$

where

(22) $$v_\theta^2 = \frac{2kT}{MA} \quad ;$$

here M is the mass of the hydrogen atom, as before, and A is the atomic weight of the element in question. In practice the thermal velocity v_θ is computed from equation 22 using for the temperature that derived from θ in equation 16, and then the turbulent velocity v_t is obtained from equation 21. This latter quantity is the same for all atoms.

From the fit of the theoretical to the empirical curve the difference between log η_o and log η_o'' is determined. Equation 17 indicates that the absolute abundance of V I can be expressed as

(23) $$\log V^\circ = \log \eta_o - \log \eta_o'' + B(\theta) - \log \frac{c}{v} - \log \frac{\delta C}{RP_e} - 17 \quad .$$

Thus if the electron pressure, the calibration constant C, and the abundance of hydrogen which enters δ can be obtained, the absolute abundance of V I can be calculated. Lacking these, another quantity of interest may be defined:

(24) $$\log \gamma^\circ \equiv \log \frac{V^\circ \delta C}{RP_e} + 17 = \log \eta_o - \log \eta_o'' + \log B(\theta) - \log \frac{c}{v} \quad .$$

This quantity is a numerical representation of the absolute strength of the V I lines, and is proportional to what would be known in the Schuster-Schwarzschild model as "the number of V I ions per square centimeter above the photosphere." It can be readily calculated.

(d) The ionization of vanadium.

As was mentioned in the preceding chapter, no lines of ionized vanadium are found in the spectral region covered in these observations. It is therefore necessary to deduce the ionization of vanadium from that of another element. Scandium is convenient for this purpose. Having obtained equivalent widths for lines of both Sc I and Sc II, one can express the abundances of these ions relative to V I by equations similar to equation 18. Then, subtraction of the equation for Sc I from that for Sc II gives

(25) $$\log \frac{Sc^+}{Sc^\circ} = \log \eta_o''(Sc\ II) - \log \eta_o''(Sc\ I) + \log \frac{B(Sc\ II)}{B(Sc\ I)} - \log \frac{gf\lambda}{\alpha}(Sc\ II) + \log \frac{gf\lambda}{\alpha}(Sc\ I) + \theta\left[E(Sc\ II) - E(Sc\ I)\right] \quad .$$

This equation applies directly to the comparison of one Sc II line with one Sc I line. However, it will also apply to the average log η_o'' values and

the average $gf\lambda/\alpha$ values for a number of lines after correction for differences in E. Actually, for the lines used in both ions except for one multiplet of Sc I, the E-values are nearly the same; thus if we correct the log η_o''-values for these latter lines to the E's for the others, then the last term in equation 25 may be dropped. Expressing the difference in the mean values of log $gf\lambda/\alpha$ in the sense ionized minus neutral as Δ, and the difference of the mean values of log η_o'' in the same sense as $\Delta\log \eta_o$ (since differences are the same in both log η_o and log η_o''), equation 25 may be written

$$(25a) \qquad \log \frac{Sc^+}{Sc^o} = \Delta\log \eta_o + \log \frac{B(Sc\ II)}{B(Sc\ I)} - \Delta \ .$$

The logarithmic form of the Saha ionization equation is

$$(26) \qquad \log \frac{N_{i+1}}{N_i} = -\theta I + 2.5 \log T - 0.48 + \log \frac{2B_{i+1}(T)}{B_i(T)} - \log P_e \ .$$

Here θ is defined as before, T is the corresponding ionization temperature, and I is the ionization potential of the lower state (in ev). Applying equation 26 to the neutral and the singly ionized states of both scandium and vanadium, and subtracting the equation for scandium from that for vanadium, one obtains

$$(27) \qquad \log \frac{V^+}{V^o} - \log \frac{Sc^+}{Sc^o} = -\theta\left[I(V\ I) - I(Sc\ I)\right] + \log \frac{B(V\ II)}{B(V\ I)} - \log \frac{B(Sc\ II)}{B(Sc\ I)} \ .$$

Now the ionization potentials of Sc I and V I are equal; therefore the first term above vanishes, and equation 27 may be added to equation 25a to give

$$(28) \qquad \log \frac{V^+}{V^o} = \Delta\log \eta_o + \log \frac{B(V\ II)}{B(V\ I)} - \Delta \ .$$

Thus if Δ can be determined, equation 28 will permit the direct determination of the ionization of vanadium from the measurements of the scandium lines. Unfortunately no laboratory or accurate theoretical determinations of the oscillator strengths f have been made for scandium. Several investigators have estimated these values in determining abundances in the sun. For the present study, the value of Δ will be obtained by applying both equation 28 and equation 25a to the sun, using measured values of $\Delta\log \eta_o$ and published values of the abundances of the ions.

Since the second ionization of vanadium can be neglected in all the stars studied here, the total abundance of vanadium is the sum of the neutral and singly-ionized states. Then

$$\frac{V}{V^o} = 1 + \frac{V^+}{V^o} \quad . \tag{29}$$

A quantity γ may be obtained, given by

$$\gamma = \gamma^o\left(\frac{V}{V^o}\right) \quad , \tag{30}$$

which is proportional to the total abundance of vanadium divided by the continuous opacity. This may be used to test the necessary assumptions concerning these quantities.

Equation 26 may now be inverted to calculate the electron pressure from the known ionization of vanadium:

$$\log P_e = -6.71e + 2.5 \log T - 0.18 + \log \frac{B(V\ II)}{B(V\ I)} - \log \frac{V^+}{V^o} \quad . \tag{31}$$

Here the numerical value of the ionization potential has been inserted.

It should be mentioned that investigations of stellar atmospheres have generally shown that the same temperature cannot be used to express both the ionization and the excitation equilibria. Thus the temperature used in equation 31 should not be the one derived from equation 16. Fortunately, the ionization temperature drops out of equation 27, so that it does not affect the determination of the ionization state of vanadium. However, it is probably also true that the excitation temperatures of Sc II and Sc I are not exactly equal, so that the dropping of the last term of equation 25 is not fully justified. But since the constant used in the ionization determination is derived assuming the equality of the temperatures, the errors introduced by this approximation are minimized.

(e) The ratio of total abundances, Li/V.

An application of the ionization equation for vanadium to the sun showed that the second ionization of this element is negligible there. Since the degree of ionization is approximately as great in the sun as in any star studied here, the ionization of V II can be neglected throughout the investigation. The ionization potential of this ion is 14 ev. Since the ionization potential of Li II is 75 ev, there is certainly no second ionization of this element. Therefore the ratio of the total abundances

may be written

$$(32) \qquad \frac{Li}{V} = \frac{Li^{o}+Li^{+}}{V^{o}+V^{+}} = \left(\frac{Li^{o}}{V^{o}}\right)\frac{1 + Li^{+}/Li^{o}}{1 + V^{+}/V^{o}} = \left(\frac{Li^{o}}{V^{o}}\right)\left(\frac{V^{o}}{V^{+}} + \frac{Li^{+}/Li^{o}}{V^{+}/V^{o}}\right)/\left(\frac{V^{o}}{V^{+}} + 1\right) \quad .$$

In this equation the factor $\underline{Li}^{o}/\underline{V}^{o}$ is obtained from equation 18. Let the coefficient of this quantity in the final form in equation 32 be called $\underline{\beta}$. The first term in the numerator and denominator of $\underline{\beta}$ is obtained from equation 28. The second term in the numerator follows from an expression similar to equation 27:

$$(33) \qquad \log \frac{Li^{+}/Li^{o}}{V^{+}/V^{o}} = -\underline{\theta}\left[I(Li\ I) - I(V\ I)\right] + \log \frac{B(Li\ II)}{B(Li\ I)} - \log \frac{B(V\ II)}{B(V\ I)} \quad .$$

Here a value of $\underline{\theta}$ must be estimated. However, the result is not extremely sensitive to this value, because the ionization potentials of the two ions differ by only 1.34 ev. Thus $\underline{\beta}$ may be calculated from equations 28 and 33, and the total abundance ratio obtained from

$$(32a) \qquad \frac{Li}{V} = \frac{Li^{o}}{V^{o}}\,\beta \quad .$$

(iv) The Curve of Growth for the Li I Doublet

In the discussion of sub-section (iii), it was assumed that the equivalent width of a single line of Li I could be obtained. However, the two lines of the resonance doublet, which are the only lines available, are completely blended at the dispersion used here. Special consideration must therefore be given to how the equivalent width of this blended feature may be related to the curve of growth for the V I lines.

It is essential to determine the source of the blending of the lines. The blending may be caused primarily by the spectrograph or by large-scale turbulence in the stellar atmosphere, the absorption coefficients remaining separate; or the absorption coefficients themselves may be blended. In the former case the absorptions add and the feature may be treated as the sum of two lines; in the latter the feature must be considered as a single line formed by an oddly-shaped absorption coefficient. The V I curve of growth would not apply directly in either case.

If the lines are weak, the equivalent width is proportional to the "fictitious absorption coefficient;" therefore it is irrelevant which of these two cases apply. It is only when the total equivalent width is sufficient to place the feature above the linear part of the curve of growth

that a distinction must be made.

It is instructive to determine the degree of blending of the absorption coefficients in two extreme cases. In HD 62345 (K Gem), the temperature and the microturbulence are both high, and the blending should be a maximum. Computing the thermal velocities v_θ for both lithium and vanadium from equation 22 using the excitation temperature, and obtaining the total velocity of the vanadium atoms from the curve of growth, the total velocity of the lithium atoms is found to be 5.5 km/sec. Taking the profile of the absorption coefficient for lithium to be determined by the velocities and Gaussian in shape, its half half-width is found to be o.10 A. Thus, since the separation of the two line centers is only 0.15 A, it would seem that there is in this case significant blending of the absorption coefficients. In HD 29139 (α Tau), the temperature and microturbulence are both low. Proceeding as above, the total velocity of the lithium atoms is found to be 3.1 km/sec, which yields a half half-width for the absorption coefficient of 0.058 A, only about one-third of the separation of the line centers. Here clearly the blending is much less. In the parts of the lines in which blending does occur, the total absorption coefficient is still probably small enough that the resultant absorption is the sum of the absorptions of the lines taken separately.

The present analysis is considerably simplified by the fact that strong Li I lines occur only in cool stars. In stars in which the temperature and turbulence are sufficiently high to cause significant blending of the absorption coefficients, the continuous opacity and the ionization of lithium are also sufficiently high to make the total absorption quite small. Nevertheless in all cases in which the doublet was strong enough for the two types of blending to produce different results, the analysis was carried out using two different approximations:

(a) The absorption coefficients are significantly, but not completely, blended. It is assumed that the profile of the total absorption coefficient remains Gaussian, and that its maximum height equals that of the stronger line of the pair, but that its width increases sufficiently to account for the total area under the absorption-coefficient curves of both lines. Thus the effect of the blend is to increase the width of the absorption coefficient, which is equivalent to an increase in the velocity of the atoms. In the analysis

the most probable velocity for the lithium atoms, derived as in the preceding paragraph, was increased by a factor 3/2 to account for the necessary increase in the absorption coefficient width, and this increased velocity was combined with the equivalent width of the whole feature to yield the proper W/b to apply to the curve of growth. This approximation certainly overestimates the effect of blending in the cooler stars by a considerable amount.

(b) The absorption coefficients are unblended. Since the effect of saturation will not be the same for the two lines of the doublet, their equivalent widths will not be in the 1:2 ratio that applies to the absorption coefficients. The following procedure was adopted: (1) the most probable velocity was determined as in the examples of the preceding paragraph; (2) this was applied to the total equivalent width to produce a total W/b; then (3) from the curve of growth two values of log η_o'' were found which differed by log 2 and gave values of W/b which added to the total W/b obtained in (2). The sum of the deduced values of η_o'' was applied to equation 18.

From the foregoing discussion it would appear that in those stars in which these two methods give different answers, method (b) would be much closer to the truth. The result from method (a) would provide an estimate of the maximum possible error from this source.

b) Procedure

In the preceding section the theoretical basis for the abundance determinations was discussed and the equations to be used in the reductions were derived. The present section will describe in detail the procedures followed, and discuss the errors inherent in each step.

(i) The Excitation Temperature

The determination of the excitation temperature, which is the only actual determination of temperature made in this analysis, is based on equation 16 and the unique relation of the value of log η_o'' to the equivalent width expressed by equation 17. As was pointed out in the discussion of these equations, two lines of the same equivalent width would have the same log η_o''; therefore the differences of their log η_o' values and excitation potentials would yield an estimate of θ. This is in principle the method

that was adopted. From the list of the V I lines in Table 2, it is seen that the lines of multiplets 34, 35, 36, and 37 have similar excitation potentials, averaging approximately 1.06 ev. The lines of multiplets 19 and 20 also have a very small range in E, averaging near 0.28 ev. The procedure followed was this:

(a) A plot was made on translucent paper of log W/λ vs. log η_o' for each group of lines separately.

(b) These two plots were superimposed with their log W/λ scales coincident, and were moved relative to each other in log η_o' until a continuous curve could be drawn to represent the combined set of points. No reference was made to the theoretical curve of growth. The ranges of strength of the lines in the two groups were always quite similar, so that the two plots overlapped for nearly all of their lengths, and it was never necessary to fit them "end-to-end."

(c) The difference of the two log η_o' scales with the points thus superimposed was noted, and was divided by the difference of the mean excitation potentials to yield the value of θ.

(d) The value of log η_o'' was computed for each line according to equation 16 using the excitation potential for that line (not the mean), and a plot was made of log W/λ vs. log η_o'' using all the V I lines in these six multiplets. This plot was inspected to detect any asymmetry in the distribution of the points from the two groups of multiplets which could have been caused by an error in θ. If such an asymmetry was found, the analysis was repeated. The success achieved in eliminating such effects may be estimated by inspecting the samples shown in Figure 6.

The accuracy of the determination with respect to internal errors was estimated in step (b). Not only was the best fit determined, but the amount that the plots could be displaced relative to each other without introducing obvious asymmetry was also noted. These displacements lead to a value 0.12 as an estimate of the mean probable error in θ, averaged over all the stars. Errors are less in the hotter stars and greater in the cooler ones.

The errors were produced not only by the errors in the photometry of the lines, but also by apparent small errors in the gf' values used. Certain groupings of points were seen through all the stars, indicating that either

the gf' values were in error, or that unsuspected blends persisted. However, some of these groupings fell below the mean curve on the plots, making the first alternative seem more likely. These effects were quite small. As the V I lines grew stronger in the cooler stars, the point was reached where they were all on the central part of the curve of growth, and little slope remained in the plots. The fitting of the two groups then became more uncertain. Nevertheless it is not likely that the probable error of θ exceeds 0.20. In the coolest stars, there appeared an apparent difference in slope between the plots from the two groups of lines. The reason for this is not clear, but it made the determination of θ quite difficult. The increase of this effect with decreasing temperature, as well as the appearance of a new blending feature near the Li I doublet (see Chapter II, section f), led to the decision not to consider stars cooler than type M0 in this study.

(ii) The Temperature Gradient

It was pointed out in sub-section (iii) of section a) that a value of the temperature gradient parameter B_0/B_1 must be computed in order to select the appropriate theoretical curve of growth to compare with the observations. This quantity was computed according to equation 19 (repeated here for convenience),

$$\frac{B_0}{B_1} = \frac{8}{3}\frac{K_\lambda}{\overline{K}}\frac{1-e^{-u}}{u} \quad , \tag{19}$$

using the tables of the H^- absorption coefficient given by Chandrasekhar and Breen (1946) and the values of the mean opacity computed by Chandrasekhar and Münch (1946). Since both of these quantities are proportional to the electron pressure, their ratio is independent of it. Thus for a given wave length, B_0/B_1 is a function of temperature only.

In order to test the necessity of correcting each value of log η_0'' to that appropriate to a single value of B_0/B_1, this was done in one case (HD 206778, ε Peg). The results were compared with those obtained by applying one of Wrubel's curves directly to the empirical curve of growth with uncorrected log η_0'' values. The theoretical curve was chosen so that its value of B_0/B_1 agreed as closely as possible with the median value computed for the V I lines. No significant differences were found.

Values of B_0/B_1 were computed for a number of temperatures which

covered the range of excitation temperatures encountered in the stars studied, and for the wave lengths λ5600 and λ6300. These wave lengths defined the range covered by the V I lines. The values of B_o/B_1 so derived were plotted as a function of θ. The curves showed that the range of values of the parameter in any star of interest did not exceed 0.10. It seemed likely that the result for HD 206778 would then hold for all the stars. It was further found that the median value (the average of the two computed extreme values at a given θ) remained in the range 0.33 and 0.60. Hence it was decided to use the excitation temperature of each star to enter these curves of B_o/B_1 to obtain a median value, reduce the data separately with the curves of growth given by Wrubel for the values 1/3 and 2/3, and then to interpolate roughly between the results. In practice, no significant difference appeared between the results from the two curves.

It should be stated that it was necessary to extrapolate the mean opacities of Chandrasekhar and Münch to higher values of θ. While this introduces uncertainty into the derived values of B_o/B_1, the insensitivity of the results to this parameter makes the uncertainty of no consequence.

(iii) Fitting the Theoretical Curve of Growth

The theoretical curves of growth computed by Wrubel for B_o/B_1 equal to 1/3 and 2/3 were plotted on semi-transparent paper, using all values of the damping constant given by him. Following Wrubel, all the curves for a single value of the temperature gradient parameter were plotted together.

The plot of W/λ vs. log η_o'' made in sub-section (i), which is the empirical curve of growth, was always plotted to the same scale as the plots of the theoretical curves. One of the sets of theoretical curves was superimposed upon the empirical points and translated in both co-ordinates until the best representation of the points by the curve was achieved. The appropriate value of the damping constant was also chosen in the process, using the slope of the central part of the curve of growth in most cases, and also the position of the beginning of the "square-root" branch where possible. The differences in the two co-ordinates of the empirical and theoretical relations were noted. The procedure was then repeated using the other set of theoretical curves. This whole process was then repeated at least twice, so that at least three sets of co-ordinate differences were obtained for each value of the temperature gradient parameter. If the scatter was large

in these values, more attempts at fitting were made. Although some effort was exerted to make each fitting process as independent as possible, it is certain that each attempt was influenced by the previous one. However, on several occasions a second attempt at fitting the curves was made several days after the first one, and good agreement was obtained.

The range in values of log η_o'' was in all cases sufficient to permit a fairly well-determined fit of the curves. Even when the lines were essentially all on the transition part of the theoretical curve, the observations covered the entire region so that relatively little uncertainty remained. For the hottest stars the vertical fit was somewhat uncertain. This has a relatively small effect on the results, since both the vanadium and lithium lines are similarly affected. Nevertheless it was always possible to determine a satisfactory value, except in the case of the sun. Here the value of the microturbulence given by Minnaert (1953) was adopted, and the thermal velocity was computed from the excitation temperature; the combined velocities were used to fix the vertical fit of the curve of growth. Estimates of the probable errors of the fitting constants averaged over all the stars would be 0.04 in log c/ν, and 0.06 in log η_o'' - log η_o. The errors in the first quantity are larger for the hotter stars; in the second, the errors are larger in the cooler ones.

Further indication of the accuracy of the fitting process can be obtained from the agreement of the independent analyses of the two spectrograms of HD 9270. The difference in the two values of log c/ν was 0.05, and the two values of log η_o'' - log η_o agreed to the second decimal place, which was the accuracy to which the computations were carried. The spectral type of this star is G8 III, so that the V I lines are just below the "knee" of the curve of growth.

Figure 6 presents three sample cases of the adopted fit of the theoretical to the empirical curve of growth. The values of log W/λ are plotted against log η_o'' for three stars--HD 9270, 6805, and 189319--of spectral types G8 III, K2 III, and K5 III (respectively). These stars indicate the variety of fits that had to be made. The adopted theoretical curve of growth is also drawn in for the case $B_o/B_1 = 1/3$. The necessity of using a theoretical curve for extrapolation to weak lines is obvious in the two cooler stars. It might be thought that the fit in the log η_o co-ordinate is extremely uncertain in the cool stars. However, the slope of the central

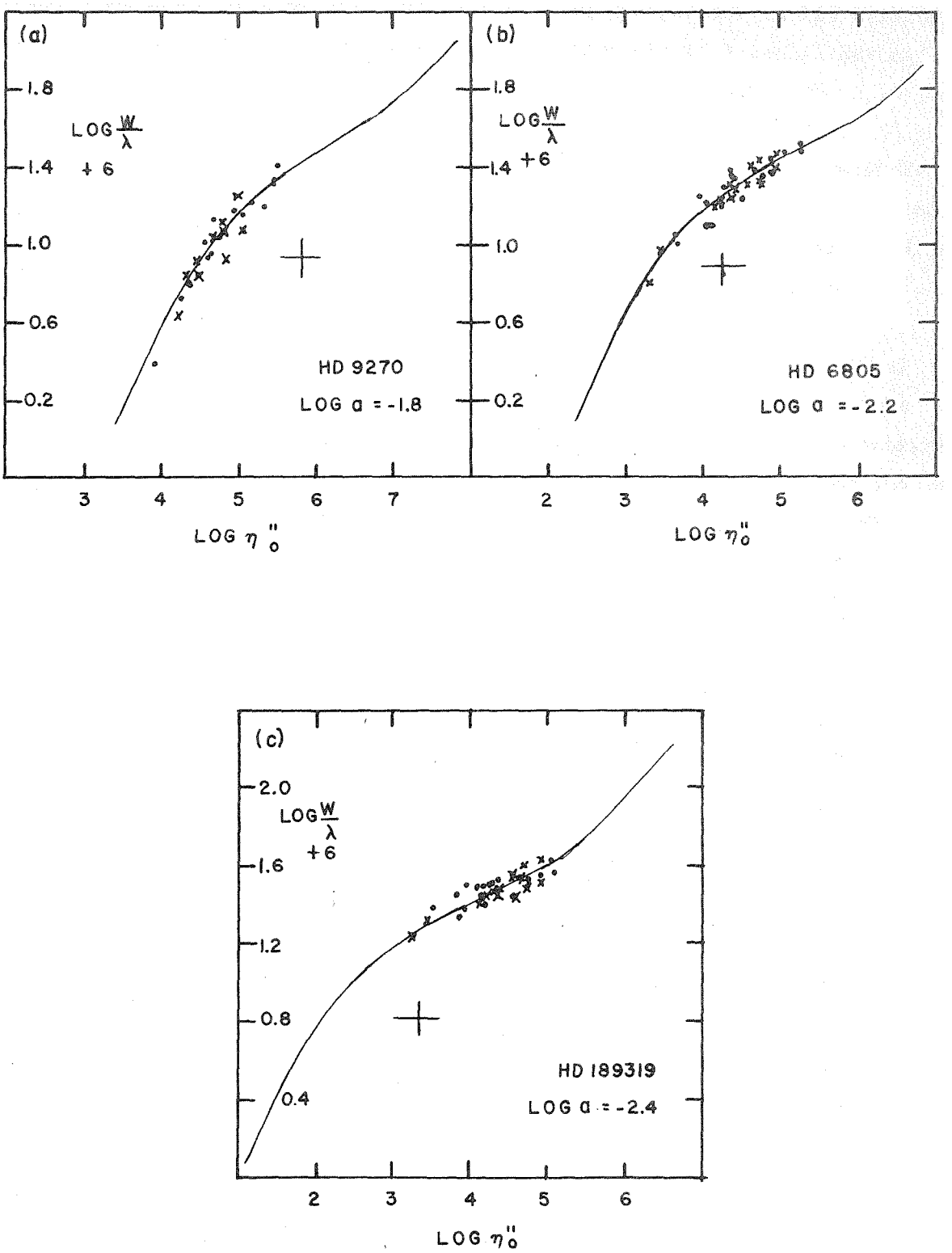

Figure 6. Empirical curves of growth (points) and adopted theoretical curves of growth for $B_0/B_1 = 1/3$. Dots indicate 1.1 ev lines; crosses, 0.3 ev lines. Spectral classes: (a) G8III, (b) K2III, and (c) K5III. Large crosses indicate the point log $W/b = 0$, log $\eta_0 = 1.5$.

region of the curve of growth is strongly affected by the damping constant; therefore the appropriate value of this quantity could be chosen with sufficient accuracy to eliminate uncertainties in the horizontal fit arising from the position of the beginning of the "square-root" branch. Having chosen a, the fit to the data could be done to within about 0.15 in log η_o in the coolest stars.

It is worth repeating at this point that the applicability of Wrubel's curves of growth to these data is assumed, and certainly cannot be tested by the limited information available here. More detailed discussions of the spectra of individual stars must be made to provide definitive tests of this assumption.

Having found the relation between the empirical and theoretical curves of growth for an individual star, no further use was made of the empirical plot. Values of log η_o'' for other lines were derived by obtaining values of log W/b, applying them to the two theoretical curves (for the two values of the temperature gradient parameter) and reading off the corresponding values of log η_o; these were then converted to log η_o'' by the known differences between these quantities. The adopted value of log η_o'' for a line was derived by interpolating between the two values from the two curves of growth, roughly linearly according to the position of the derived median B_o/B_1 with respect to 1/3 and 2/3. As was stated before, the two values were rarely significantly different. The use of both curves helped to reduce accidental errors.

The quantity Υ^o was derived from the fitting constants of the curves of growth according to equation 24, repeated here for reference.

$$(24) \qquad \log \gamma^o = \log \eta_o - \log \eta_o'' + \log B(V\,I) - \log \frac{c}{v} \quad .$$

Υ^o is proportional to the abundance of neutral vanadium divided by the continuous opacity. The values applied to equation 24 were interpolated between those derived from the two curves, and the partition function was obtained as discussed below.

In one case, the adopted theoretical curves of growth were used to determine the value of log η_o' listed in Table 4. The V I line λ5706.973 was found in the analyses of the hot stars--which were done first--to fall consistently above the mean empirical curve of growth. This line is one of the strongest used, and it was clear that in the cooler stars it would be

needed to help determine the damping constant. Therefore a new value of log η_o' was determined for this star from the stellar data. Using the equivalent widths and adopted theoretical curves of growth for eleven G8 and K0 stars and two cooler stars, values of log η_o' were determined using the general procedure described in this section in reverse--proceeding from W to log η_o by the theoretical curve, obtaining log η_o'' from the fit, and then log η_o' from the temperature. The mean value of this latter quantity derived from these stars differed from the value computed from the laboratory gf' by more than ten times its probable error. The derived value was therefore adopted and used in the cool stars. No indications of further changes were noted. The deviation from the laboratory value may have been caused by blending, but if so, the blend was sufficiently constant throughout the stars to permit use of the total equivalent width.

(iv) The Partition Functions

Nothing has been said heretofore about the computation of the partition functions, beyond stating their definition subsequent to equation 3. Since these quantities enter into all the reduction equations, their calculation should be discussed.

For convenience, the definition of the partition function is repeated here:

$$B(T) = \Sigma_j g_j e^{-X_j/kT} \quad .$$

In principle, there is no reason to suppose that the series converges, but in practice the statistical weights of g_j of the highest energy levels must vanish because of the effect of collisions with other particles.

Claas (1951) made extensive computations of B(T) for various ions in the sun. He took into account the effects of collisions in considerable detail, and found that for levels whose effective principal quantum number (computed from the level energy and effective nuclear charge by the hydrogenic formula) is greater than six, the effects of collisions are significant. He also found that in the outer layers of the solar atmosphere the temperature is sufficiently low that these levels do not affect the partition function. This will clearly also be the case in the cooler stars considered in this study. Thus in calculating the partition functions, no particular account was taken of the effect of collisions except to cut off the summa-

tion after including all levels whose effective principal quantum number is less than seven.

The date used in the calculations were taken from Atomic Energy Levels, Vol. 1 (Moore 1949). Following a method similar to that of Claas, the contributions of all levels were added explicitly for those terms whose mean energy was less than 1.5 electron-volts. For terms with excitation energy greater than this but less than 3.0 ev, the exponential was computed using the mean term energy and multiplied by the total statistical weight for the term. For the higher terms, all levels in a 1-ev energy range were considered together; the exponential was computed from the energy at the center of the range, and multiplied by the total statistical weight of the levels included. The computations were carried out at temperatures of 2500°, 4000°, and 5000° for the ions Li I, Li II, V I, and V II. The results are given in Table 5, below.

Table 5

Partition Functions, log B(T)

T	V I	V II	Li I	Li II	θ
5000	1.638	1.634	0.320	0.000	1.01
4000	1.565	1.572	0.308	0.000	1.26
3000	1.489	1.503	0.301	0.000	1.68
2500	1.443	1.462	0.301	0.000	2.01

These values of log B(T) were plotted as a function of θ, and smooth curves were drawn through the results. These curves were entered to obtain the partition functions at the stellar temperatures.

The values above overlap somewhat those computed by Claas for the outer layers of the solar atmosphere, and show small systematic differences. But since Claas used older sources for his spectroscopic data, the differences probably arise from revisions in this material.

(v) The Abundance of Neutral Lithium

The steps involved in determining the abundance ratio of neutral lithium to neutral vanadium have all been discussed already; little more need be done here than to bring them all together in sequence.

Having obtained a value (or an upper limit to the value) of the

equivalent width of the blended doublet of Li I, a value of the most probable velocity is calculated from that of the V I lines, obtaining the thermal contribution for both lithium and vanadium from equation 22 using the excitation temperature. For lithium, the contribution of the thermal motion to the total velocity always exceeds the turbulent contribution, while the reverse is usually true for vanadium.

In all cases, a value of log η_o'' representing the sum of both lines was calculated on the assumption of blended absorption coefficients, as explained in subsection (iv) of the previous section (method "a"). In those stars in which the equivalent width of the doublet was greater than 40 mA, a value of log η_o'' for the entire feature was also computed assuming that the absorption coefficients were unblended (method "b"), since here differences between the methods might be expected. The stars in which the two values disagreed were all among the cooler ones, so that the unblended approximation was the most accurate, and the value of log η_o'' computed on this assumption was used to derive the final results. The blended assumption was used in the weak-line cases to simplify the computations. Note that the actual values of log η_o'' are different in the different assumptions in all cases, but for weak lines the difference is exactly cancelled in equation 18 by a difference in the lithium velocity.

The abundance ratio of neutral atoms was computed from equation 18, using this value (or values) of log η_o'', the partition functions from the curves described above entered with the excitation $\underline{e}$ value, and the values of log $\underline{c/v}$ for lithium and vanadium. The excitation potential for the lithium doublet is zero; the remaining constants are left unevaluated and written as a single constant $\underline{K}$, so that the equation takes the form

$$\log \frac{Li^o}{V^o} = \log \eta_o'' + \log \frac{B(Li\ I)}{B(V\ I)} - \log \frac{c/v(Li)}{c/v(V)} + \log K, \text{ and} \tag{34}$$

$$\log K \equiv \log C - \log \frac{gf\lambda}{\alpha} + 17 \quad . \tag{35}$$

The value of $\underline{K}$ cannot be determined with any accuracy until a reliable determination of $\underline{C}$, the calibration constant of the V I $\underline{f'}$ values, is made. $\underline{K}$ was calculated roughly both from equation 35 and from equation 34 using abundance determinations in the sun by other authors, but the results of this investigation will be quoted with $\underline{K}$ left unevaluated.

(vi) A Test for Systematic Errors

The possibility remains that in the cool stars and the supergiants some systematic effect, possibly due to stratification in the atmospheres, persists which produces spurious abundance ratios between the ground-state lines of lithium and the slightly excited lines of neutral vanadium used for comparison, especially when the V I lines are quite strong. As a test of this, a very weak line of V I, λ5632.469, which has an excitation potential of only 0.07 ev, was used to obtain the abundance ratio $\underline{V}^{o}/\underline{V}^{o} = \underline{V}/\underline{V}$ by the same procedure used for the lithium line, excluding, of course, the compensation for blending. This line was not used in obtaining the curve of growth. In applying equation 18 to this line, the terms in the partition functions and the velocities drop out,

$$(36) \qquad \log \frac{V^{o}}{V^{o}} = \log \eta_{o}'' + \theta E - \log \frac{gf\lambda}{a} + \log C + 17 \quad ,$$

and the constants may be replaced by a term $\log \underline{K}'$ as was done for the lithium case, but here it is clear from equation 14 that $\log \underline{K}' = - \log \underline{\eta_{o}'}$. This weak vanadium line was used to compute the quantity $\log \underline{V}/\underline{V}$, which must be constant in all the stars. It should also be near zero, but any small constant deviation would not affect the conclusions of this study regarding the variations of the $\underline{Li}/\underline{V}$ ratio.

A similar procedure was applied to the equivalent width of the strong line λ5727.024, which has an excitation potential of 1.08 ev. If the values of $\log \underline{V}/\underline{V}$ derived from both the weak and the strong line remain constant in the stars studied, then reasonable confidence may be had in the absence of serious systematic errors arising from either curve-of-growth, ~~or~~ excitation-potential, or excitation-temperature effects.

(vii) The Ionization of Vanadium

The ratio of ionized to neutral vanadium atoms was determined from the equivalent widths of the scandium lines using equation 28, repeated here:

$$(28) \qquad \log \frac{V^{+}}{V^{o}} = \Delta \log \eta_{o} + \log \frac{B(V\ II)}{B(V\ I)} - \Delta \quad .$$

Basically, the values of $\log \underline{W}/\underline{b}$ for the scandium lines and the adopted curves of growth were used to obtain values of $\log \underline{\eta_{o}}$, and the values for the lines from multiplet 2 of Sc I were corrected to agree in excitation

potential with the other lines using θ derived from the V I lines; then the mean log η_o's were computed for each ion, and the difference, ionized minus neutral, was inserted into equation 28 as $\Delta \log \eta_o$. The constant Δ was obtained from the sun as described below.

One difficulty in applying the above procedure occurs when one of the Sc lines is not measured. Since the value of Δ depends on which lines are used, a new value would have to be obtained from the sun each time a different Sc line were omitted. This places considerable weight on the accuracy of the individual equivalent widths of these lines in the sun, where they are quite small. To reduce this dependence on the individual values, a method was adopted in which each individual line in a star provides an estimate of the mean log η_o for all the lines of that ion listed in Table 2; therefore a mean value for all the lines could be obtained even if all were not observed. In this way a single value of Δ applied in all cases, and depended on the mean of all the lines observed in the sun. Systematic differences in the state of ionization will not appear between stars because of different photometric errors in the solar lines.

In order to apply this method, a table was first constructed of the log η_o values for the Sc lines from the best plates, selected on the basis of good contrast and low tracing noise. Only those stars in which all the Sc lines were measured were used here. Then, systematic differences between stars were eliminated by subtracting the value of log η_o for a selected line in each ion from all the values in that ion in every star. This provided a table of "adjusted" log η_o values which reflected only the fluctuations of this quantity from line to line in a single star.

At this point it was possible to determine whether the V I excitation temperature was adequate to use in adjusting the log η_o's from the two ground-state Sc I lines. This was done by computing the mean adjusted log η_o values for Sc I from all four lines and from the two excited lines alone, averaging both these means over all the stars, and obtaining the variances (σ^2) of these grand means. The variance of the mean obtained from the four lines was slightly less than that obtained from the two, indicating that although the accuracy was not improved as much by including these lines of different excitation as would be expected for lines of the same excitation, the accuracy was certainly not reduced by their inclusion, and probably would be increased in cases where one of the excited lines was

unobservable. Hence the two ground-state lines were retained.

A mean value of log η_o was then obtained for each ion in each star from the original table, and the deviation of each line from the appropriate mean was recorded. These deviations were each averaged over all the stars, providing a mean deviation from the mean for each line. Thus in the reductions, the appropriate mean deviation was applied to each observed log η_o to estimate the mean log η_o of all the lines of that ion. All of the available estimates of the mean were averaged to provide the adopted mean for the ion. The difference of the adopted values became $\Delta \log \eta_o$ in equation 28.

From Table 5 it may be seen that the term in the partition functions which enters equation 28 is always approximately zero.

The value of Δ was determined from the abundances derived for the sun by Unsöld (1948) and Wright (1951a). Both equation 28 (vanadium) and 25a (scandium) were used after determining $\Delta \log \eta_o$ from the Utrecht Atlas data and the curve of growth fitted in this study. Partition functions were taken from the work of Claas (1951). Both Unsöld and Wright used the Schuster-Schwarzschild model and gave abundances in numbers of atoms "above the photosphere." Since only ratios are used, this makes no difference. Unsöld's values are based on the equivalent widths of Allen (1934), and Wright's were determined using his own relatively low-dispersion sky and moon plates. Wright gives the total abundance of each ion, while Unsöld gives only the abundance in each excited state and the total abundance of the element. The Boltzmann equation was applied to Unsöld's results to give the values needed here. Six determinations of Δ were made treating both scandium and vanadium abundances from three sources: (a) Wright's results, (b) Unsöld's results applying his value of θ (0.868), and (c) Unsöld's results applying the value of θ derived here from the solar V I lines (1.11). This latter determination was included because Unsöld's θ was derived to apply to both the excitation and ionization of a large number of ions with lines of a large range in excitation potential; therefore it may be less accurate for the ions in question than a value derived for one of them. The best agreement for the two elements was for case (c), where the results were negligibly different. The adopted value, +0.38, was the mean for this case, and agreed very closely with the mean of all six determinations.

The resultant of Δ remains a source of uncertainty ~~in the~~

in the results, since it is ultimately based on Unsöld's and Wright's estmates of the absolute oscillator strengths of the scandium and vanadium lines which they measured. However, since it is the difference in the log $gf\lambda$ values for the two ions that enters Δ, the uncertainty is perhaps less than in the absolute values themselves. Any error in Δ is most important in the coolest stars, since it affects the value of V^o/V^+ which appears in the factor β in equation 32a, and of course this ratio is larger at lower temperatures. If Δ is too large, the ratio V^o/V^+ will be too large, and β will be too near unity--i.e., too small. Thus a large Δ will tend to reduce the abundances for cool stars. However, in the M0 III star HD 6860 (β And) a decrease of 1.0 in Δ (a factor of 10 in V^o/V^+) increases the value of β by only a factor of 2. There is no way to estimate the uncertainty in Δ, but it seems unlikely that it is enough to have a major effect on the results.

Having obtained the ratio V^+/V^o for a star by the above procedure, the quantity γ, which is proportional to the abundance of vanadium divided by the continuous opacity, was calculated from the value of γ^o obtained in subsection (iii) above, using equations 29 and 30; i.e.,

$$\gamma = \gamma^o\left(1 + \frac{V^+}{V^o}\right) \quad .$$

(viii) The Ionization Temperature

In order to determine the ratio of total abundances of lithium to vanadium from the ratio of neutral ions determined according to subsection (v), it is necessary to have both the ionization of vanadium determined as in subsection (vii) and the relative ionization of lithium to vanadium, determined from equation 33. For this purpose, and in order to estimate the electron pressure, a value of the ionization temperature is needed. This cannot be derived from the data of Table 4, but must come from other sources.

Detailed investigations of stellar atmospheres, including those of Greenstein (1948) of F stars of several luminosities, and the Burbidges (1957) of a G8 giant and a "Ba II" star, indicate that the ioniation temperature is usually higher than the excitation temperature, and is, in fact, better approximated by the effective temperature. Since, however, the excitation temperatures seem to show variation among stars of the same

spectral type, it might be the case that the ionization temperature shows similar effects. The effective temperature, however, is usually taken to be same for all stars with the same spectral classification. It was decided, therefore, to make two estimates of the ionization temperature, each based on the effective temperature but being differently sensitive to individual differences between stars.

Popper (1958) has investigated the problem of the effective temperatures of stars of late types, and has concluded that to a good approximation a unique relation exists between a color index obtained from the long wave length part of the spectrum and the effective temperature. A color index such as the $\underline{I} - \underline{R}$ of Stebbins and Whitford (1945) would be desirable, but, lacking values of this index for a sufficient number of stars, the $\underline{B} - \underline{V}$ of Johnson and Morgan (1953) can be used. Popper has also concluded that the table of effective temperatures as a function of spectral classification given by Keenan and Morgan (1951) is most reliable for the dwarfs.

Following Popper's suggestions, a list was made of stars with accurately determined color indices on the $\underline{B} - \underline{V}$ system and good spectral classifications on the MK system, taking all stars from G0 to M2 in the lists of Johnson and Morgan (1953), Johnson and Harris (1954), and Johnson (1955). Using the dwarfs from this list, a plot was made of $\underline{B} - \underline{V}$ vs. $\underline{\theta}$(eff), deriving $\underline{\theta}$ from the table of Keenan and Morgan. These points (Figure 7) appear to fall on a linear relation, except that only three points fall between $\underline{B} - \underline{V} = 0.9$ and $\underline{B} - \underline{V} = 1.4$, and these are somewhat below the line (up to 0.1 in $\underline{\theta}$). But since the remaining points suggest a linear relation, a linear one was adopted. From this relation, values of $\underline{\theta}$(eff) were determined for all the stars in the list. Eighteen stars studied here are included.

These eighteen stars were used to construct a correlation plot of $\underline{\theta}$(eff) and $\underline{\theta}$(exc). This relation, when extended to include the sun, can be fairly well represented by a straight line (Figure 8). The scatter is fairly small (± 0.07), and no significant segregation of points according to luminosity class appears, except for the two supergiants. The color indices for these stars are not well determined, and the excitation temperature of one of them (HD 200905, ξ Cyg) is obviously much too high for its spectral class, judging by the other stars studied. The relation between the $\underline{\theta}$'s can be expressed by the equation

$$\theta(\text{eff}) = \theta(\text{exc}) - 0.19 \quad . \tag{37}$$

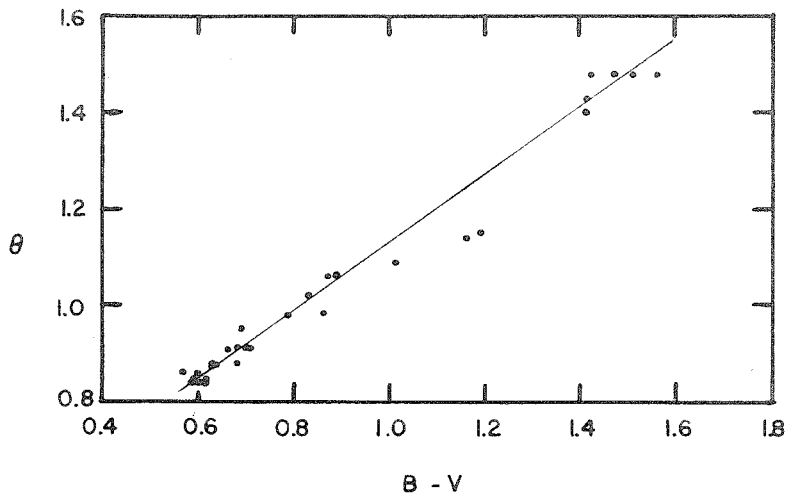

Figure 7. B-V color index vs. effective temperature parameter for dwarfs

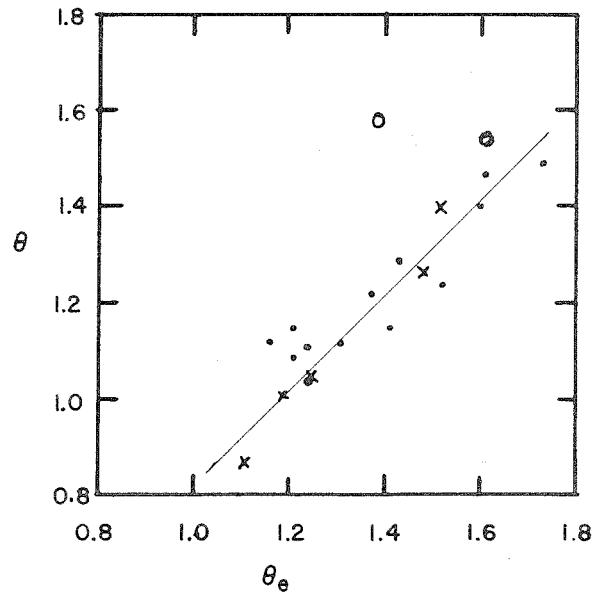

Figure 8. Relation between observed excitation temperature parameter (abscissa) and effective temperature parameter (ordinate). Crosses indicate dwarfs; dots, giants; circles, supergiants.

Thus equation 37 was used to obtain one estimate of the ionization temperature, replacing $\underline{\theta}$(ion).

The second estimate was to use the $\underline{\theta}$(eff) obtained from the color index where this quantity was available, and to estimate it from the spectral class otherwise. This latter step was made by way of a correlation of the effective temperatures of the stars on the color-index list with their spectral classification. Since a sufficient sample was not available for each temperature and luminosity subdivision, the table of Keenan and Morgan was used to establish trends. Table 6 below gives the values adopted.

Table 6

Effective Temperatures $\underline{\theta}$(eff)

	V	IV	III	II	Ib
G8	0.94	1.03	1.04	1.19	1.36
K0	0.98	1.08	1.11	1.25	1.42
K1	1.02	1.13	1.16	1.31	1.46
K2	1.06	1.18	1.24	1.36	1.50
K3	1.09		1.34	1.50	1.57
K4	1.15		1.45	1.52	1.58
K5	1.26		1.50	1.55	1.60
K7	1.39				
M0	1.42		1.55	1.60	1.65

These values of $\underline{\theta}$ are close to those which may be computed from the temperatures of Keenan and Morgan; in general, the dwarfs agree with the published values except at K4 and K5 (no values are given at K7), the giant values of $\underline{\theta}$ are less in types earlier than K5 and more in K5 and M0 than the published temperatures give, and the supergiant values are all greater. In all cases the differences are too small to significantly affect the derived $\underline{Li}/\underline{V}$ abundance ratios.

Thus for each star two estimates of the ionization temperature were made: one using the effective temperature given by equation 37; and the other by using the color index $\underline{B} - \underline{V}$ to derive a temperature from Figure 7, or by taking the value for the proper spectral class from Table 6 if no color index was available. Separate estimates of the abundance ratio and the electron pressure were made from the two temperatures, unless they were in agreement.

(ix) The Electron Pressure and the Total Abundance Ratio

Having two estimates of the ionization temperature for each star and determinations of the ratios $\underline{V}^+/\underline{V}^0$ and $\underline{Li}^0/\underline{V}^0$, values of the total abundance ratio $\underline{Li}/\underline{V}$ were calculated from equations 33 and 32a, and electron pressures were computed from the Saha equation, 31. Two values of each quantity were obtained.

In order to obtain a final value of the abundance ratio, some choice or interpolation had to be made between the two computed ones. The electron pressure was used as the indicator of the most likely value, and the derived results were regarded as indicating the range of possible choices. In quite a few cases, the two estimates of the ionization temperature coincided so that no choice was possible or necessary, and in other cases the two values were quite close. Results of this type established a run of electron pressure with spectral classification, which served as a criterion to guide the choices in the other cases. In addition, O. C. Wilson has kindly furnished estimates of the absolute visual magnitude for twenty-nine of the stars studied here derived from measurements of the emission width in the "K" line of Ca II (see Wilson and Vainu Bappu 1957). These values constitute an extension and an improvement of the published list, and the writer is most grateful to Dr. Wilson for permitting their use here in advance of publication. The absolute magnitudes showed that two stars of the same classification may differ considerably in luminosity; therefore presumably also in electron pressure, with the brighter star having the lower pressure. Whenever this criterion could be brought to bear, it was used in choosing the electron pressure from the prescribed range for each star. The $\underline{Li}/\underline{V}$ ratio was then chosen according to the adopted electron pressure.

An extreme example of the divergence of the two results is the case of the supergiant HD 200905 (ξ Cyg). The excitation temperature derived here was extraordinarily high--much in excess of its effective temperature according the Table 6. Thus in deriving an ionization temperature from the excitation temperature, a high value also resulted, giving a high electron pressure--specifically, $\log \underline{P}_e = +0.41$. The ionization temperature based on the color index was lower, giving an electron pressure $\log \underline{P}_e = -2.43$ -- a range of almost a factor of 10^3 in $\underline{P}_e$. The ratio of abundances had a range of less than a factor of 4. Since the K3 supergiant HD 225212 (3 Cet) gave coincident results in the temperature estimates and a computed electron

pressure log P_e = -2.65, it was obvious that the lower limit of the electron pressure range (and the maximum abundance ratio) should be chosen for HD 200905. The K2 giant HD 12533 (γ And A) had a permitted range of about 1.8 in log P_e (and a factor of 2 in the abundance ratio). Had no value of the absolute magnitude been available, the electron pressure would have been chosen to agree with the other K2 III stars. But Wilson's measurement showed this star to be almost three magnitudes brighter than these other stars; therefore a lower electron pressure was adopted.

Usually the two values of the abundance ratio were in good agreement, differing by a factor less than 2. In the extreme cases a reasonable choice could always be made, so that the uncertainty involved in this step is less than a factor of 2.

(x) The Absolute Abundance of Vanadium

Since the principal result of this paper is a set of values of the abundance ratio of lithium to vanadium, and since it will be assumed that any variation in this ratio is due to variations in the abundance of lithium, it is of interest to make at least a rough check on the constancy of the vanadium abundance. This assumption is really quite a safe one, since it is possible to see by inspection of the spectrograms that the strength of the lithium feature fluctuates rather wildly with respect to the other spectral lines. If one is not inclined to question the constancy of the vanadium abundance in these stars, the computation can be regarded as a test of the adopted electron pressure and temperature values which enter the calculation.

The determination rests upon the quantity χ defined in equation 30, an observational result which is fairly well determined and which is proportional to the abundance of vanadium divided by the continuous opacity. Combining the definitions of χ and χ^o in equations 30 and 24 gives

$$\log V = \log \gamma + \log R P_e - \log \delta C - 17 \quad . \tag{38}$$

Here it should be recalled that R is the ratio of the H^- absorption coefficient at the temperature of interest to that at $\theta = 1.4$ (for the same P_e), C is the calibration of King's relative gf' values for V I, and

$$\delta = \sqrt{\pi}\, \frac{1}{X}\, \frac{M}{m}\, \left(\frac{\varepsilon}{c}\right)^2 \quad .$$

It is not necessary to evaluate the constant term δC in order to test the constancy of log V, but it is of interest to do so to see if the result is of a reasonable order of magnitude. A value of C may be obtained from Allen's (1955) list of absolute gf values for V I, based on an f-sum rule. From these, and King's relative values, one obtains

$$C = 1.39 \times 10^{-4} \quad .$$

The constant δ may be evaluated from the known physical constants, taking a reasonable value for X. Adopting $X = 0.70$, often used for solar-type stars, one obtains

$$\delta = 1.19 \times 10^{-36} \quad .$$

Finally,

$$\log V = \log \gamma + \log RP_e + 22.78 \quad . \tag{39}$$

Thus the absolute vanadium abundance may be calculated from the adopted electron pressure and the value of R deduced from the tables of Chandrasekhar and Breen (1946) for the adopted ionization temperature, since this temperature is probably closer to the one responsible for the opacity. Of course the adopted electron pressure is very subject to error, and the vanadium abundance reflects this directly.

IV. RESULTS

This chapter presents the numerical results of this study. Those quantities which bear upon the physical properties of the stellar atmospheres are given first; in those cases in which two values of a quantity have been derived, both are presented, along with the final adopted value. The second section presents the principal results of this study--the relative abundances of lithium to vanadium. Here also duplicate values and final choices are given where appropriate. Finally, the errors involved in the various steps of the analysis are discussed with regard to their influence upon the final results.

a) Physical Properties of the Atmospheres

Table 7 presents the results which refer to the physical conditions in the stellar atmospheres. All the values related to a single star are collected in a column, and the stars are ordered according to spectral classification rather than in order of HD numbers. This arrangement groups together stars of similar physical characteristics. The left-hand column in each section of the table identifies the quantities in each row. The first row identifies the star by its HD number; the second gives the spectral classification; the third line (omitted in later types) gives the spectroscopic group according to Roman (1952), either strong-line (st-l), weak-line (wk-l), strong CN absorption at λ4150 (4150), or weak CN absorption (CN); the fourth rw6 gives the observed excitation temperature parameter; the fifth, the most probable velocity for V I atoms, including both thermal motion and microturbulence; the sixth, the half-widths for weak lines, which includes the effect of macroturbulence; the seventh, the degree of ionization of vanadium; the eigth, the quantity χ_λ^h proportional to the abundance of vanadium divided by the continuous opacity; the ninth, the absolute visual magnitude derived from the width of the Ca II emission by Wilson; the tenth, the absolute visual magnitude from Roman's (1952) calibration of the luminosity classes; the eleventh (a double row), the ionization temperature parameter derived from both the color index (or the spectral class) and the excitation temperature; the twelfth (also double), the electron pressure derived from these two sources; the thirteenth, the adopted electron pressure; and the fourteenth, the absolute abundance of vanadium in atoms per gram of stellar material.

Table 7

Physical Parameters

HD	(Sun)	104979	62345	219615	9270
Type	G2V	G8III	G8III	G8III	G8III
Group	---	wk-1	st-1	CN	st-1
e_e	1.11	1.24	1.24	1.37	1.24
v(km/sec)	1.9	3.7	4.7	2.8	2.7
$\Delta\lambda$ (A)	---	0.30	0.29	0.27	0.34
$\log \frac{V^+}{V}o$	1.69	1.55	1.22	1.74	1.47
log γ	-7.28	-6.61	-6.74	-6.28	-6.24
M_V(W)	+4.7	---	---	+1.9	-0.2
M_V(R)	+4.6	0.0	0.0	0.0	0.0
e_i(B-V)	0.88	1.04	1.08	1.04	1.11
(e_e)	0.92	1.05	1.05	1.18	1.05
log P_e(B-V)	+1.62	+0.50	+0.53	+0.31	+0.04
(e_e)	+1.30	+0.43	+0.76	-0.76	+0.50
log P_e	+1.5	+0.5	+0.6	+0.3	0.0
log V	16.1	16.0	16.1	16.1	15.9

HD	90537	98430	168723	76294	4128
Type	G8III-IV	G8III-IV	G8IV	KOIII	KOIII
Group	st-1	wk-1	wk-1	4150	st-1
e_e	1.33	1.52	1.21	1.42	1.35
v(km/sec)	2.7	2.6	2.4	3.5	2.8
$\Delta\lambda$ (A)	0.27	0.27	0.28	0.29	0.32
$\log \frac{V^+}{V}o$	0.99	0.87	1.30	1.39	1.20
log γ	-6.48	-6.54	-6.45	-6.25	-6.14
M_V(W)	---	---	---	+0.5	+0.8
M_V(R)	+1.3	+1.3	+3.5	+0.7	+0.7
e_i(B-V)	1.04	1.04	1.09	1.11	1.11
(e_e)	1.14	1.33	1.02	1.23	1.16
log P_e(B-V)	+1.06	+1.18	+0.37	+0.12	+0.31
(e_e)	+0.29	-1.02	+0.91	-0.78	-0.06
log P_e	+0.9	+0.8	+0.6	0.0	+0.1
log V	16.6	16.5	16.3	16.1	16.3

Table 7 cont'd.

HD	8512	197989	27697	28305	27371	165341
Type	KOIII	KOIII	KOIII	KOIII	KOIII	KOV
Group	wk-1	st-1	st-1	wk-1	st-1	---
e_e	1.43	1.41	1.31	1.21	1.16	1.10
v(km/sec)	2.9	3.0	4.1	3.2	3.0	1.8
$\Delta\lambda$ (A)	0.29	0.33	0.29	0.29	0.27	0.26
$\log \frac{V^+}{V^o}$	1.18	1.29	1.03	1.37	1.37	1.14
$\log \gamma$	-6.21	-6.29	-6.63	-6.20	-6.25	-7.06
M_v(W)	+1.0	+1.3	+0.7	+0.5	+0.7	+5.4
M_v(R)	+0.7	+0.7	+0.7	+0.7	+0.7	+6.0
e_i(B-V)	1.11	1.15	1.12	1.15	1.12	0.98
(e_e)	1.24	1.22	1.12	1.02	0.98	0.91
$\log P_e$(B-V)	+0.33	-0.07	+0.38	-0.15	+0.07	+1.38
(e_e)	-0.29	-0.61	+0.38	+0.84	+1.15	+1.92
$\log P_e$	+0.3	-0.1	+0.4	+0.1	+0.5	+1.7
log V	16.3	15.9	16.0	16.1	16.6	16.6

HD	96833	108381	10476	11909	206778
Type	K1III	K1III-IV	K1V	K1p	K2Ib
Group	wk-1	4150	---	---	---
e_e	1.37	1.44	1.18	1.04	1.61
v(km/sec)	3.0	2.8	2.1	1.8	2.7
$\Delta\lambda$ (A)	0.28	0.32	0.26	0.30	0.42
$\log \frac{V^+}{V^o}$	1.03	0.99	1.14	1.53	0.83
$\log \gamma$	-5.97	-5.69	-6.89	-6.30	-4.93
M_v(W)	+0.7	---	+6.5	---	-4.3
M_v(R)	+0.8	+1.3	+6.2	---	---
e_i(B-V)	1.22	1.14	1.01	---	1.50
(e_e)	1.18	1.25	0.99	0.85	1.42
$\log P_e$(B-V)	-0.36	+0.29	+1.15	---	-2.25
(e_e)	-0.04	-0.54	+1.33	+2.02	-1.65
$\log P_e$	-0.2	0.0	+1.2	+2.0	-2.0
log V	16.2	16.7	16.4	17.5	15.9

Table 7 cont'd.

HD	20468	124897	12533	12929	6805	22049
Type	K2II	K2IIIp	K2III	K2III	K2III	K2V
e_e	1.60	1.43	1.67	1.52	1.51	1.25
v(km/sec)	3.0	2.5	2.9	2.3	2.4	2.9
$\Delta\lambda$ (A)	0.30	0.31	0.32	0.26	0.32	0.27
$\log \frac{V^+}{V_o}$	1.08	0.80	0.99	1.26	0.94	0.66
$\log \gamma$	-5.35	-6.05	-5.26	-5.65	-6.03	-7.37
M_v(W)	---	+0.5	-1.6	+1.3	+1.1	+6.5
M_v(R)	-2.5	+0.9	+0.9	+0.9	+0.9	+6.4
e_i(B-V)	1.36	1.29	1.24	1.24	1.24	1.06
(e_e)	1.41	1.24	1.48	1.33	1.32	1.06
$\log P_e$(B-V)	-1.44	-0.64	-0.46	-0.73	-0.41	+1.24
(e_e)	-1.83	-0.27	-2.26	-1.41	-1.01	+1.24
$\log P_e$	-1.6	-0.5	-1.6	-1.0	-0.7	+1.2
log V	15.8	16.0	15.8	15.9	15.8	16.0

HD	225212	176670	186791	20644	98262	3627
Type	K3Ib	K3II	K3II	K3II-III	K3III	K3III
e_e	1.75	1.75	1.74	1.51	1.60	1.75
v(km/sec)	2.3	2.8	3.0	3.2	2.8	2.5
$\Delta\lambda$ (A)	0.40	0.28	0.37	0.32	0.28	0.26
$\log \frac{V^+}{V_o}$	0.79	0.59	0.85	0.98	0.54	0.43
$\log \gamma$	-4.25	-5.49	-5.21	-5.55	-5.67	-5.86
M_v(W)	---	---	-2.0	---	-0.7	+0.2
M_v(R)	---	-2.5	-2.5	-1.0	+0.1	+0.1
e_i(B-V)	1.56	1.50	1.50	1.42	1.41	1.34
(e_e)	1.56	1.56	1.55	1.32	1.41	1.56
$\log P_e$(B-V)	-2.65	-2.00	-2.27	-1.80	-1.21	-0.65
(e_e)	-2.65	-2.45	-2.64	-1.05	-1.21	-2.29
$\log P_e$	-2.6	-2.2	-2.4	-1.6	-1.2	-0.6
log V	16.1	15.2	15.3	15.6	15.9	16.1

Table 7 cont'd.

HD	81797	35620	201251	30504	69267
Type	K3III	K3p	K4II	K4II	K4III
e_e	1.55	1.57	1.73	1.42	1.51
v(km/sec)	2.6	2.2	2.5	2.2	2.4
$\Delta\lambda$ (A)	0.28	0.30	0.30	0.30	0.27
$\log \frac{V+}{V_o}$	0.20	0.28	0.53	-0.04	0.12
$\log \gamma$	-5.65	-5.43	-4.86	-5.63	-5.57
M_V(W)	-1.0	---	---	---	+0.2
M_V(R)	+0.1	---	-2.5	-2.5	-0.1
e_i(B-V)	1.34	---	1.52	1.52	1.47
(e_e)	1.36	1.38	1.54	1.23	1.32
$\log P_e$(B-V)	-0.50	---	-2.17	-1.52	-1.32
(e_e)	-0.50	-0.88	-2.17	+0.65	-0.19
$\log P_e$	-0.5	-0.9	-2.2	-1.5	-1.0
log V	16.5	16.4	15.9	15.8	16.2

HD	50778	90432	200905	196321	29139
Type	K4III	K4III	K5Ib	K5II	K5III
e_e	1.61	1.50	1.39	1.48	1.73
v(km/sec)	2.3	1.9	2.0	2.0	1.7
$\Delta\lambda$ (A)	0.28	0.29	0.38	0.30	0.32
$\log \frac{V+}{V_o}$	-0.08	-0.08	+0.42	-0.26	+0.02
$\log \gamma$	-5.63	-5.37	-4.37	-5.32	-4.47
M_V(W)	---	---	-4.0:	---	+0.2
M_V(R)	-0.1	-0.1	---	-2.5	-0.2
e_i(B-V)	1.45	1.45	1.58	1.55	1.49
(e_e)	1.42	1.31	1.20	1.29	1.54
$\log P_e$(B-V)	-0.96	-0.97	-2.43	-1.53	-1.37
(e_e)	-0.74	+0.08	+0.41	+0.41	-1.74
$\log P_e$	-0.8	-0.9	-2.4	-1.5	-1.4
log V	16.3	16.5	16.2	16.1	17.0

Table 7 cont'd.

HD	189319	201091	201092	6860
Type	K5III	K5V	K7V	MOIII
e_e	1.65	1.48	1.52	1.64
v(km/sec)	2.0	1.5	1.3	1.8
$\Delta\lambda$ (A)	0.30	0.25	0.23	0.30
$\log \frac{V^+}{V^o}$	-0.23	-0.40	-0.95	-0.23
$\log \gamma$	-5.32	-6.97	-6.52	-4.86
M_V(W)	-1.0	+6.6	+8.4	-0.8
M_V(R)	-0.2	---	---	---
e_i(B-V)	1.50	1.27	1.40	1.55
(e_e)	1.46	1.29	1.33	1.45
$\log P_e$(B-V)	-1.19	+0.63	+0.28	-1.56
(e_e)	-0.89	+0.63	+0.80	-0.82
$\log P_e$	-1.2	+0.6	+0.8	-1.2
log V	16.2	16.2	16.9	16.8

The latter quantity is given in this table because it is of interest mostly as a check on the assumed and derived atmospheric parameters. It depends on the adopted electron pressure and ionization temperature, as well as the abundance of vanadium and the theory of the H^- absorption coefficient.

Table 7 is of interest not only because of its bearing on the final results presented in the next section, but also because no such extensive table of the spectroscopic properties of cool stars has been published heretofore. While the accuracy of the values suffers from the limited amount of material entering each one, their comparative magnitudes gain from the homogeneity of the data.

First, it is encouraging to note the constancy of the derived values of the vanadium abundance. All the values are contained in the range of log $\underline{V}$ from 15.2 to 17.5, inclusive, and all but six are in the range from 15.8 to 16.8, inclusive. These values have been plotted as a function of spectral type in Figure 9. A different symbol has been used for each luminosity class (intermediate classes, i.e., II-III, have been omitted for simplicity). No systematic trend is evident. In view of the large uncertainty of the adopted electron pressures, this is quite satisfactory. The agreement of the solar value with those for the other stars indicates that no serious differences arise from the different source of data.

It is interesting to notice a few of the extreme cases. All of the values below the lower limit of the smaller range are K3 stars, the two lowest being HD 176670 (λ Lyr) and 186791 (γ Aql), both K3 II. In these cases it seems likely that the electron pressures are too low, since the adopted values are almost as low as that adopted for the K3 Ib star HD 225212, which has a normal value of log $\underline{V}$. The highest value of log V was found for the star HD 11909, classed as K1p. More will be said of this star later. A high value is also indicated for the K5 III star HD 29139 (α Tau). This star is, according to Wilson, over a magnitude fainter than the other K5 III star observed. Moreover, the excitation temperature is lower, the degree of ionization of vanadium is greater, and the value of $\underline{\gamma}$ is almost ten times greater than that of the other star. This value of $\underline{\gamma}$ is quite near to that observed for the supergiant HD 200905 (ξ Cyg), which must have a lower opacity. It would seem possible that the abundance of vanadium is high in HD 29139.

Also worthy of note is the considerable variation of the derived parameters among stars of the same spectral classification. For example, three of the four giants in the Hyades cluster are included here (HD 27371, 27697, and 28305). A spectrogram was also taken of the fourth, but it was found to be improperly exposed, and no further opportunity existed for obtaining a plate. These stars are all classified as K0 III, and one of them, HD 28305 (ε Tau), is classified as "weak-line" by Roman. All the others are "strong-line" stars. It is certainly unlikely that these stars have different metal abundances. However, HD 28305 is 0.2 magnitudes brighter than the other two stars studied here. The data in Table 7, on the other hand, show considerably less difference between HD 28305 and 27371 than between these two and HD 27697 (δ Tau). Its excitation temperature, proportion of ionized vanadium, and value of γ are all significantly lower than in the other two stars. Of course the spectral classifications are fairly coarse, and variations within classes are to be expected. Another case of this is the K2 III star HD 12533, in which the values of all the parameters are considerably closer to those of the K2 II star HD 20468 than to those of the other K2 III stars. Also it is nearly three magnitudes brighter than the other giants. In short, there would seem to be evidence of significant differences among stars of the same spectral classification. In this regard it may be pointed out that according to the evolutionary processes discussed by Sandage, Schwarzschild, Hoyle, and others (see, for example, Sandage 1957a, and Hoyle and Schwarzschild 1955), two giant stars of the same surface temperature and luminosity may have different masses. Perhaps, then, some spectroscopic differences can be expected. Also, of course, the spectral classifications, which are done at low dispersions, are not necessarily highly accurate even with respect to the coarse subdivisions used.

Several of the most luminous stars show peculiar excitation temperatures. This is especially true of the K5 Ib star HD 200905 (ξ Cyg), which has an excitation temperature as high as some K0 III stars. The excitation temperatures of HD 196321 and HD 30504 (K5 II and K4 II, respectively) are almost this high. It is known that the atmospheres of the highly luminous stars are very tenuous and can by no means be in thermodynamic equilibrium. Therefore while these temperatures can serve no other purpose than

to describe the populations of the two excited states of V I from which they were derived (note that they lead to absurd electron pressures), there is little ground for doubting their correctness for this purpose.

A brief examination of the three stars studied which are called "peculiar" from the low-dispersion spectrograms is in order. HD 11909 (ι Ari) is classed as K1p by Roman, who states that the H-lines and λ4290 are strong and indicate luminosity class II, while the CN bands and Sr II are weak, indicating class III. In any case, she obviously regards the star as a giant. The present results conflict quite strongly with this classification. The vanadium lines are quite strong (as indicated by a γ value ten times that of the sun) and permitted a reasonable estimate of the damping constant. This value appeared to be quite high, on the order of that for the sun (see Aller 1953, p. 292) or greater. The excitation temperature is slightly higher than that of the sun, and the ionization temperature based on it is sufficient to demand a high electron pressure even with the rather high degree of ionization. Thus the excitation temperature, the damping, the electron pressure, and also the low derived velocity parameter indicate that this star is a dwarf of near solar temperature. However, the high value of γ demands either a high abundance of vanadium or a low opacity. The H^- opacity computed for the ionization temperature and electron pressure indicates a high abundance of vanadium. If there were any contribution to the opacity by neutral hydrogen, a still higher abundance would be required. Perhaps this star is actually a metal-rich dwarf. The data presented here are not sufficient to answer this question, but it would be of interest to investigate the star further.

HD 35620 (ϕ Aur) is classified K3p by Roman, with the remark that CN and Sr II are too strong for class III, and H is too weak. The results obtained in this study do not differentiate it from the K3 III stars.

HD 124897 (α Boo) is a well-known high-velocity star, and is classified by Roman as K2 III, but Johnson and Morgan (1953) append the "peculiar" designation. The results given in Table 7 do not set it off from the other K2 III stars except possibly in its excitation temperature, which seems significantly higher than those of the others. Its value of γ is somewhat lower than that of one of the K2 III stars and about equal to the other's (HD 12533, mentioned above as over-luminous, is not considered here). Otherwise its parameters conform quite well to the other stars.

Putting aside individual peculiarities, it is instructive to note the general trends of the quantities. The excitation temperatures generally decline with advancing spectral class, and the electron pressures decline with increasing luminosity, as is to be expected. In addition, the mean half-width for weak lines ($\Delta\lambda$) increases with luminosity, which is anticipated from inspection of the spectrograms. Surprisingly, however, the most probable velocity declines with temperature and is quite insensitive to luminosity, except that it is lower for dwarfs than for more luminous stars. It has been thought that this quantity should show the same correlation with luminosity that the line width does; in fact, it does show such a correlation in hotter stars (see Greenstein 1948). But since the lines used here are largely on the central part of the curve of growth in the cooler stars, and the derived velocity cannot be much affected by errors in θ_e, it would seem that the values giving this discordant result are quite well determined. Only a few comparisons with other observers are possible. The Burbidges (1957) in their analysis of K Gem (HD 62345) gave a velocity derived from many lines, mostly of higher excitation than used here; their value of log v/c is approximately 0.1 less than that derived here. Wright (1951b) in his analysis of α Boo (HD 124897), derived a value of log v approximately 0.1 greater than derived in this study, using approximately the same lines. It was noted with respect to Figure 3 that Wright's equivalent widths are systematically larger than those derived here, but the difference does not seem sufficient to account for this result. This star was also studied by van Dijke (1946) who obtained a value close to Wright's. However, she used stronger lines of Fe in a crowded part of the spectrum, measuring by the triangle approximation. Probably this comparison is not particularly significant. It does not seem likely that the values of v derived here for the cool stars can be in error by 0.1 in the logarithm, since that implies errors of the equivalent widths of the same order. Quite likely there are differences in velocity for lines from levels of different excitation, but this has not been investigated sufficiently in the cool stars. It seems likely that the values given in Table 7 represent fairly well the ion and levels from which they were derived.

Figure 10 is the result of an attempt to correlate several of the quantities in Table 7 with Roman's spectroscopic groups. Her "strong-line" group is associated with the low-velocity, presumably younger, stars, and the other three groups tend to be high-velocity stars, especially the

"4150" and "CN" groups. The quantities examined are log $\underline{\gamma}$, which is a measure of the absolute strength of the vanadium lines, log $\underline{V}^+/\underline{V}^\circ$, the degree of ionization of vandium, $\underline{\theta}$, the excitation temperature parameter, and $\underline{v}$, the microscopic velocity parameter. All these quantities should be related to the strength of the lines seen at low dispersion. In Figure 10 an average value for each quantity is given for all the giant stars observed in each spectroscopic groupdin each spectral class. These averages are plotted as a function of spectral class with a different symbol for each spectroscopic group. The vertical bars are estimates of the probable error. These estimates depend on the values derived for the KO III strong-line stars, which were the only averages based on more than two values. The four stars in this group provided values of the probable error of a single observation for each quantity, and the probable error given for each point in Figure 10 is this value divided by the square root of the number of stars entering the average. The figure indicates no segregation of the groups in log $\underline{\gamma}$ or $\underline{v}$, but possibly the high-velocity stars have high ionization and low excitation temperatures. This latter effect was noted also be Greenstein and Keenan (1958). Because of the very small sample, the present results cannot do more than suggest these correlations.

In conclusion, it would appear from Table 7 that in general the results of the photometry are reasonable and real, and it is possible to proceed to the results on the abundance of lithium with the expectation that they will be meaningful.

b) Relative Abundances

The principal results of this study, the relative abundance of lithium to vanadium for all the stars studied, are given in Table 8. In addition, the ratio of neutral lithium to neutral vanadium, a preliminary quantity which is subject to a minimum uncertainty, is presented; as is also the ratio of vanadium to vanadium, computed from two different lines as a test for errors.

The quantities involving the lithium abundance are given as logarithms of the abundance ratios divided by the constant $\underline{K}$. The vanadium-to-vanadium ratios are also given as logarithms. The symbols ($<$) and ($\leq$) have the same significance as in Table 4, and a colon (:) following an entry indicates unusual uncertainty in the value.

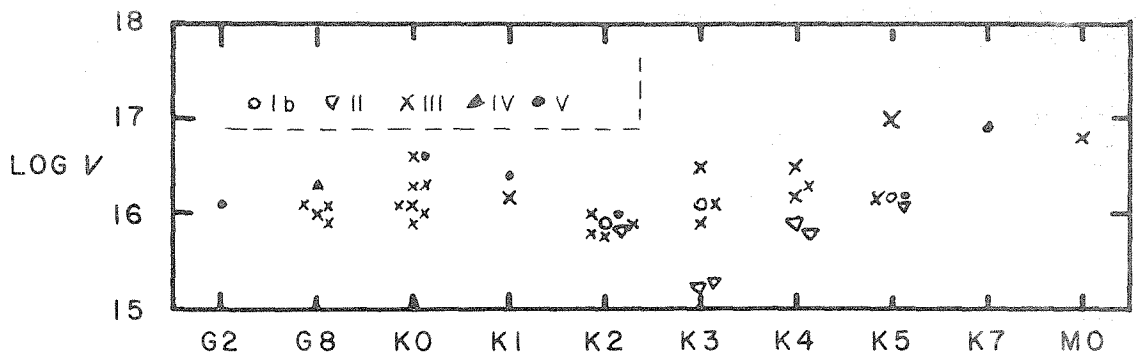

Figure 9. Correlation between the absolute abundance of vanadium, spectral type, and luminosity class. Individual star values are plotted.

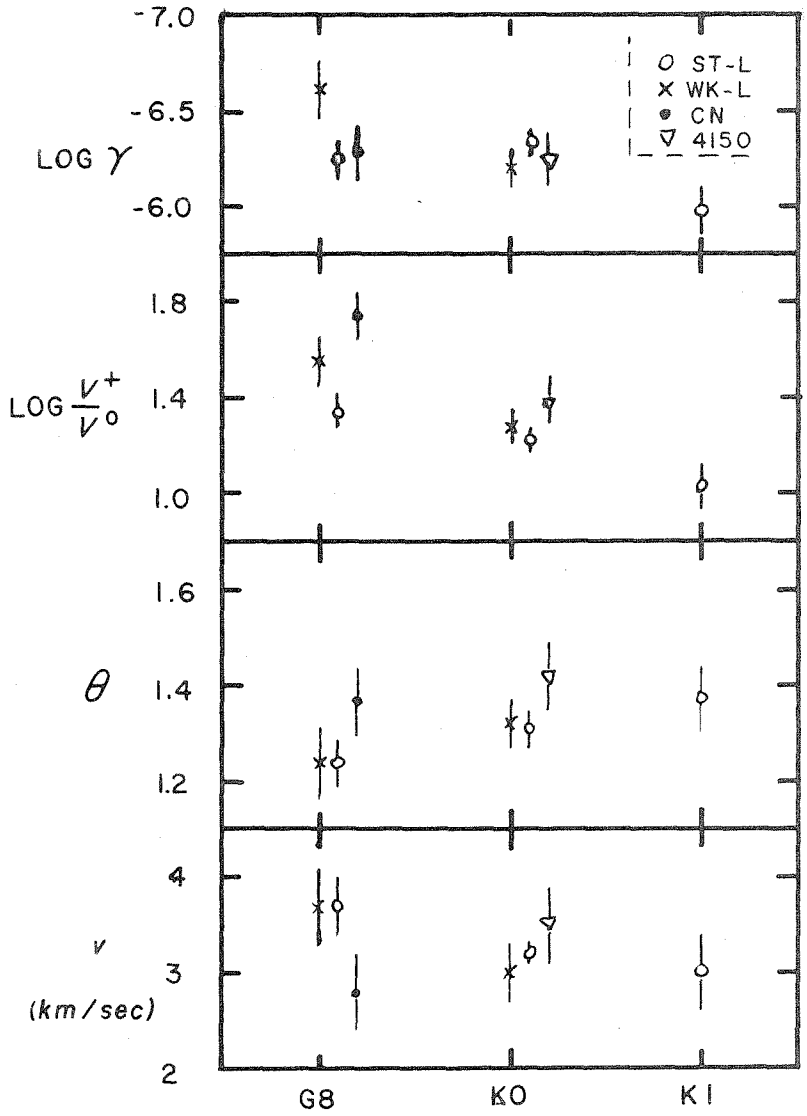

Figure 10. Correlation between means of quantities affecting line strengths, spectral type, and spectroscopic group for giant stars. Probable errors are indicated.

The arrangement of the table is similar to that of Table 7. The quantities derived for a given star are collected in a column, and the stars are ordered according to spectral classification. The column at the left of each group identifies the quantity in each row. The first row identifies the stars by their HD numbers; the second gives the spectral type; the third (omitted in later types) gives the spectroscopic group according to Roman; the fourth gives the ratio of neutral lithium to neutral vanadium, divided by the constant K (in later types this is made a double row, giving the quantity computed for both unblended (ub) and blended (bl) absorption coefficients); the fifth (a double row) gives the ratio of total lithium to total vanadium divided by K, with the ionization correction computed from the temperature derived from both the color index or spectral class (B-V) and the excitation temperature (θ_e); the sixth gives the final adopted abundance ratio of lithium to vanadium, still divided by K; the seventh gives the abundance ratio of vanadium to vanadium derived from the weak line at λ5632; and the eighth gives the same quantity derived from the strong line at λ5727. Only one figure is given for the ratio of neutral lithium to neutral vanadium when the doublet is sufficiently weak that the blending of the absorption coefficient is irrelevant to the results; in this case the value is always given under the "unblended" heading. The abundances of total lithium to total vanadium are all computed using the ratio for neutral atoms derived on the unblended approximation when a choice is necessary. It was explained previously that this approximation is certainly nearer the truth than the other; and since the total abundance ratio is proportional to the ratio of neutrals, the two values for the latter quantity give an estimate of the maximum error from this cause.

An important difference between the results presented in Table 8 and those in Table 7 is that while in the latter each depends on the average properties of a fairly large number of lines, all the numbers in Table 8 result from the photometry of only one spectral feature. It is therefore to be expected that the values in Table 8 show a considerably greater scatter than those in Table 7. Since it is at once clear that the principal feature of the lithium-to-vanadium abundances is their large range, it is essential to determine how much of this may be attributed to random errors. This is one of the reasons for obtaining the abundance ratio of vanadium to vanadium, which must be unity in all stars.

Table 8

Relative Abundances

HD	(Sun)		104979	62345	219615	9270
Type	G2V		G8III	G8III	G8III	G8III
Group	---		wk-l	st-l	CN	st-l
$\log \frac{Li^o}{KV^o}$	3.09		<2.64	2.27	2.86	2.92
$\log \frac{Li}{KV}(B-V)$	3.93		<3.70	3.38	3.92	4.08
(e_e)	4.00		<3.72	3.33	4.12	4.00
$\log \frac{Li}{KV}$	3.96		<3.71	3.36	3.92	4.08
$\log \frac{V}{V}(wk)$	<0.72		<0.47	<0.16	<0.28	<0.15
$\log \frac{V}{V}(st)$	-0.01		-0.12	-0.13	-0.04	+0.01

HD	90537	98430	168723		76294	4128
Type	G8III-IV	G8III-IV	G8IV		KoIII	KoIII
Group	st-l	wk-l	wk-l		4150	st-l
$\log \frac{Li^o}{KV^o}$	<2.23	<1.74	<2.05		≤2.22	<1.84
$\log \frac{Li}{KV}(B-V)$	<3.27	<2.76	<3.17		≤3.38	<3.00
(e_e)	<3.41	<3.14	<3.08		≤3.53	<3.05
$\log \frac{Li}{KV}$	<3.30	<2.83	<3.12		≤3.40	<3.02
$\log \frac{V}{V}(wk)$	<0.26	-0.12	≤0.33		<0.03	<-0.42
$\log \frac{V}{V}(st)$	-0.19	-0.04	-0.07		-0.08	-0.18

HD	8512	197989	27697	28305	27371	165341
Type	KoIII	KoIII	KoIII	KoIII	KoIII	KoV
Group	wk-l	st-l	st-l	wk-l	st-l	---
$\log \frac{Li^o}{KV^o}$	<2.03	<1.94	2.36	2.17	2.70	<2.33
$\log \frac{Li}{KV}(B-V)$	<3.18	<3.14	3.52	3.37	3.87	<3.30
(e_e)	<3.34	<3.23	3.52	3.20	3.67	<3.20
$\log \frac{Li}{KV}$	<3.18	<3.14	3.52	3.32	3.80	<3.25
$\log \frac{V}{V}(wk)$	-0.07	<-0.17	0.48	<0.35	0.48	<0.33
$\log \frac{V}{V}(st)$	-0.11	-0.10	-0.28	-0.12	-0.07	+0.01

Table 8 cont'd.

HD	96833	108381	10476	11909		206778
Type	K1III	K1III-IV	K1V	K1p		K2Ib
Group	wk-1	4150	---	---		---
$\log \frac{Li^o}{KV}_o$ (ub)	2.91	1.88	<2.40	3.13		≤ 0.51
(bl)	2.98			3.14		
$\log \frac{Li}{KV}$ (B-V)	4.20	3.06	<3.40	---		≤ 2.15
(e_e)	4.13	3.20	<3.38	3.91		≤ 2.04
$\log \frac{Li}{KV}$	4.16	3.11	<3.39	3.91		≤ 2.11
$\log \frac{V}{V}$ (wk)	-0.09	-0.63	<0.38	<0.59		-0.85
$\log \frac{V}{V}$ (st)	-0.06	-0.03	+0.01	+0.04		+0.08

HD	20468	124897	12533	12929	6805	22049
Type	K2II	K2IIIp	K2III	K2III	K2III	K2V
$\log \frac{Li^o}{KV}_o$ (ub)	2.20	≤ 0.83	1.29:	<1.49	2.42	< 2.31
(bl)	2.27				2.47	
$\log \frac{Li}{KV}$ (B-V)	3.68	≤ 2.18	2.59:	<2.81	3.71	< 3.28
(e_e)	3.75	≤ 2.11	2.92:	<2.93	3.82	< 3.28
$\log \frac{Li}{KV}$	3.72	≤ 2.16	2.80:	<2.86	3.76	<3.28
$\log \frac{V}{V}$ (wk)	-0.06	-0.17	-0.39	-0.09	-0.20	<0.48
$\log \frac{V}{V}$ (st)	+0.34	+0.12	+0.02	+0.44	+0.14	-0.11

HD	225212	176670	186791	20644	98262	3627
Type	K3Ib	K3II	K3II	K3II-III	K3III	K3III
$\log \frac{Li^o}{KV}_o$ (ub)	-0.08:	1.79	2.15	1.84	1.34	0.97
(bl)		1.84	2.25	1.84		
$\log \frac{Li}{KV}$ (B-V)	1.63:	3.39	3.79	3.39	2.80	2.32
(e_e)	1.63:	3.47	3.85	3.25	2.80	2.62
$\log \frac{Li}{KV}$	1.63:	3.43	3.82	3.36	2.80	2.32
$\log \frac{V}{V}$ (wk)	-1.01	-0.01	-0.41	-0.19	-0.17	-0.37
$\log \frac{V}{V}$ (st)	+0.02	-0.14	+0.36	+0.01	+0.20	+0.05

Table 8 cont'd.

HD	81797	35620	201251	30504	69267
Type	K3III	K3p	K4II	K4II	K4III
$\log \frac{Li^o}{KV}_o$ (ub)	1.80	0.78:	$\leq$ 0.36	1.66	$<$ 0.50
(bl)	1.85			1.72	
$\log \frac{Li}{KV}$ (B-V)	3.10	---	$\leq$ 1.99	3.07	$<$ 1.92
(e_e)	3.10	2.15:	$\leq$ 1.99	2.69	$<$ 1.71
$\log \frac{Li}{KV}$	3.10	2.15:	$\leq$ 1.99	3.07	$<$ 1.86
$\log \frac{V}{V}$ (wk)	-0.22	-0.29	-0.46	-0.10	-0.11
$\log \frac{V}{V}$ (st)	+0.04	+0.26	+0.29	+0.12	+0.19

HD	50778	90432	200905	196321	29139
Type	K4III	K4III	K5Ib	K5II	K5III
$\log \frac{Li^o}{KV}_o$ (ub)	$<$ 0.45	$<$ 0.33	1.11	$<$ 0.34	$<$ -1.14
(bl)			1.25		
$\log \frac{Li}{KV}$ (B-V)	$<$ 1.75	$<$ 1.63	2.78	$<$ 1.67	$<$ 0.27
(e_e)	$<$ 1.71	$<$ 1.43	2.27	$<$ 1.33	$<$ 0.33
$\log \frac{Li}{KV}$	$<$ 1.73	$<$ 1.61	2.78	$<$ 1.67	$<$ 0.27
$\log \frac{V}{V}$ (wk)	-0.04	+0.20	-0.64	-0.15	-0.35
$\log \frac{V}{V}$ (st)	+0.31	+0.03	+0.04	+0.19	+0.07

HD	189319	201091	201092	6860
Type	K5III	K5V	K7V	MoIII
$\log \frac{Li^o}{KV}_o$ (ub)	1.07	$\leq$ 1.92	1.70	$<$ -0.03
(bl)	1.13			
$\log \frac{Li}{KV}$ (B-V)	2.35	$\leq$ 2.82	2.37	$<$ 1.31
(e_e)	2.30	$\leq$ 2.82	2.28	$<$ 1.17
$\log \frac{Li}{KV}$	2.35	$\leq$ 2.82	2.28	$<$ 1.24
$\log \frac{V}{V}$ (wk)	-0.15	$\leq$ -0.11	-0.67:	+0.15
$\log \frac{V}{V}$ (st)	+0.03	-0.03	+0.03	+0.12

Before investigating the scatter in the derived vanadium ratios, it is necessary to examine possible systematic trends which might discredit the lithium results. The weak vanadium line, as previously remarked, should be subject to all the stratification effects that the lithium doublet is, for in all cases when the abundance of lithium is high for the spectral class, the total strength of the Li I doublet is greater than that of the weak V I line. First it is necessary to observe that in the G8 and K0 stars most of the entries under the weak line vanadium-to-vanadium ratio indicate that a maximum was computed, and even in those cases where none is indicated it is unlikely that the value may be taken for other than a maximum, because the line is extremely weak in these stars. Note that in this case the plates were not critically inspected for defects at this wave length, as was done for the Li I feature. Then considering only the values from K1 onward, it is seen that they are systematically negative, indicating a possible error in the laboratory $\underline{gf}$' or a depression of the continuum at this wave length, but there is no trend with temperature. However, the values for the three supergiants are all low. A plot was made of log $\underline{Li}/\underline{KV}$ vs. log $\underline{V}/\underline{V}$(wk); no correlation was found.

The abundance derived from the strong line is not affected by the disappearance of the line in the hotter stars. It is, however, dependent more strongly on the excitation temperature, since this line originates in a 1.08 ev level, and also by the choice of the damping constant in the cooler stars. Inspection of the values indicates a slight systematic increase, amounting to about 0.20 to 0.25 in the logarithm from the hotter stars to the cooler ones. This is likely due to increasing blending with another line of the same multiplet located 0.64 A to the longward. There is no systematic effect connected with the supergiants.

Thus the vanadium-to-vanadium ratios indicate that no significant systematic error has been introduced into the results by the application of a simple curve-of-growth analysis to lines of the range of strength and excitation used here. This conclusion applies both to the principles involved and the actual procedure applied. The only possible exception to this statement is in the case of the supergiants, where the vanadium ratios indicate that the final results may be low, but probably by a factor less than five.

It is next desirable to evaluate the scatter in the vanadium results. Assuming that the two vanadium-to-vanadium ratios can be represented as constants with randomly-scattered errors, it is possible to derive values of the probable error of a single measurement by the usual procedures. Such an analysis gives 0.10 as the probable error of log $\underline{V}/\underline{V}$ for the strong line, including all stars; and 0.12 for the weak line, including all stars later than K1 except those in which a maximum is indicated and HD 201092, in which the exposure was too weak in this region to give a reliable result. These values are negligible compared to the range of 4 found in the log $\underline{Li}/\underline{V}$ values. The computed probable errors for the vanadium-to-vanadium ratios include all the errors involved in selecting the appropriate theoretical curve of growth, but not in determining the ionization correction.

It would appear, then, that the values of the abundance ratio of lithium to vanadium given in Table 8 are devoid of serious systematic errors, and, as will be shown in the next section, the random errors are sufficiently small that differences of a factor greater than three are probably real. Examination of the lithium-to-vanadium ratios then indicates a high variability among stars of the same spectral classification, and a decline of the maximum value for a classification with temperature. Of course the high opacity in the hotter stars precludes observing any but the largest abundance ratios--that is, a G8 III star with an abundance ratio equal to the largest found in a K5 star would not show a Li I line at the dispersion used here. Nevertheless, some of the observed abundances are significantly above the limit set by the opacity.

It might be thought that the high abundance ratios in the G8 and K0 stars are spurious because the lines were quite weak, especially since some apparent lines measured for the weak-line vanadium-to-vanadium ratio have high values. But the lithium line region on the plates was inspected for defects, and in the highest-abundance-ratio cases, the Li I feature could be easily seen. Further, the two separate analyses of HD 9270 based on different plates gave lithium-to-vanadium ratios differing by only 30 per cent.

Some of these effects are illustrated in Figure 11. In this figure reproductions are presented of four of the spectrograms used in this study. Three of them are of stars with large lithium-to-vanadium ratios: HD 9270, type G8 III; HD 6805, K2 III; and HD 200905, K5 Ib. The other spectrogram, HD 12929, is of a star of the same classification as HD 6805, but shows

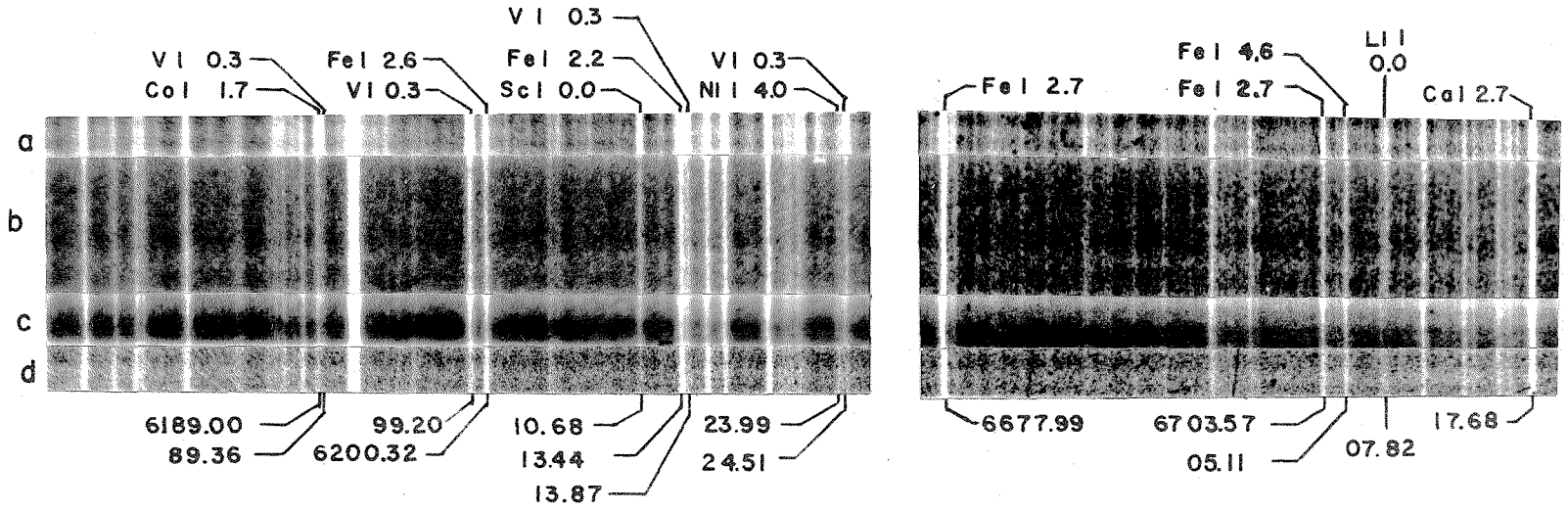

Figure 11. Sections of sample spectrograms. Li I doublet and other lines showing excitation effects are indicated by ion and excitation potential (ev) above and wavelength (A) below. Stars are (a) HD 200905 (ξ Cyg), K5Ib; (b) HD 6805 (η Cet), K2III; (c) HD 12929 (α Ari), K2III; and (d) HD 9270 (η Psc), G8III.

no lithium. The spectral regions shown are the region of the Li I doublet at λ6708 and a region at λ6200 containing lines of various elements and excitation potentials as indicated. The relative strengths of the high- and low-excitation lines indicate the expected dependence of excitation upon spectral class. Note that in general the excitation appears lower in HD 200905 (ξ Cyg) than in the K2 III stars, although it was found that the excitation temperature for the V I lines used was higher than in those stars. In the three stars that show the Li I feature, its strength increases as the stars become cooler, and the strengths of the V I lines of 0.3 ev excitation also increase. But their increase coupled with the decreased population of the 0.3 ev level relative to the ground state, the increased relative ionization of lithium, and especially the effect of the broader absorption coefficient of lithium, gives the result that the strong Li I doublet in HD 200905 represents an abundance ratio twenty times smaller than does the weak feature in HD 9270. The similarity of the spectra of the two K2 stars in all respects except the Li I doublet is also apparent.

It is interesting, but not essential to the interpretation of the results, to evaluate the constant K which appears in the abundance ratios. This constant is given in equation 35 of Chapter III as

$$\log K = \log C - \log \frac{gf\lambda}{\alpha} + 17.$$

The value of C was given in Chapter III, section b), as 1.39×10^{-4}. The value of gf, according to the method of reduction used here, should be the total for the entire doublet, and can be found from Allen's (1955) table. Since this is a simple transition in a light atom, this value is well determined from theory. The value of α can be found by interpolation in the tables of Chandrasekhar and Breen, using $\theta = 1.4$ and $P_e = 1$. As a result, one obtains

$$\log K = -7.70; \quad K = 2.0 \times 10^{-8}.$$

An alternate procedure is to use the ratio of lithium to calcium in the sun determined by Greenstein and Richardson (1951) and the ratio of calcium to vanadium given by Unsöld (1948) to determine a ratio of lithium to vanadium devoid of an undetermined constant. The comparison of this ratio with the one in Table 8 will evaluate K. The result of this procedure is

$$\log K = -7.96; \quad K = 1.1 \times 10^{-8}.$$

In view of the various evaluations of transition probabilities and analyses of the solar atmosphere involved in these two values, the agreement is quite satisfactory. It is sufficient for the present purpose to know that $\underline{K}$ is of the order of 10^{-8}. The agreement of the two values reflects favorably upon the results obtained here for the sun, and upon the procedure used in general.

c) Discussion of Errors

In various places in the foregoing discussion, estimates have been made of the probable errors involved in various steps of the analysis. It is necessary to consider these all together, and estimate their effect upon the final results.

Since the reduction procedure is a complex of graphical and arithmetical steps, it is not possible to derive an analytical expression for the probable error of the result in terms of the probable errors of the various quantities which enter. Therefore what was done was to choose a particular star and subject the various initial and intermediate quantities in its reduction procedure to perturbations, and then carry each perturbation separately through the procedure to determine its effect upon the results. The perturbations chosen were estimates of the probable error of the quantity involved. The reduction used for this estimate of error was that of HD 96833, a K1 III star, probably a little hotter than the average star of the study.

Because in general the reductions were carried out in terms of logarithms, the present treatment of errors will derive the probable errors in the logarithms of the quantities. Each source of error will be treated separately, an estimate of the magnitude of the error will be made, and its effect upon log $\underline{Li}^{o}/\underline{V}^{o}$ and log $\underline{\beta}$ will be determined. Since the sum of these two quantities equals the logarithm of the total abundance ratio, the sum of the squares of the errors in these two quantities will be an estimate of the square of the error in log $\underline{Li}/\underline{V}$.

Errors in the partition functions and in the temperature gradient parameter will not be treated, since their effects on the results must be very small.

(i) Photometry

It was shown in Chapter II, both by comparison of the assumed and observed line profiles and by the comparison of the results of the photometry of two plates of the same star, that there is probably little systematic error in the photometry. Further, a small systematic error affecting all the lines would have no significant effect upon the results, since these essentially depend upon the ratio of the strengths of the lithium and vanadium lines. It is therefore necessary to consider only the random errors in the photometry.

Errors in the photometry can be caused by blends, plate defects, tracing noise (plate grain), and errors in the calibration curves. The plotted position of a V I line in the empirical curve of growth is also affected by errors in the laboratory gf' value. The effects of blending have been minimized by careful choice of the lines used and examination of each line before measurement. It seems probable that since approximately 35 V I lines were used to determine the empirical curve of growth, the errors will tend to average out and leave only a scatter in the plot for the curve. This will have the effect of permitting a range of possible fits of the theoretical curve, centering on the correct one. The magnitude of this effect will be considered under "Fitting the Theoretical Curve of Growth" below.

Since only one measurement is involved in determining the strength of lithium in the spectrum, there is no opportunity for the errors of photometry to average out. An estimate has therefore been made of the probable error in the value of $\log \eta_o''$ derived for the Li I doublet. Since this line is usually on the linear part of the curve of growth, it is possible to estimate this error from other lines also on this part of the curve. In the G8 stars, almost all the vanadium lines come in this category. Therefore what was done was to take the equivalent widths of the V I lines observed in the G8 III stars HD 62345 and HD 104979, correct these to values of $\log W/b$, enter the theoretical curves of growth to obtain $\log \eta_o$, and apply the appropriate fitting constant to obtain values of $\log \eta_o''$. These values were then compared with those derived from the laboratory gf' values and the excitation temperature. The mean square difference between the two values of $\log \eta_o''$ was obtained by averaging over all the lines. From this, a value of 0.08 for the probable error of a single measurement was derived. This

value is taken as the probable error in log η_o'' for the Li I doublet, and as such produces an error of equal magnitude in log Li^o/V^o. This figure is probably a slight overestimate, because it includes the effects of errors in the gf' values.

Up to seven lines are used in determining the ionization of vanadium; thus there should be some cancellation of random errors. Nevertheless, since this number is quite a bit smaller than the number of V I lines, it seems necessary to estimate an error here also. Each of the scandium lines used in this step provides an estimate of the mean log η_o for all the lines of its ion. Therefore the difference between this estimate and the final adopted mean may be taken as an estimate of the error in the photometry. Such differences were taken for all the Sc lines measured in ten of the hottest and ten of the coolest stars in this study, and the mean square difference was determined. Since the value of $\Delta\log \eta_o$ in equation 28 of Chapter III results from at least six lines in each star studied, the probable error of six measurements was derived from the above analysis as an estimate of the error of $\Delta\log \eta_o$. The resultant value was 0.05, which produces an error of equal magnitude in log V^o/V^+. But since this quantity is itself quite small in HD 96833, the effect of the error on log β is negligible. The effect would be greater in cooler stars, but would be compensated by a decreased effect of the error in the estimated ionization temperature.

(ii) The Excitation Temperature

Errors in the derived excitation temperature parameter θ_e may be regarded as due to errors in judgment in superimposing the two plots of log W/λ vs. log η_o'. The error has been estimated by determining the range of fits over which no obvious asymmetry of the positions of the points from the two initial plots was seen in the final combined plot. A fairly generous attitude was adopted in deciding what constituted "obvious asymmetry." The resultant estimates of errors ranged from about 0.08 in the G8 stars to about 0.20 in the K5 and M0 stars. Thus it seems fair to adopt 0.15 as a generous mean.

The error in the excitation temperature parameter has several effects, which are given below:

(a) The error changes the value of log η_o'' calculated for each V I line, and thereby shifts the abscissae of the empirical curve of growth, producing an error in the fitting constant of the theoretical

curve, log η_o'' - log η_o. This error is in this case 0.10. Since the fitting constant is used to obtain the value of log η_o'' for Li I, the error enters log Li°/V° directly, giving an error of 0.10 there also.

(b) The error changes the correction applied to the values of log η_o of the ground-state Sc I lines to bring them into consonance with the other lines used in the ionization determination. The error of 0.15 in θ_e will produce an error of 0.10 in log V^o/V^+, which in turn yields an error of 0.01 in log β.

(c) The error in θ_e produces errors in the thermal motions computed for lithium and vanadium. The latter produces an error in the velocity of microturbulence, which combines with the error in the thermal velocity in computing the most probable velocity for lithium. The resultant error in log Li°/V° is only 0.01, since the error in W/b is almost entirely cancelled by the error in the c/v(Li) term which appears in the reduction equation. The cancellation is complete if no saturation effects are present.

(d) An error of 0.15 in the value of θ_e produces an error of 0.15 in one of the estimates of θ_i. This produces an error of 0.20 in the corresponding estimate of log β. This ignores the fact that the relation applied here assumes the identity of the effective and ionization temperatures. Furthermore, the final value of log Li/V depends on two estimates of log β--the one discussed here and one based on the color index or spectral class. It does not seem possible to evaluate the error in the second estimate, or the error involved in the basic assumption. But assuming that the second estimate is no worse than the first, perhaps the error of 0.20 in log β is a reasonable estimate of the total effect of the uncertainty in the ionization temperature.

(iii) Fitting the Theoretical Curve of Growth

In fitting a chosen theoretical curve of growth to the empirical one, errors arise because of the scatter in the results of the photometry of the V I lines. Each of the two fitting constants, log c/v and log η_o'' - log η_o, may be in error. Since at least six sets of these quantities were obtained in each analysis before adopting final values, estimates can be made of the uncertainty of the fit. Since the sets of constants are not

really independent estimates, it does not seem justified to apply the usual statistical procedures. A mental average based on an examination of the values, and considering the lack of independence, seems to be the best that can be done. Estimates of the probable errors in the fitting constants are then 0.04 in log c/v, and 0.06 in log η_o'' - log η_o. The latter error directly produces an error of the same magnitude in log Li^o/V^o.

The error in log c/v produces an error in the determination of the velocity of microturbulence, which affects both the lithium line and the scandium lines. In addition, the quantity log $c/v(V)$ itself appears in the reduction equation giving log Li^o/V^o. The effect on the Sc lines produces an error of 0.03 in log V^o/V^+, which is not large enough to affect log β. The total effect on the value of log Li^o/V^o is an error of 0.06.

(iv) Total Errors

Having surveyed the sources of errors in each reduction, and estimated the effects on the values of log Li^o/V^o and log β, it is now possible to calculate the total probable errors of these quantities and that of the final result, log Li/V.

The total error is given by the square root of the sum of the squares of the partial errors. For log Li^o/V^o, the total probable error is 0.15. It is interesting to compare this value to the probable error derived for the quantity log V/V, which includes essentially the same errors but could be derived without examining the sources of error in detail. The error derived in the previous section for log V/V was 0.12. These two results agree satisfactorily.

The error derived for log β is entirely due to the estimated error in the ionization temperature. The test star is too hot for the degree of ionization of vanadium to be effective in determining β. In a cooler star the effect of ionization would be more, and of the temperature, less. In cooler stars a possible error in the ionization constant Δ would also be important. The probable error in log β is found to be 0.20 in this case.

The probable error of the total abundance ratios is then the sum of the squares of the errors in log Li^o/V^o and log β. The value derived is 0.25. This corresponds to an estimated probable error in Li/V of a factor of 1.8. Although there are many uncertainties in this value, it seems reasonable to conclude that differences in the abundance ratios of 0.5 or more in the logarithm are significant.

It is worth pointing out again that the two independently-derived abundance ratios from the two spectrograms of HD 9270 differed by only 30 per cent. This star is one of the hotter ones used and has a very weak Li I feature. While one cannot estimate a probable error from two measurements, at least it is well within the factor of 1.8 calculated here.

V. DISCUSSION

a) The Abundance of Lithium

In section b) of Chapter IV the results on the relative abundance of lithium to vanadium are tabulated. The figures indicate that in any spectral classification the ratios are highly variable, but that the observed maximum declines with spectral type. The observed range of variation is small in the G8 and K0 stars, but here the high opacity and ionization prevent observation of a Li I doublet if the abundance is much less than the maximum. The indication of the later classes is that two stars with the same spectral classification may have abundance ratios differing by a factor of as much as 100, and there is no reason to believe that this cannot also be true of the earlier classifications. The abundance ratio derived for the sun is among the highest observed, which is consonant with its relatively early type. In general, it seems unlikely that very much of the variation can be accounted for by changes in the abundance of vanadium, both from the evidence of the absolute abundance of vanadium as given in section a) of Chapter IV, and from the appearance of the spectra in which the lithium line changes considerably more among stars of similar type than do the vanadium lines. It was suggested earlier that two stars, HD 29139 (α Tau) and HD 11909 (i Ari) might have high vanadium abundances. If the vanadium abundance in the latter is ten times normal as the derived value suggests, then the lithium abundance in this star is the highest observed. No lithium feature was seen in the spectrum of HD 29139, and an increase of a factor of ten in the vanadium abundance here would merely increase the upper limit for lithium to a value similar to other stars of similar classifications. If both these stars have high vanadium abundances, then apparently the abundance of lithium is not correlated with the abundance of vanadium. Furthermore, there is no correlation with any of the other properties of the stars given in Tables 7 or 8, such as luminosity, electron pressure, opacity, temperature (except in the sense indicated above), or Roman's spectroscopic groups.

The hope expressed in the Introduction that the lithium abundance might be found to be correlated with a gross property of the stars does not seem to have been realized except in a limited sense. Possibly it is a sensitive indicator of the efficiency of some process in the star which has no obvious effect upon its general characteristics.

It is also conceivable that the results obtained here do not reflect real changes in the abundance of lithium nuclei at all, but rather different equilibria between lithium atoms and an unobservable state not considered in the reductions, namely molecules. It seems *a priori* unlikely that these equilibria can change enough between stars of similar atmospheric conditions to account for the variations exhibited in Table 8, but it is nevertheless worthwhile to consider molecules in a little detail.

A molecule likely to account for some of the lithium is lithium hydride, LiH. This substance, which is analogous to H_2, has a covalent bond. The equilibrium between a diatomic molecule and its constituent atoms may be expressed by a relation similar to the ionization equation, and may be written for LiH as

$$(1) \qquad p(Li)p(H)/p(LiH) = K(T).$$

Here the p's are the partial pressures of the gases, and the function $K(T)$ involves both the dissociation potential and a term in the moment of inertia which arises from a degree of freedom not possessed by an atom. Aller (1953, p. 92) gives a convenient expression for log K. It is of interest to compare the equilibrium for Li and LiH with the analogous case, H and H_2. Writing equation 1 in the logarithmic form and subtracting it from the similar expression for H_2 gives

$$(2) \qquad \log LiH/Li = \log H_2/H + \log K(H_2) - \log K(LiH);$$

here expressions of the form $p(Li) = LiKT$ have been applied. Note that a ratio LiH/Li of at least 10^3 is needed to account for the observations. Thus if the difference of the log K's is not positive, a ratio of at least this magnitude is also required for H_2/H. Such a depletion of hydrogen would be easily detectible in the spectrum. For instance, if the abundance of H were highly variable due to the formation of H_2, the constant result for the absolute abundance of vanadium (Table 7) derived on the assumption of a constant hydrogen abundance would not have been obtained. The dissociation constants for H_2 and LiH are known from both experiment and theory, and values of log K can be calculated. For a temperature of 4000°, such a calculation gives for the difference of the log K's in equation 2 a value of approximately -2, distinctly non-positive. Hence it seems certain that no significant amount of LiH is formed in the stars studied here.

Another possibility is the radical LiO, analogous to OH. No dissociation constants are available for this molecule, but it seems likely that since the bond in this case is ionic, and the ionization potential of lithium is much lower than that of hydrogen, that LiO is the more strongly bound. However, NaO must be quite similar to LiO; therefore if the observable lithium is strongly depleted by the formation of this substance, the sodium must be similarly affected. No quantitative investigation has been made of the sodium abundance, but there was no obvious correlation between the strength of the "D" lines of Na I and the Li I doublet in the spectra studied. It was mentioned in the introduction that McKellar and Stilwell obtained the same result in the carbon stars. Furthermore, VO is a stable compound with a two-electron bond. It seems likely that vanadium would be more strongly oxidized than lithium if oxidation were important, and in this case one would expect the Li/V abundance ratio to increase with declining temperature instead of the opposite effect observed.

In general, then, it seems possible to neglect the effects of molecule formation.

The data indicate that stars cooler than the sun have less lithium than the sun. If the vanadium abundance of HD 11909 is actually high, as suggested, then the lithium abundance may significantly exceed the solar value. But it also seems likely that this star is hotter than the sun. The results of Greenstein and Richardson (1951) indicate that the lithium abundance of the earth exceeds the solar abundance by a factor of 100. If the terrestrial abundance is typical of the material out of which the solar system has formed, the conclusion is inescapable that the net effect of the processes acting on the material of the solar surface has been to destroy lithium. Greenstein and Richardson suggest that the material is convected to regions of sufficiently high temperature to destroy lithium. But aside from the specific process, the results of this study indicate that the net effect in cooler stars is also destruction. Certainly it is conceivable that the initial compositions of the stars were different, but there is no reason to suppose that the present temperatures of the stars are related to the initial compositions. It seems then that basically the stars cooler than the sun destroy lithium, and that the efficiency of destruction is highly variable but increases with decreasing temperature.

b) The Production and Destruction of Lithium

Although it does not seem likely that the results of this study can lead to any definite conclusions, it is interesting to examine the various methods that have been proposed by which stars may manufacture and destroy lithium and to note any suggestions that may be made about them on the basis of these results.

(i) Processes in Stellar Atmospheres

Burbidge and Burbidge (1955a,b) studied the spectra of two A stars which show strong magnetic fields, and found that the heavy elements are overabundant by a factor of the order of 1000. Fowler, Burbidge, and Burbidge (1955) suggested that these overabundances may be caused by nuclear reactions at the surfaces of the stars resulting from the acceleration of particles in varying magnetic fields. They also proposed that Li, Be, and B may be formed by spallation reactions on heavier nuclei, and indicated that a good possibility is that such reactions are produced by high energy protons ($>$ 100 Mev) in low-density regions high in the atmosphere. Much of this material would then be injected into the interstellar gas. They suggested that if similar processes, probably of lower efficiency, operate in the M dwarfs, it may be possible to account for the cosmic abundances of the light elements.

Nothing is known, either from theory or observations, as to how the strength and variability of the magnetic field depends on the other properties of the star; thus it is not possible to say how the data on the lithium-to-vanadium ratios fit the idea that lithium is either produced or destroyed by surface magnetic fields. Babcock (1958) has given a catalogue of stars which he has examined for variable magnetic fields. Only a few of the stars studied here are included in his lists, and these show no evidence of fields, although in stars with broad lines no field can be detected. He has observed magnetic fields in a few M stars which show peculiar emission lines, and of course in many A and F stars. Since the sun also shows complex magnetic fields, it seems likely that they are a property of all stars, but no correlation with the lithium abundances can yet be established.

(ii) Convection

As was mentioned earlier, Greenstein and Richardson have suggested that the abundance of lithium is low on the sun relative to the earth because

convection in the outer layers of the sun circulates the surface material to sufficient depths to cause the destruction of the lithium by energetic protons. The requirement that the lithium abundance be reduced to its present level in the lifetime of the sun sets a lower limit on the temperature to which the material must be convected. In this way, these authors were able to estimate the minimum depth of the solar convection layer.

Indeed, recent calculations indicate that the general requirements for a satisfactory model of a stellar interior demand an outer convection zone for the sun (Schwarzschild, Howard, and Härm 1957; Weymann 1957). Earlier, Osterbrock (1953) had demonstrated the need for a considerable convection zone in the outer part of K dwarfs. A recent rediscussion of the pertinent observational material by Limber (1958a) reduced the discrepancy noted by Osterbrock between his models for the middle and late M dwarfs and the observations, and further theoretical work (Limber 1958b) indicates that the cool dwarfs have completely convective interiors. The general trend of the results of these authors is that the cooler the star, the more of its mass must be included in an outer convection zone. Hoyle and Schwarzschild (1955), in attempting to fit models for the giant stars to the evolutionary tracks deduced from globular-cluster color-magnitude diagrams, found it necessary to invoke outer convection zones for stars more than two magnitudes above the main sequence. They do not give sufficient details of their calculations to show how the convection zone changes with temperature, and, since they emphasize the preliminary nature of their calculations, they would probably regard any conclusions based on the details of their models as unwarranted. Nevertheless, it seems clear that the giants also must have outer convection zones, which are presumably of different depths in stars of different surface temperatures.

Since detailed models for the sun and the K dwarfs are available, it is interesting to reverse the procedure of Greenstein and Richardson and estimate the mean lifetime of a lithium nucleus at the bottom of the convection zones of these stars. Presumably, the longer the lifetime at the bottom of the convection zone, the more lithium should appear at the surface if convection is primarily responsible for the destruction of this element. Greenstein and Richardson give the following formula for the mean lifetime of Li^7 (the most stable isotope) under stellar conditions:

$$(3) \qquad t = (1.8 \times 10^{-7}) \frac{e^{\tau}}{\rho \tau^2} \; ;$$

$$(4) \qquad \tau = 85 \, T_6^{-1/3} \; .$$

Here T_6 is the temperature in millions of degrees, and ρ is the density. Using these equations and the conditions at the bottom of the convection zones given in the interior models, the lifetimes given in Table 9 below were computed. Here the first column gives the spectral classification, the second and third columns give the temperature and the density at the bottom of the convection zone, the fourth column gives the lifetime of Li^7 in years (equation 3 gives the lifetime in seconds), and the final column gives the reference for the data in the second and third columns.

Table 9

The Lifetime of Li^7 at the Bottom of Convection Zones

Type	T_6	ρ	t(yr)	Reference
G2V	1.04	0.020	1.0×10^{20}	Weyman 1957
K1V	2.5	0.545	4.1×10^{9}	Osterbrock 1953
M0V	2.6	1.93	6.1×10^{8}	"

It is clear at once that the lifetime in the sun is too long to account for the destruction of lithium as suggested by Greenstein and Richardson. However, Hoyle and Schwarzschild have pointed out that the depth of convection in the giant models is extremely sensitive to the assumptions made about the atmosphere. In particular, the efficiency of convective transport of energy in the lower atmosphere, where the process is driven by the ionization of hydrogen, is critical, and cannot be accurately calculated. This is probably true also in the dwarf models, as Osterbrock hinted. Therefore it is quite possible that the conditions here given for the bottom of the convection zones are considerably in error. But since Weymann used Osterbrock's procedure for taking the atmosphere into account it is likely that all the errors are in the same sense. Also, in deriving equations 3 and 4 Greenstein and Richardson used early values of the lithium reaction cross-sections, which are probably inaccurate. Both of these considerations cast doubt upon the absolute values of t, but probably their relative values are of the correct order. In particular, one would not be surprised on the basis of these results to see considerably less lithium in the atmospheres

of K dwarfs than in G dwarfs. Unfortunately not many dwarfs were included in this program, but the K0, K1, and K2 dwarfs studied indicate abundances at least five to ten times less than the sun, the K5 dwarf a deficiency of at least a factor of 15, and the K7 dwarf a deficiency of about a factor of 40. Clearly this is in the right sense. Unfortunately no two dwarfs studied are of the same spectral type, so no information about possible variations within a spectral class is available.

No detailed giant models are available to permit a similar analysis for these stars, but it is reasonable to assume that the trend would be similar. Thus it would seem possible to account qualitatively for the general decline of lithium abundance with surface temperature through its destruction at the bottom of outer convection zones, which increase in depth with declining temperature.

Although it may be possible to account for the general decline of the lithium abundance in this way, nothing has been said about the considerable variations of the abundance under similar surface conditions. But it does not seem unlikely that the depth of convection is different among stars of the same spectral and luminosity class, at least among the giants. As was pointed out above, the depth of the convection zone is influenced by the efficiency of the convective transport of energy near the surface. If two stars differ in the general metal abundance, the electron pressure and hence the continuous opacity would vary proportionally. However, the appearance of the spectrum at low dispersion might be very little affected, since the strengths of the lines depend on the ratio of abundance to opacity. But a lower opacity would mean more effective radiative transport of energy, and less need to transport it by convection; thus the surface convection, and, in turn, the deeper convection would be influenced by a difference which would not be observed in a qualitative examination of the spectrum. Furthermore, according to the semi-empirical evolutionary tracks of Sandage (1957a) it is possible, as was mentioned earlier, that two giant stars of the same radius and luminosity have different masses. Necessarily the more massive of the two must have a higher central temperature, and therefore a different temperature distribution in the interior. Probably, then, the depth of the convection zone would be different. But since the surface conditions of the two stars are quite similar, no gross differences in the spectrum would appear. Thus it appears that there are mechanisms which can change the depth of convection without producing profound changes in the spectrum, and thereby produce lithium abundance differences in superficially similar stars.

It seems to be possible to construct a fairly reasonable case linking the abundance of lithium to convection. It is, of course, completely speculative, except for a small degree of substantiation in the dwarfs. It is quite likely, however, that further investigation could shed some light on the matter. For example, according to present understanding of stellar structure, two dwarfs of the same radius and luminosity must have the same mass. Thus in the dwarfs one of the causes mentioned above for different depths of convection in stars of similar surface conditions is eliminated. An extension of the present study to more dwarfs would therefore be valuable. More detailed studies of high-dispersion spectra of the stars studied here could reveal differences in the opacities, metal abundances, and so forth. Differences in mass between two giants of the same radius would require differences in the surface gravities which might be reflected in the damping constants. All the stars in this program are bright enough so that spectrograms of the highest dispersion could be obtained, and spectrophotometric analyses of the highest precision could be performed. Detailed comparison of two stars with the same spectral classification but different lithium-to-vanadium ratios might be quite revealing.

The observation of lithium in the spectra of S stars beclouds this undoubtedly oversimplified picture of the effect of convection. S stars exhibit strengthened lines of those heavy elements which, according to Burbidge, Burbidge, Fowler, and Hoyle (1957), are formed by the slow capture of neutrons by elements in the iron group (s-process). The source of neutrons is α-particle captures by neutron-rich isotopes near oxygen in mass in regions of the interior which have contracted and heated after the exhaustion of hydrogen. The appearance of the elements formed in the s-process at the surface indicates mixing to depths of extremely high temperature. This interpretation of the observations is strengthened by the discovery of technetium in R Andromedae (Merrill and Greenstein 1956). There are no known stable isotopes of this element, indicating that the time-scale of mixing from the interior to the surface must be on the order of 10^5 years or less. Clearly lithium cannot survive mixing to such high temperatures unless the hydrogen is exhausted in all regions in which the temperature is of the order of 10^6 degrees or more. However, the lithium line in R And is quite weak. According to Merrill and Greenstein's estimates, its strength is slightly less than that of the 0.07 ev V I line at λ5632. In HD 200905, in which the abundance ratio was found to be about 0.07 of the solar value,

the Li I doublet is twice as strong as the V I line. Since the lithium feature in HD 200905 is strong enough to be slightly above the linear part of the curve of growth, it would seem that the lithium abundance in R And is less than half that in HD 200905.

It is also possible that the proper kind of mixing can increase the surface lithium abundance. Cameron (1955) proposed that the proton-proton chain of hydrogen burning may end in part by the reactions

$$He^3(\alpha,\gamma)Be^7(e^-,\nu)Li^7.$$

Fowler (1958) has discussed the consequences of this reaction with respect to energy production in stars near solar type, taking into account the newly-discovered high cross-section for the first of these reactions. In the sun, the Li^7 would be destroyed by proton capture. In hot stars, the Be^7 would capture a proton before it would capture an electron, and Li^7 would not be formed. In the case of stars with mixing to a hydrogen-burning zone, if the Be^7 could be removed to a cool region before the time necessary to capture an electron (the order of a year, at the most), Li^7 might be produced and preserved. But since in a zone where hydrogen is exhausted, He^3 would also be exhausted, the reaction would not proceed at the bottom of the mixed region in S stars.

The above reactions were first proposed by Cameron to explain the carbon stars, which show both lithium and bands of C^{13}; the latter results from hydrogen burning in the CN-cycle and indicates mixing to depths where that process is taking place. It would seem more likely that these reactions will produce lithium in carbon stars than in S stars. However, even in S stars possibly an element of mass may pass through a region in which these reactions are taking place on its way upward from greater depths and may accumulate a small amount of lithium, which is destroyed as the element returns downward on the next half of the cycle. The greatest difficulty with any of these suggestions is the short lifetime of Be^7 against electron capture. Further judgments on the feasibility of this process must await a better understanding of the interiors of giant stars.

In general it seems possible that there is a connection between the abundance of lithium on the surfaces of stars and the depths of convection and mixing. Certainly no cause-and-effect relation has been established, but it appears worthwhile to make further investigations along the lines indicated above.

Assuming that convection is solely responsible for the depletion of lithium in the cool stars, the present results can be used to make a rough estimate of the mixing time. According to the evolutionary tracks of Sandage (1957a), stars slightly more massive than those in the galactic cluster M67 evolve through the K-giant region at nearly constant absolute visual magnitude. If the rate of depletion of lithium in the stellar atmosphere depends on the mass, the G8 giants with the most lithium are similar in mass to the corresponding K5 giants, provided both are sufficiently massive to evolve at constant M_V. The results of Table 8 indicate a difference of about a factor of 50 in lithium abundance between the G8 giant and the K5 giant with the highest Li/V ratios. It may be objected that only two K5 giants were studied, so that the value used is probably low. However, it cannot be extremely low because it is higher than that for any of the other five giants observed later than K3. Let then the factor 50 be assumed for the depletion of the atmospheric lithium for a certain star of moderate mass as it evolves from G8III to K5 III. If 1/e of the surface lithium is destroyed in each convective cycle, four cycles are required to produce this depletion. Sandage (1957b) has studied the evolutionary times for the less massive stars of M67 in this part of the H-R diagram, and obtains a value of about 5×10^8 years for the time spent by these stars in the corresponding stages. More massive stars will evolve more rapidly, but they also pass through a larger range in surface temperature. Perhaps 1×10^8 years is a reasonable guess for the evolutionary time of the star discussed above. Then the mean time for a convective cycle is about 2×10^7 years. This value is large compared to the mixing time of 10^5 years required for the S stars, as discussed above. Possibly the value of 1×10^8 years for the evolutionary time is too long, but a decrease of a factor of 100 seems unlikely in view of Sandage's results. More likely the efficiency of destruction of lithium per cycle is smaller than supposed here; furthermore it is likely that the mixing rate is more rapid in the cooler S stars than in the K giants. The mixing time derived from the lithium results does not therefore contradict the shorter time required for the S stars.

c) WZ Cassiopeiae

It has apparently become customary for any author who discusses lithium in an astrophysical context to attempt an interpretation of the

extremely strong lithium lines found in certain cool carbon stars. In view of the fact that the present investigation has produced more data on lithium and on the general properties of cool giants than any of these authors had at their disposal, it would seem remiss of the present writer to neglect a similar effort.

It was mentioned in the introduction that McKellar and Stilwell (1944) have measured the equivalent width of the Li I doublet in WZ Cas as 8.4 A. The strongest Li feature measured in this study was in the supergiant HD 200905 (ξ Cyg), in which the equivalent with is 0.20 A. But this strength represents an abundance only 0.07 of that in the sun. It seems possible then that if WZ Cas is much cooler than ξ Cyg, the strength of the doublet may be caused more by low temperature than high abundance.

Keenan and Morgan (1941) devised a classification system for carbon stars to replace the older R and N classification. The classification is two-dimensional, depending on the temperature as deduced from atomic lines and the carbon abundance deduced from the C_2 bands. Their temperature classification of WZ Cas is C9, at the extreme cool end of the carbon sequence. By comparison with the atomic features in normal stars, they give temperatures for their classes C0 through C5 only. In order to derive a value for class C9, these temperatures were extrapolated. First converting them to values of $\underline{\theta}$, they were plotted against the class number, and a curve was fitted by eye. This curve was chosen to have slightly decreasing curvature so that $\underline{\theta}$ for class C9 would be underestimated and the temperature overestimated, so that the effect of temperature on the line strength would be underestimated. The result of the estimate was $\underline{\theta} = 1.9$ ($\underline{T} = 2700°$), which seems hot compared to other estimates of the temperature of this star.

The values of log $\underline{V^+/V^0}$ and log $\underline{\chi}$ observed for the giant stars were then plotted as a function of $\underline{\theta}$ (effective) and extrapolated linearly to $\underline{\theta} = 1.9$. The plotted points fitted fairly well to linear relations. This permitted the calculation of the horizontal shift between the empirical and theoretical curves of growth--using equations 24, 29, and 30 of Chapter III--and the ionization correction from equations 32 and 33. Here the thermal motion was calculated from the effective temperature and the microturbulence was neglected. Then assuming a lithium-to-vanadium ratio of 10^4 $\underline{K}$ (essentially the solar value) equation 34 of Chapter III was applied to obtain log $\underline{\eta_o''}$ and the deduced shift was applied to derive the total log $\underline{\eta_o}$. Then

the equivalent width was computed on the assumption of unblended absorption coefficients. The result was $\underline{W}$ = 0.9 A, and order of magnitude low. Reducing the temperature to $\underline{\theta}$ = 2.2 (which is as good an extrapolation as 1.9, but a less conservative guess) yields $\underline{W}$ = 3.1 A.

The result is quite inconclusive. The extrapolations required are enormous and cannot be regarded as more than educated guesses. In any case it seems possible to get the required line strength with no more than the solar abundance of lithium and certainly not more than the terrestrial abundance. It seems likely that the abundance is higher by at least an order of magnitude than in normal late K stars. The difference between the line strengths in the carbon stars remains to be explained, but the effects of temperature may be quite large. Equivalent widths of the order of 1 A occur frequently in the list of McKellar and Stilwell.

d) Summary

The observed variations in the lithium-to-vanadium abundance ratios--which can be ascribed to changes in the lithium abundances--cannot yet be "explained" in any final way. It appears likely that the cool stars basically destroy lithium by processes which increase in efficiency with decreasing temperature, but which are very strongly variable.

It has been suggested that magnetic activity at the surfaces of stars may accelerate protons, and, especially in regions of very low density, produce the light elements by spallation reactions. If this process operates, it seems likely that it will contribute more light elements to the interstellar gas than to the stellar atmosphere itself. However, too little is known of the relation of stellar magnetic activity with the other observable properties of the atmosphere to permit any detailed connection with the present results.

A possible connection exists between the depths of surface convection zones in cool stars and the abundance of lithium in the surface. Models of dwarf interiors indicate that the lifetime of lithium at the bottom of the convection zones decreases with surface temperature. If reactions in the convected gas destroy the surface lithium, a decrease in the surface abundance with temperature would be expected, and is observed. If a similar effect operates in the giants, and if the depth of convection is strongly affected by surface opacity or total mass, it may be possible to account

for both the trend and the fluctuations observed. It seems possible to test these ideas observationally.

The results of this study and the preceding discussion suggest a general picture such as the following: the light elements are produced in magnetically-induced reactions in the outer atmospheres of stars (whence they are injected into the interstellar gas) and/or in the interstellar medium. The abundances observed in stellar atmospheres are the remains of the initial material reduced by destruction in convective mixing. In this picture the abundances in the hot stars should have suffered no depletion. It therefore becomes of interest to extend the search for lithium to include all the G stars, and to search for beryllium in stars of earlier type.

This study has not provided any definite answers to the general question of the origin of the light elements, but it has provided useful data and led to suggestions for further investigation. Since it is of the nature of a first survey, such results are quite satisfying.

REFERENCES

C. W. Allen, 1934. Mem. Comm. Solar Obs. Canberra 1, No. 5.

" , 1955. Astrophysical Quantitites, p. 68. London: The Athlone Press.

L. H. Aller, 1953. Astrophysics, Vol. 1. New York: The Ronald Press Company.

H. W. Babcock, 1958. Ap. J. Supp. 3, 141.

B. Bell, 1951. Thesis, Harvard University.

E. M. Burbidge and G. R. Burbidge, 1955a. Ap. J. 122, 396.

" , 1957. ibid. 126, 357.

G. R. Burbidge and E. M. Burbidge, 1955b. Ap. J. Supp. 1, 431.

E. M. Burbidge, G. R. Burbidge, W. A. Fowler, and F. Hoyle, 1957. Revs. Mod. Phys. 29, 547.

A. G. W. Cameron, 1955. Ap. J. 121, 144.

S. Chandrasekhar and F. H. Breen, 1946. Ap. J. 104, 430.

S. Chandrasekhar and G. Münch, 1946. Ap. J. 104, 446.

W. J. Claas, 1951. Recherches Astronomiques de l'Observatoire d'Utrecht XII, Part 1.

D. N. Davis, 1947. Ap. J. 106, 28.

S. E. A. van Dijke, 1946. Ap. J. 104, 27.

M. W. Feast, 1953. Les Processus Nucléaires dans les Astres, p. 413. Liège: Colloque International d'Astrophysique.

W. A. Fowler, 1958. Ap. J. 127, 551.

W. A. Fowler, G. R. Burbidge, and E. M. Burbidge, 1955. Ap. J. Supp. 2, 167.

J. L. Greenstein, 1948. Ap. J. 107, 151.

J. L. Greenstein and P. C. Keenan, 1958. Ap. J. 127, 172.

J. L. Greenstein and R. S. Richardson, 1951. Ap. J. 113, 536.

S. G. Hacker, 1935. Contr. Princeton Univ. Obs., No. 16.

F. Hoyle and M. Schwarzschild, 1955. Ap. J. Supp. 2, 1.

H. C. van de Hulst and J. J. M. Reesinck, 1947. Ap. J. 106, 121.

H. L. Johnson, 1955. Ann. d'Ap. 18, 292.

H. L. Johnson and D. L. Harris III, 1954. Ap. J. 120, 196.

H. L. Johnson and W. W. Morgan, 1953. Ap. J. 117, 313.

P. C. Keenan and W. W. Morgan, 1944. Ap. J. 94, 501.

" , 1951. Astrophysics, ed. Hynek, Ch. 1. New York: McGraw-Hill Book Company, Inc.

P. C. Keenan and R. G. Teske, 1956. Ap. J. 124, 499.

R. B. King, 1947. Ap. J. 105, 376.

D. N. Limber, 1958a. Ap. J. 127, 362.

" , 1958b. Ap. J. 127, 387.

A. McKellar, 1941. Observatory 64, 4.

A. McKellar and W. H. Stilwell, 1944. J. R. A. S. Canada 38, 237.

P. W. Merrill and J. L. Greenstein, 1956. Ap. J. Supp. 2, 225.

M. Minnaert, 1953. The Sun, ed. Kuiper, Ch. 3, Chicago: University of Chicago Press.

M. Minnaert, G. F. W. Mulders, and J. Houtgast, 1940. Photometric Atlas of the Solar Spectrum. Amsterdam: I. Schnabel.

C. E. Moore, 1945. Contr. Princeton Univ. Obs., No. 20.

" , 1949. National Bureau of Standards Circular, No. 467.

D. E. Osterbrock, 1953. Ap. J. 118, 529.

D. M. Popper, 1958. Paper given at an Astrophysics Research Conference, California Institute of Technology.

N. G. Roman, 1952. Ap. J. 116, 122.

A. Sandage, 1957a. Ap. J. 125, 435.

A. Sandage, 1957b. ibid. 126, 326.

R. F. Sanford, 1950. Ap. J. 111, 262.

M. Schwarzschild, R. Howard, and R. Härm, 1957. Ap. J. 125, 233.

L. Spitzer, 1949. Ap. J. 109, 548.

J. Stebbins and A. E. Whitford, 1945. Ap. J. 102, 318.

C. E. St. John, C. E. Moore, L. M. Ware, E. F. Adams, and H. D. Babcock, 1928. Washington: Carnegie Institution of Washington.

H. E. Suess and H. C. Urey, 1956. Revs. Mod. Phys. 28, 53.

R. G. Teske, 1956. Publ. A.S.P. 68, 520.

A. Unsöld, 1948. Zs. f. Ap. 24, 306.

" , 1955. Physik der Sternatmosphären, 2nd ed., p. 436. Berlin: Springer-Verlag.

R. Weymann, 1957. Ap. J. 126, 208.

O. C. Wilson and M. K. Vainu Bappu, 1957. Ap. J. 125, 661.

K. O. Wright, 1951a. Publ. Dom. Ap. Obs. Victoria 8, 1.

" , 1951b. ibid., p. 281.

M. Wrubel, 1949. Ap. J. 109, 66.